FEB 7 1962
LIBRARY

MONTHLY NOTICES

OF THE

ROYAL ASTRONOMICAL SOCIETY

XUM

NOW AVAILABLE

MEMOIRS

OF THE

ROYAL ASTRONOMICAL SOCIETY

VOL. LXVIII—PART III

CONTENTS

CLASSIFICATION AND RADIAL VELOCITIES OF BRIGHT SOUTHERN GALAXIES

by

GERARD DE VAUCOULEURS

AND

ANTOINETTE DE VAUCOULEURS

AND

ANALYSIS OF LINE BLANKETING [illegible]

by

A. KATE [illegible] AND JOHN E. [illegible]

PRICE £3 (US $9)

Orders to:

ASSISTANT SECRETARY, ROYAL ASTRONOMICAL SOCIETY,

BURLINGTON HOUSE, LONDON W.1

XUM

MONTHLY NOTICES
OF THE
ROYAL ASTRONOMICAL SOCIETY
Vol. 123 No. 3

DISTANCES OF SOUTHERN B-STARS AND GALACTIC STRUCTURE FROM Hγ-LUMINOSITIES

Arthur Beer

(Received 1961 May 11)

Summary

The equivalent widths of Hγ have been determined for 137 Southern B-stars (tabulated in Section 5), using material obtained from the Radcliffe Observatory in Pretoria (on the average 3 spectra per star). Most of the spectrophotometric reductions were carried out at the Dominion Astrophysical Observatory in Victoria, B.C. Detailed analysis, described in Sections 3 and 4, showed that there were no systematic differences, either between different observers, or between the present southern work and the previous investigations of northern stars by Petrie at Victoria. The internal error derived for the present determinations of Hγ intensities is 7 per cent per star, equivalent to $0^m.23$ in the absolute magnitudes. To convert these absolute magnitudes into stellar distances, a uniform system of star-magnitudes and colour-indices has been established for the southern hemisphere (Section 7). The preceding Section 6 discusses the luminosity-spectrum array.

Section 8 provides satisfactory tests of the newly-determined spectroscopic distances, in particular with the help of mean proper-motion parallaxes and, furthermore, by using mean distances derived from galactic-rotation effects on the radial velocities. In the latter case, it is shown (Section 8.4.3), that we may not be justified in using the south " calcium-cloud distances " (i.e. " effective half-distances ", based on the K-line) since, differing from the north, lines of sight in the south mostly run through cloud-free inter-arm regions.

Section 9 relates the new material to the structure of the Milky Way, and makes use of recent work on H I-areas, clusters, associations, H II-regions and various proposed Milky-Way arm-patterns. A general colour-excess diagram, illustrating the dependency on galactic longitude, is derived in Section 9.3. Figs. 9, 10 and 11 represent the B-stars and other Milky-Way constituents in their relation to different galactic regions out to about 4, 1·5, and 7 kiloparsecs, respectively. Particular attention is drawn to the occurrence of a conspicuous group of reddened B-stars which are clearly situated between hydrogen arms, lying especially outside the Sagittarius arm. Various significant discrepancies between location of stars, neutral hydrogen, and rotational models of the Galaxy are pointed out. Evolutionary aspects are indicated.

1. *Introduction.*—" It has long been recognized that one of the main difficulties in galactic studies is the uncertainty in the distance of the B-stars. Direct measurements are too few and uncertain . . . we are therefore compelled to develop the method of spectroscopic absolute magnitudes and thus to assign distances to the individual B-stars . . . ". There can hardly be a better introduction to this

XUM

paper than this remark made by Petrie early in his work on the determination of absolute magnitudes of B-stars by measurement of the total intensity of the hydrogen lines. Petrie's papers (1953, 1956a, 1956b, 1956c, 1958a, 1958b, 1958c, 1960) give bibliographical notes on work in this field by other authors. Special attention may also be drawn to the recent publications by Kopylov (1958a, 1958b) and Sinnerstad (1961).

The fundamental basis of this type of work is the existence of a close correlation between the total strength of Hγ and the absolute magnitude of the star in whose spectrum it occurs—a relation which has been calibrated by standard stars of known luminosities. By combining absolute magnitudes inferred in this way with other data (apparent brightness, colour, proper motion, radial velocity) we can derive the individual distances of these stars and check at least the statistical accuracy of the results. All work of this kind has so far been restricted to B-stars accessible to northern observatories. However, an extension to the southern sky has been made possible by the use of spectroscopic material from the Radcliffe Observatory, Pretoria, obtained by Feast, Thackeray, and Wesselink (1955, 1957, 1958), primarily for measuring B-star velocities. Dr Thackeray has very kindly put this material at the writer's disposal.

2. *The southern B-star spectra.*—The Radcliffe Observatory's B-star programme was specially designed to be complementary to the northern B-star work that has been carried out for many years at the Dominion Astrophysical Observatory, Victoria, B.C., first by J. S. Plaskett, who was later joined by J. A. Pearce, and then more recently by R. M. Petrie.

Although the Radcliffe and Victoria spectrographs are of quite different design —in the arrangements in which they have been used for most of this work—they give very nearly the same dispersions, so that methods successfully developed at Victoria could be applied with very little modification directly to the Pretoria material. The Pretoria spectrograms were obtained with two cameras, the b-camera giving 29 A/mm at Hγ, and the c-camera giving 49 A/mm; the spectra belong to the Pretoria " OBD "- and " OBC "-series which contain mainly fainter stars. The plates used were Kodak IIaO or 103aO emulsions; on each one were two calibration exposures, made with a tube-sensitometer, supplying 12 spots which were arranged so as to minimize the effects of emulsion irregularities. The spectrograms were intended primarily for radial velocity work, not for spectrophotometry, and this must be remembered when judging the errors of the line-intensities. Doubtless somewhat greater accuracy would have been obtained, had it been possible to introduce all the special precautions of accurate photographic photometry.

Between 1 and 9 spectrograms were available for each of 137 southern B-stars, with an average of three spectrograms per star. The stars ranged down to $10^{m}\cdot2$ (visual). Fig. 1 shows their galactic distribution; the data for the southern stars come from Table III (Section 5), and for the northern stars are those referred to in Section 9.1. The galactic coordinates used here are l^{I} and b^{I} (Ohlsson 1932); see also Blaauw, Gum, Pawsey, and Westerhout (1960).

3. *Spectrophotometry and equivalent widths of Hγ.*

3.1. The measurement of the plates, as far as the main programme was concerned, was carried out with the Cambridge microphotometer, using tracings at a magnification 100: 1, and covering about 100A centred on Hγ. The calibration

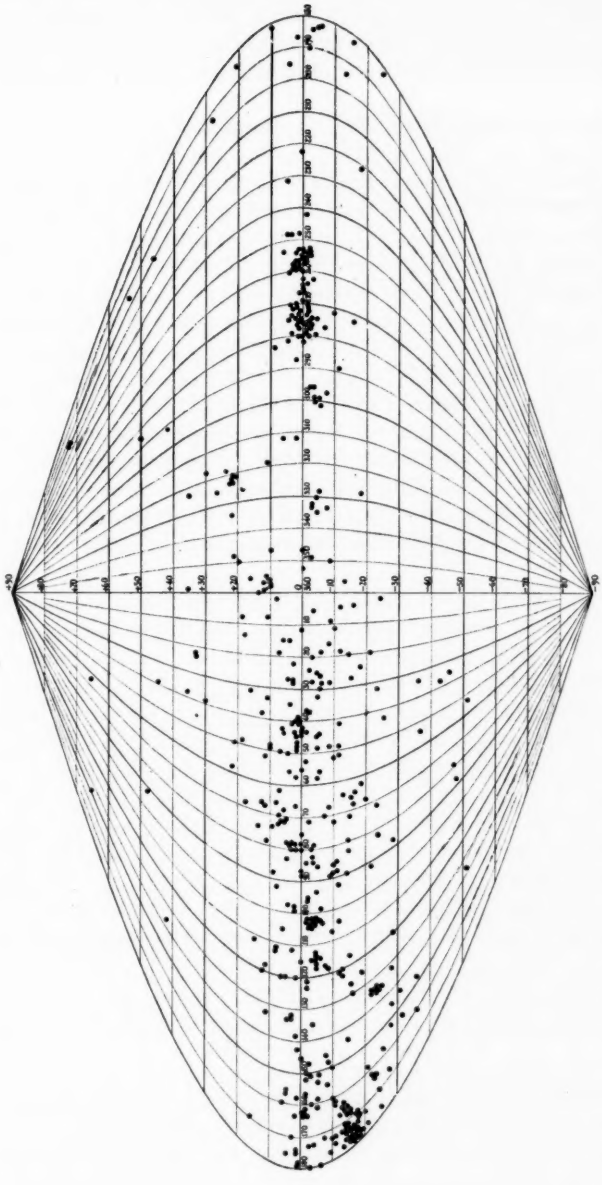

FIG. 1.—*Galactic distribution of B-stars with Hγ-luminosities, derived from Pretoria and Victoria spectra, and referred to in Sections 5 and 9.*

spots were recorded at 10 : 1. The tracings usually included the λ4388A He I-line, although normally this line lay well outside the wings of Hγ. Later work showed that occasionally Hγ has very extensive wings, making it necessary to record a greater length of the spectrum—up to 200A—to ensure a better determination of the continuous background, and a number of plates were re-photometered on this account.

3.2. Several other lines, mainly O II, may occur in appreciable strength within the Hγ-wings (see, e.g., Struve, 1931; and Butler and Seddon, 1958). In allowing for these lines, and also in determining the line wings, the same general procedure was used as had been followed in the original Victoria work, in the hope that in their error-characteristics the new southern measures would be closely similar to the earlier northern measures.

3.3. In outline, the procedure was to measure the equivalent width of Hγ, to read off the corresponding absolute magnitude from the calibration-curve (Petrie 1953, p. 264) and finally to add a correction for spectral type (*l.c.*, p. 263).

Preliminary Cambridge results for a few stars showed that satisfactory accuracy was being achieved with relatively few spectrograms. For instance, 8 spectrograms of HD 149438 gave a mean equivalent width 3·62A with a standard error ±0·15, or 4 per cent. Three spectrograms of HD 93128 gave 1·51 ± 0·16, i.e. an error of 11 per cent. These and other samples indicated that a mean of only 3 plates would usually give an equivalent width with a standard error less than 10 per cent. The general aim, therefore, was to use not less than three spectrograms per star.

3.4. However, before the work had gone very far, Dr Petrie offered very helpful assistance. He kindly arranged that the writer should spend four months at the Dominion Astrophysical Observatory, so that the very efficient semi-automatic intensity-reduction machine there could be used (Beals 1944). The visit to Victoria also permitted much closer consultation with Dr Petrie, and a more thorough intercomparison of all Victoria and Pretoria results available up to date.

3.5. In examining the errors of the Hγ-intensities we first note that, if N is the number of stars for which n plates were measured, the distribution $n(N)$ of the observations falls into the following n groups: 1(8), 2(33), 3(58), 4(32), 5(3), 6(1), 8(1), 9(1). The values of n are given in Column 11 of Table III. The average number of plates per star is 3·02. There are 129 stars with $n \geqslant 2$, i.e. altogether 7 groups, which can contribute to the error-examination.

The standard errors were first computed from internal agreement, using the formula

$$\Delta W = \pm \sqrt{\frac{\sum_i \delta_i^2}{n(n-1)}}, \qquad (1)$$

where the δ-values are individual deviations from the mean of n measures. The ΔW-values (in units of 0·01 A) are given in Column 13 of Table III.

Two diagrams were then drawn, one of which was a plot of the absolute values ΔW against W, the other of the percentage errors ΔW (per cent) against W. These showed that ΔW tended to vary with W, and that for some purposes it is better to deal with the percentage error in W rather than with the absolute error. If, then, Δ_i is the percentage-deviation of the equivalent-width determination (derived from the ith plate) from the mean (based on n plates), we find the r.m.s. deviation

for each star by

$$\sigma^2 = \frac{1}{n-1} \sum_{i=1}^{n} (\Delta_i)^2. \qquad (2)$$

The mean value of σ^2 per plate, averaged over all the N stars in one group, each having n plates per star, is therefore

$$\overline{\sigma_n^2} = \frac{1}{N(n-1)} \sum_{k=1}^{N} \left[\sum_{i=1}^{n} (\Delta_i)^2 \right]_k . \qquad (3)$$

The values of $\overline{\sigma_n^2}$ were then derived for each group using the above formulae. Finally, the mean $[\sigma^2]$ over all 7 groups was formed by weighting each one according to Nn.

From the above-mentioned 129 stars we thus obtained $[\sigma^2] = 66755/406$, i.e., $[\sigma] = \pm 12{\cdot}8$ per cent; so that the average star, with 3·02 plates, has an error of $\pm 7{\cdot}4$ per cent in its Hγ-intensity.

We may convert this Hγ error into the equivalent error in absolute magnitude, using Petrie's equation $M = a.10^{bW}$, where $a = -10{\cdot}96$ and $b = -0{\cdot}145$. It will be shown in Section 4 that we are entitled to apply this equation to the Pretoria material, although the formula was originally derived for the northern stars only.

3.6. Were there a constant 7·4 per cent error in the Hγ intensity, the errors in M would range between about $0^m{\cdot}2$ and $0^m{\cdot}3$, according to the value of M. We have, however, computed errors in more detail for Table III, to try to give some indication of the relative reliabilities of the M-values. By differentiating Petrie's formula, we obtain

$$\Delta M \,.\, \log_{10} e = b \,.\, \Delta W \,.\, M,$$

and

$$\Delta M / M = -0{\cdot}335 \,.\, \Delta W. \qquad (4)$$

Table III gives the ΔW-values computed from the interagreement of different spectrograms; its Column 15 contains the corresponding ΔM from this formula, expressed in units of $0^m{\cdot}01$. The values of M used are, however, not quite those given in the preceding Column 14 of Table III, but those which were derived before the spectral-type correction was applied (see Section 3.3). The mean value of all the ΔM in Table III is $0^m{\cdot}23$.

Petrie (1953, p. 265; 1960) has given the standard error of the absolute magnitudes in his work as $0^m{\cdot}3$. He has also remarked that the scatter of individual points about the calibration-curve is $0^m{\cdot}5$. This scatter may arise from errors in the assumed parallaxes of the standard stars, or from an intrinsic scatter in the (Hγ, M)-relation. From whichever source this standard scatter arises, the internal consistency of both the Victoria and the Pretoria work appears to be quite satisfactory in view of our present knowledge of B-star luminosities.

4. *The correspondence between Pretoria and Victoria luminosities.*

4.1. It is of the greatest importance that there should be as little systematic difference as possible between Pretoria and Victoria magnitudes, and that the error-characteristics of the one should closely resemble those of the other, so that the results may be used for the study of B-stars equally all round the Milky Way.

4.2. The first important question is whether there are systematic differences between different observers when dealing with the same material, differences such as may arise from individual judgments as to the position of the continuum, etc.

Dr Petrie kindly repeated 22 of the author's measurements and found that for B-stars his measured Hγ equivalent-widths were on the average about 10 per cent smaller than the author's, and that for O-stars the differences were somewhat larger, possibly due to variation in the interpretation of the blended lines lying within Hγ. A 10 per cent difference would correspond to about $0^{m}\cdot3$ in absolute magnitude. Later, however, the author was able to increase the overlapping material between the two observers to 46 spectrograms of 10 stars, and the result was then: mean difference $\overline{\Delta W}$ (Beer-Petrie) $= -0\cdot02$ A; the difference was still less if each star was weighted according to the number of spectrograms involved. The values for individual stars are shown in Fig. 2. It might be mentioned that there appears to be a slight tendency for the $\overline{\Delta W}$ (Beer-Petrie) to increase with

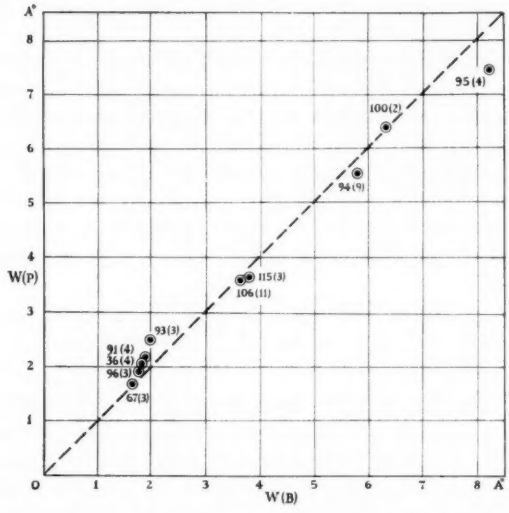

FIG. 2.—*Individual differences in measured equivalent widths of the same stars as obtained by different observers; following the No. of the star (Table III) is the number of plates (in brackets).*

photographic density in the continuous spectrum. On the whole, however, systematic differences in the absolute magnitudes arising from personal judgments of the two observers appear to be certainly less than $0^{m}\cdot1$.

4.3. However, a wider investigation is needed. Not only have there been two different observers; there have been two telescopes, two spectrographs, different photographic emulsions differently calibrated for photometry, two microphotometers, etc. Originally there were only 5 stars on the Pretoria list (Table III: Nos. 94, 95, 98, 100 and 106) for which absolute magnitudes had already been obtained at Victoria, and these covered a range of 2·5 magnitudes only, while the Victoria calibration-curve covers altogether 6·7 magnitudes. Further examination of material available at Pretoria and Victoria revealed a much more satisfactory overlap. There were 39 stars outside the original programme for which radial velocity work had been done on photometrically calibrated plates both at Victoria and Pretoria; to help widen the range of intercomparison, a number of additional

spectrograms were specially obtained at Pretoria. Eventually there were thus 44 stars in common, with 128 spectrograms from Pretoria and 88 from Victoria.

Thanks to the kindness of Dr Petrie, all the microphotometer work on these plates was carried out at the Dominion Astrophysical Observatory, following the procedure he used in his previous work on northern stars. His comparison of the

TABLE I

Comparison of the equivalent widths of Hγ between Pretoria (R) *and Victoria* (DAC) *plates*

		R		DAC	
	Star	*W*	*n*	*W*	*n*
1	HD 23408	6·10	3	6·70	3
2	23793	6·90	4	7·20	2
3	30677	2·12	2	2·93	3
4	35730	5·92	1	7·75	2
5	36013	6·18	3	5·98	2
6	36895	6·06	2	6·32	1
7	36960	3·28	2	4·14	2
8	37018	4·13	2	4·01	1
9	37128	1·98	6	1·42	2
10	37209	4·53	6	4·95	4
11	37742	1·50	1	1·74	2
12	46056	2·93	2	3·80	2
13	46202	3·82	2	3·96	2
14	46573	2·17	3	2·36	2
15	46883	2·33	1	3·34	2
16	50868	4·01	3	5·54	2
17	66665	3·17	3	3·36	2
18	138485	5·54	9	5·90	1
19	142096	7·13	5	7·87	1
20	144218	6·29	2	5·64	2
21	149438	3·62	8	3·85	4
22	154445	4·58	2	4·04	2
23	160233	3·89	3	4·62	2
24	162365	4·81	2	5·63	1
25	163472	4·80	4	4·34	2
26	167785	5·98	2	6·10	2
27	170580	6·41	3	5·44	2
28	174391	5·13	4	5·62	2
29	175803	5·98	2	6·80	2
30	176304	4·42	3	4·39	2
31	176542	6·42	2	7·86	1
32	178129	2·29	3	2·13	2
33	181858	6·41	1	6·58	2
34	181963	4·76	1	4·82	2
35	184279	3·41	3	3·70	2
36	187320	3·52	1	2·98	2
37	189550	4·54	2	5·30	2
38	189921	7·15	3	6·62	2
39	196025	5·16	4	5·29	2
40	201254	5·86	2	5·52	1
41	207563	5·56	4	5·67	3
42	209008	5·69	3	6·35	2
43	215733	2·64	2	1·99	2
44	219188	2·84	2	2·69	2

TABLE II

Comparison of the equivalent widths of He I λ4388 *between Pretoria* (R) *and Victoria* (DAO) *plates*

Star	R	*n*	DAO	*n*
HD 30677	0·76	2	0·75	2
36013	0·84	2	0·94	2
46202	0·74	2	0·68	2
66665	0·66	2	0·60	2
160233	1·23	2	1·04	2
189550	0·87	2	0·94	2
207563	1·16	3	0·77	2

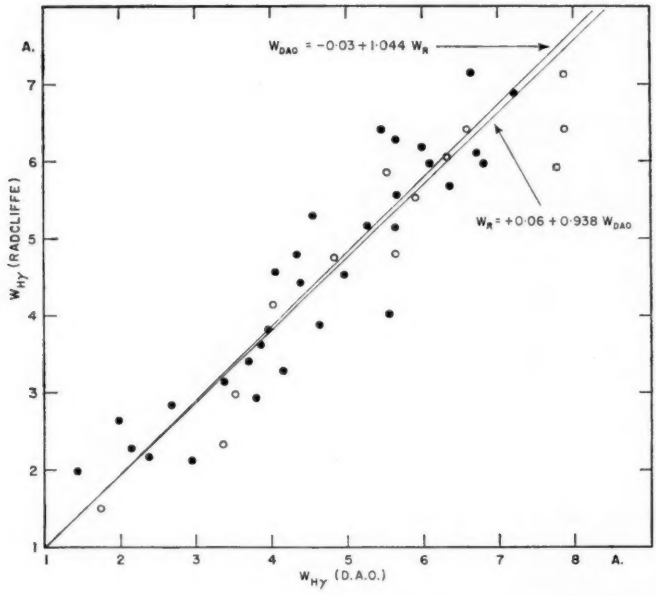

FIG. 3.—*Comparison of Hγ intensities from spectra obtained at Pretoria* (*Radcliffe Observatory*) *and Victoria* (*Dominion Astrophysical Observatory*). *Open circles have a smaller weight* (*stars with one plate only*).

individual Hγ intensities is plotted in Fig. 3, with Victoria values as abscissae and Pretoria as ordinates. Table I shows the results for Hγ, and Table II for λ4388A, He I. The computation of regression lines by least squares gave

$$W_{DA0} = -0·03 + 1·044\,.\,W_R \qquad (5)$$

$$W_R = +0·06 + 0·938\,.\,W_{DA0} \qquad (6)$$

Taking these relations at their face value, the Pretoria equivalent widths are about 5 per cent smaller than the Victoria equivalent widths. In view of the general level of errors involved, this difference has been neglected in what follows. The

Victoria calibration curve and the Victoria spectral-type corrections have been used unchanged for the Pretoria measures, and it should be possible to regard the Pretoria values as on exactly the same footing as the Victoria values.

5. *Absolute magnitudes of southern B-stars.*—The following data are tabulated in Table III which comprises all stars investigated in the present Hγ-programme.

Column:

1 Current number
2 HD number
3 Galactic longitude, l^{I}
4 Galactic latitude, b^{I}.
5 Spectral and luminosity classification, Sp.
6 Proper motion in right ascension, μ_α.
7 Proper motion in declination, μ_δ.
8 Visual magnitude, V.

Column:

9 Colour index, $B-V$.
10 3 × colour-excess, 3CE.
11 Number of spectra measured, n.
12 Equivalent width, W.
13 Standard error of W in units of 0·01 A, $\pm\Delta W$.
14 Absolute magnitude, M.
15 Standard error of M in units of $0^{m}\cdot01$, $\pm\Delta M$.
16 Distance of star in kiloparsecs, r.

6. *The luminosity-spectrum array.*—Fig. 4 (*a*) and (*b*) represents the luminosity-spectrum relation for all the 137 stars listed in Table III, which may be compared (in Fig. 4 (*b*)) with the corresponding relationship for 313 northern stars (derived

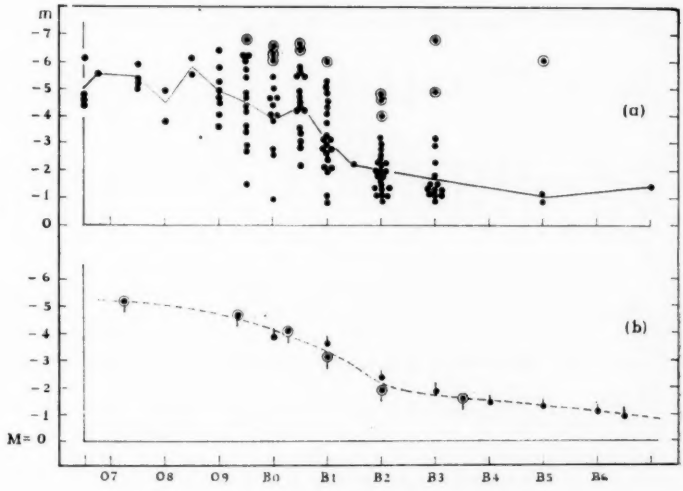

FIG. 4

(*a*) *Single southern values.*
● : *"normal" stars.*
⊙ : *supergiants.*
———: *mean relation for spectral sub-classes, (supergiants omitted).*

(*b*) *Group-means.*
● : *northern spectral-groups.*
⊙ : *southern spectral-groups.*
– – –: *mean Sp-M relation.*

TABLE III

1	2	3	4	5	6	7	8	9	10	11	12	13	14	15	16
No.	HD	l^{I}	b^{I}	Sp	μ_a	μ_δ	V	$B-V$	3CE	n	W	$\pm\Delta W$ (0·01A)	M	$\pm\Delta M$ ($0^{m}\cdot01$)	r
		°	°		″	″	m	m	m				m		
1	23408	134	−22	B 7 III	+·026	−·045	3·96	−0·02	+0·30	4	6·10	25	−1·45	12	0·10
2	23793	145	−31	B 3	+·028	−·020	5·08	−0·12	0·18	4	6·90	55	−0·90	20	0·15
3	30677	158	−21	B 1 V:	...	...	6·95	−0·02	0·72	2	2·12	22	−5·13	40	1·87
4	35730	167	−15	B 3 V:	−·005	+·001	7·20	−0·15	0·15	1	5·92	...	−1·34	...	0·48
5	36013	169	−16	B 3 V: n	...	...	6·88	−0·13	0·21	3	6·19	27	−1·21	13	0·46
6	36895	163	−11	B 2 V	+·018	+·002	...	...	...	2	6·06	28	−1·23	14	...
7	36960	177	−18	B 1	+·004	+·004	4·71	−0·22	0·06	2	3·28	65	−3·39	79	0·40
8	37018	176	−17	B 2	+·003	+·001	4·70	−0·11	0·33	2	4·13	41	−2·53	38	0·29
9	37128	173	−15	B 0 Ia	·000	·000	1·71	−0·16	0·18	6	1·98	15	−5·35	28	0·36
10	37109	178	−17	B 1	−·006	−·012	5·67	−0·15	0·27	10	4·35	17	−2·29	14	0·34
11	37742	174	−15	B 0 ne	+·004	−·002	1·91	−0·20	0·30	1	1·50	...	−6·32	...	0·40
12	46056	174	− 1	O 8	...	...	8·10	+0·18	1·44	2	2·93	6	−3·75	8	1·21
13	46202	174	0	O 9·5 III	...	...	8·19	+0·13	1·29	2	3·82	5	−2·73	5	0·84
14	46573	176	− 1	O 8	...	...	7·92	+0·30	1·80	3	2·17	7	−4·94	12	1·63
15	46883	170	+ 3	B 2 V: n	...	...	8·15	+0·39	1·89	1	2·33	...	−4·80	...	1·63
16	49798	221	−18	O 6	+·012	−·002	8·26	−0·27	0·15	2	2·32	24	−4·63	40	3·53
17	50868	176	+ 5	B 2 Vne	...	...	...	...	...	3	4·01	24	−2·65	23	...
18	66665	184	+21	B 0·5 III	...	...	7·65	−0·15	0·39	3	3·17	30	−3·51	38	1·43
19	69106	222	0	B 0·5 V	+·002	−·012	7·08	−0·04	0·72	2	3·20	24	−3·48	30	0·93
20	77581	231	+ 5	B 0 I	−·016	−·001	6·86	+0·05	2·34	2	1·36	11	−6·67	26	1·81
21	81370	242	− 1	B 1 V	−·005	+·001	8·71	+0·16	1·26	3	2·97	12	−3·80	16	1·78
22	87380	248	+ 1	B 1 IVn	−·015	−·008	9·02	−0·03	0·69	2	4·26	46	−2·36	41	1·37
23	89137	248	+ 5	O 9·5 V	−·045	−·022	7·90	−0·06	0·72	4	1·94	16	−5·41	30	3·30
24	89174	248	+ 4	B 1 III	+·013	+·010	7·83	+0·24	1·50	3	2·62	10	−4·29	15	1·33

25	90087	253	− 2	O	9·5 V	−·002	−·005	7·78	−0·02	0·84	4	2·27	10	−4·81	17	2·24
26	91651	254	− 2	O	9·5 Vn:	...	...	8·79	0·00	0·90	3	2·27	4	−4·81	7	3·47
27	92206	254	0	O	6	+·003	−·012	7·61	+0·13	1·35	3	2·26	14	−4·72	24	1·57
28	92504	254	+ 1	O	9:	+·014	−·008	8·46	−0·02	0·84	3	3·03	27	−3·65	36	1·79
29	92554	255	− 2	B	0 V:	...	...	8·58	+0·28	1·74	3	2·37	7	−4·65	11	1·99
30	92850	254	+ 2	B	0 I	−·023	−·001	8·01	+0·08	0·90	3	2·17	16	−5·00	28	2·64
31	92982	254	0	B	1 II	...	...	8·79	+0·38	1·86	4	2·28	5	−4·83	9	2·25
32	93028	255	− 1	O	9 I	+·002	+·002	8·34	−0·04	0·72	3	2·44	16	−4·51	26	2·67
33	93128	255	0	O	6 e	+·011	−·008	...	...	...	3	1·51	16	−6·19	35	...
34	93206	255	− 1	O	9·5 I:	+·003	·000	6·46	+0·16	1·23	2	1·30	5	−6·76	12	2·50
35	−59·2623	255	0	O	6	+·004	+·007	8·04	+0·01	0·99	3	2·32	25	−4·63	42	2·17
36	93843	256	− 1	O	6·5	−·002	−·009	7·42	−0·02	0·90	4	1·84	7	−5·52	14	2·56
37	94663	256	+ 1	O	9·5 III	...	...	9·28	+0·18	1·44	4	3·17	3	−3·47	4	1·83
38	94909	256	+ 2	B	0 I	+·004	+·002	7·24	+0·50	2·16	3	1·53	14	−6·26	31	1·85
39	95029	254	+ 7	B	2 V	−·012	+·001	8·79	+0·03	0·81	4	4·02	3	−2·64	12	1·33
40	95461	257	0	B	0 I	...	...	8·85	+0·40	1·86	2	1·28	5	−6·82	12	5·78
41	95731	257	+ 1	B	0·5 III	−·008	−·008	9·00	+0·20	1·44	3	2·28	10	−4·82	17	2·99
42	97471	258	+ 2	B	0 V	+·003	+·021	9·28	0·00	0·90	2	3·98	48	−2·60	46	1·57
43	97848	258	+ 2	O	9 III	+·006	·000	8·66	−0·01	0·90	3	2·36	17	−4·65	28	3·03
44	97913	259	+ 1	B	1 V:	+·004	−·017	8·79	+0·03	0·93	5	2·50	16	−4·47	25	2·92
45	97966	259	+ 1	O	7·5	−·005	−·007	8·78	+0·07	1·14	3	1·65	11	−5·93	23	5·18
46	98614	259	+ 1	B	1 III	+·008	+·002	8·41	+0·12	1·14	3	3·35	15	−3·31	18	1·31
47	99160	260	0	O	9 II:	+·023	−·026	9·11	+0·18	1·47	4	2·68	18	−4·14	27	2·36
48	99890	260	+ 4	B	0·5 V:	−·013	−·003	8·27	−0·02	0·78	3	2·47	8	−4·52	13	2·52
49	100099	262	− 3	O	9·5 III	−·007	−·006	8·02	+0·14	1·32	4	2·66	18	−4·18	27	1·50
50	100943	262	0	B	5 I	−·011	−·005	7·12	+0·14	0·66	4	1·66	5	−6·20	11	3·40
51	102475	263	− 1	B	0·5 II	+·004	+·012	8·53	−0·02	0·72	3	3·80	34	−2·79	35	1·32
52	102997	264	0	B	3 I	−·003	−·011	6·53	+0·32	1·52	4	1·35	12	−6·79	28	2·51
53	103146	264	0	B	I III:	+·017	+·013	8·29	+0·08	1·02	3	4·00	24	−2·61	23	0·95
54	105627	266	0	O	9 V	−·008	·000	8·06	+0·08	1·17	3	1·98	7	−5·32	13	2·77
55	106325	266	0	B	1 III	+·011	−·017	8·45	+0·23	1·56	3	2·75	4	−4·10	6	1·57
56	109978	269	0	O	9 III	+·007	−·015	8·75	+0·40	2·13	3	2·20	14	−4·92	25	2·03

TABLE III (*continued*)

1	2	3	4	5	6	7	8	9	10	11	12	13	14	15	16
No.	HD	l^{I}	b^{I}	Sp	μ_α	μ_δ	V	$B-V$	3CE	n	W	$\pm\Delta W$ (0·01A)	M	$\pm\Delta M$ ($0^{m}\cdot01$)	r
		°	°		″	″	m	m	m				m		
57	110360	270	+ 2	O˜ 7·5	−·019	+·007	9·28	+0·17	1·44	3	2·15	8	−4·95	14	3·61
58	110660	270	− 1	B 2 V:	...	...	9·88	+0·52	2·28	2	4·40	55	−2·30	46	0·96
59	110785	270	+ 3	B 2 V	−·025	+·011	9·84	+0·04	0·84	3	4·64	21	−2·10	16	1·66
60	110863	270	+ 2	B 2 V	−·025	+·011	8·91	+0·38	1·86	3	4·00	38	−2·65	37	0·87
61	110946	270	− 2	B 1 V:	−·005	−·011	9·24	+0·36	1·86	3	3·55	23	−3·07	26	1·23
62	111952	271	+ 2	B 3 Vn	+·004	−·002	9·45	+0·10	0·90	4	4·44	27	−2·28	22	1·46
63	112485	271	+ 2	B 2 V	+·005	−·018	9·44	+0·28	1·56	3	5·06	20	−1·80	14	0·86
64	112843	271	−10	B 2 III:	...	...	9·52	+0·15	1·17	4	3·46	14	−3·22	16	2·06
65	113016	272	− 2	B 2 V:	...	...	9·04	+0·26	1·50	1	4·35	...	−2·34	...	0·95
66	114011	273	+ 1	B 0·5 III	−·003	−·011	9·13	+0·84	3·36	3	2·66	22	−4·22	33	1·00
67	114340	273	+ 3	B 1 I	−·014	−·015	8·08	+0·48	1·98	3	1·68	26	−5·97	54	2·59
68	114733	274	+ 4	B 0·5 V	...	...	9·48	+0·27	1·65	3	4·39	10	−2·25	7	1·04
69	115034	273	− 1	B 1 V	−·018	+·002	8·68	+0·08	1·02	4	3·79	23	−2·81	23	1·24
70	116168	275	+ 1	B 2 IV:	−·007	−·010	9·13	+0·18	1·26	2	4·24	14	−2·38	12	1·12
71	116282	275	+ 2	B 0 IV	−·013	+·009	9·57	+0·44	2·22	2	2·52	7	−4·42	11	2·26
72	116328	275	+ 1	B 2 V	+·032	−·003	9·11	+0·19	1·29	3	3·66	14	−3·00	15	1·46
73	116766	275	− 2	B 2 V	...	...	10·04	+0·18	1·26	3	5·98	6	−1·27	30	1·02
74	116852	272	−16	O 9 III	...	...	8·42	−0·10	0·63	3	1·76	20	−5·75	41	5·10
75	117216	275	− 3	B 1 III:	...	...	10·20	+0·26	1·56	3	4·75	27	−1·97	20	1·32
76	117357	275	0	B 0 V ne	...	...	9·06	+0·18	1·44	1	1·36	...	−6·65	...	7·14
77	117707	275	− 3	B 0·5 I	−·007	+·016	9·36	+0·56	2·28	3	1·90	22	−5·52	43	3·31
78	117797	276	0	O 8·5	...	...	9·12	+0·45	2·25	4	1·59	21	−6·07	45	3·89
79	118571	276	+ 1	B 1 Vn	−·006	+·003	8·72	+0·02	0·84	3	3·76	8	−2·85	8	1·40
80	118681	277	+ 1	B 2 V	...	...	9·36	+0·14	1·52	2	6·55	34	−1·01	14	0·59

XUM

81	118969	276	− 2	B	1·5 V	−·032	+0·12	9·89	+0·04	0·87	2	4·49	45	−2·20	38	1·75
82	119646	277	− 1	B	2 I	−·007	−·009	6·59	+0·12	0·84	3	2·34	4	−4·68	6	1·22
83	120521	279	+ 3	O	9 I	+·010	−·012	8·56	+0·25	1·59	4	1·45	19	−6·41	42	4·74
84	122324	281	+ 5	B	0·5 I	−·013	+·011	8·99	+0·42	1·89	4	1·85	20	−5·62	40	3·55
85	122691	279	− 1	B	0·5 Vn	−·007	−·002	9·12	+0·28	1·18	2	2·36	5	−4·70	8	3·37
86	122831	277	− 7	B	1 III	−·002	−·013	8·97	+0·07	0·99	4	4·67	18	−2·03	14	1·00
87	122879	280	+ 1	B	0 I	−·004	+·006	6·41	+0·08	0·90	3	1·37	5	−6·62	12	2·67
88	123008	279	− 3	O	9·5 I	−·016	−·011	8·85	+0·44	2·07	3	1·81	16	−5·66	32	3·08
89	123056	280	0	O	9·5 III	−·004	−·010	8·12	+0·12	1·26	4	3·06	21	−3·62	28	1·25
90	124298	280	− 1	B	2 V	+·026	+·005	9·48	+0·21	1·35	3	5·11	3	−1·76	2	1·51
91	124979	284	+ 9	O	8·5	−·018	+·011	8·49	+0·08	1·14	4	1·89	4	−5·47	8	3·66
92	125241	281	0	O	9·5 I	+·004	−·013	8·34	+0·36	1·83	2	1·57	9	−6·15	19	3·40
93	130298	287	+ 2	O	7·5	+·014	−·002	9·25	+0·44	2·25	3	1·97	5	−5·28	10	2·99
94	138485	317	+30	B	2 V:	−·014	−·021	5·49	−0·14	0·30	9	5·54	25	−1·50	14	0·22
95	142096	319	+24	B	3 n	−·014	−·031	4·99	−0·10	0·45	3	6·99	42	−0·88	15	0·12
96	142468	296	− 2	B	0·5 I	−·002	+·005	7·90	+0·53	2·19	3	1·76	15	−5·80	30	2·00
97	142565	296	− 2	B	0 I	−·014	+·010	8·92	+0·45	2·01	3	2·39	24	−4·62	39	2·02
98	142983	325	+27	B	3	−·016	−·025	4·85	−0·01	0·45	3	3·76	11	−2·94	12	0·25
99	143104	288	−11	B	2 V	−·014	−·024	9·23	−0·04	0·60	3	5·96	18	−1·28	9	0·96
100	144218	322	+22	B	3	−·021	−·027	5·01	−0·01	0·69	2	6·34	25	−1·14	11	0·12
101	146919	299	− 3	B	0·5 I	−·025	−·002	8·53	+0·48	2·04	4	2·39	17	−4·64	28	1·68
102	147331	300	− 3	O	9·5 I	−·012	−·019	8·76	+0·21	1·38	5	1·64	9	−6·00	19	4·74
103	147421	299	− 4	B	0 II	−·010	−·008	8·94	+0·08	1·11	3	2·83	11	−3·96	16	2·28
104	148422	297	− 7	B	0·5 II	−·014	−·002	8·67	+0·09	1·05	4	1·94	18	−5·47	34	4·15
105	148546	311	+ 6	O	9·5 I	+·002	−·005	7·67	+0·28	1·59	2	1·56	23	−6·18	50	2·83
106	149438	319	+11	B	0 V	−·012	−·028	2·89	−0·25	0·13	8	3·62	15	−2·97	16	0·14
107	149729	301	− 5	B	2 Vn	−·013	+·012	9·05	+0·04	0·84	4	4·70	14	−2·06	11	1·13
108	151397	312	+ 2	B	0·5 V	...	...	9·66	+0·24	1·56	2	3·48	43	−3·13	48	1·76
109	154445	347	+22	B	1 V:	·000	−·005	5·67	+0·06	0·96	2	4·58	16	−2·10	13	0·28
110	160233	356	+17	B	1 V:	+·022	+·007	...	...	...	3	3·89	13	−2·72	13	...
111	162365	8	+19	B	2 V	+·012	+·010	8·05	−0·06	0·54	2	4·81	25	−1·98	18	0·82
112	163472	355	+11	B	2 V	−·009	·000	5·78	−0·02	0·66	4	4·79	17	−1·99	13	0·26

TABLE III (*continued*)

1	2	3	4	5	6	7	8	9	10	11	12	13	14	15	16
No.	HD	l^{II}	b^{II}	Sp	μ_α	μ_δ	V	$B-V$	3CE	n	W	$\pm\Delta W$ (0.01A)	M	$\pm\Delta M$ ($0^m.01$)	r
		°	°		″	″	m	m	m				m		
113	164019	330	− 4	O 9.5 I	−·031	+·002	9·31	+0·21	1·38	4	2·88	17	−3·86	24	2·28
114	164032	329	− 5	B 1 II	−·011	+·007	7·48	+0·14	1·14	3	2·07	25	−5·21	46	2·94
115	164741	333	− 3	B 1 III	−·005	+·018	9·05	+0·32	1·74	3	3·78	27	−2·83	28	1·07
116	165016	334	− 3	B 0 III:	−·003	+·011	7·53	−0·06	0·72	4	2·82	10	−3·97	14	1·43
117	167785	6	+11	B 2 V	...	...	...	...	...	2	5·98	24	−1·27	12	...
118	168941	334	− 8	O 9.5 II	+·026	−·028	9·34	−0·01	0·87	3	2·58	20	−4·30	31	3·58
119	170580	2	+ 5	B 2 V	−·010	−·020	6·55	+0·14	1·14	3	6·41	12	−1·07	5	0·22
120	173987	355	− 4	B 0.5 I	−·005	+·007	9·05	+0·27	1·41	2	1·42	38	−6·52	86	6·79
121	174391	15	+ 6	B 3 V	+·006	+·008	6·59	−0·06	0·42	4	5·13	23	−1·79	15	0·39
122	175803	19	+ 7	B 3 V	+·013	+·005	8·02	+0·17	1·11	2	5·98	48	−1·31	23	0·44
123	176304	10	− 2	B 2 V	+·020	−·013	6·57	+0·25	1·47	3	4·42	43	−2·28	36	0·30
124	176542	15	+ 4	B 2 V	+·007	−·012	8·99	+0·15	1·17	2	6·42	32	−1·06	14	0·60
125	178129	6	− 3	B 3 II	+·004	−·008	7·63	+0·47	1·95	3	2·29	32	−4·91	54	1·31
126	181858	357	−13	B 5	−·020	+·025	6·54	+0·02	0·42	1	6·41	...	−1·21	...	0·26
127	181963	27	+ 4	B 2 V	−·020	−·009	7·31	+0·08	0·96	1	4·76	...	−2·02	...	0·47
128	184279	9	− 9	B 1 V: n	+·016	−·001	6·80	−0·06	0·00	3	3·41	45	−3·25	53	1·02
129	187320	25	− 4	B 3 V n	+·007	−·015	7·55	+0·08	0·84	1	3·52	...	−3·20	...	0·96
130	189550	26	− 6	B 2 V	+·016	−·009	7·55	−0·04	0·60	2	4·54	18	−2·19	15	0·67
131	189921	19	−12	B 5 V	−·002	−·012	6·85	−0·04	0·36	3	7·15	36	−0·93	12	0·30
132	196025	20	−21	B 2 V	+·009	+·015	6·91	−0·09	0·45	4	5·16	12	−1·73	8	0·44
133	201254	32	−23	B 3 V	−·022	−·015	6·91	−0·02	0·54	2	5·86	8	−1·37	4	0·35
134	207563	44	−26	B 3 V	−·015	·000	6·21	−0·04	0·48	4	5·56	24	−1·53	14	0·28
135	209008	34	−37	B 3 V	+·006	−·002	6·04	−0·10	0·30	4	5·76	20	−1·42	11	0·27
136	215733	54	−37	B 0.5 III	−·016	−·027	7·25	−0·09	0·57	2	2·64	18	−4·26	27	1·54
137	219188	53	−51	B 2 n	−·021	−·014	6·98	0·00	0·84	2	2·84	6	−3·96	8	1·05

from Petrie, 1956b, p. 299; and 1958a). In obtaining mean magnitudes for each spectral sub-type of our southern stars, (Tables IV a and IV b), we have followed Petrie's procedure of excluding, more or less arbitrarily, certain thinly scattered high-luminosity stars, regarded as supergiants. Fig. 4 (*a*) shows the individual southern stars, while in Fig. 4 (*b*) these have been brought together into six groups, with the addition of the corresponding mean values for the northern stars. It is apparent that southern and northern stars show very much the same relation between mean absolute magnitude and spectral type. It should be noted that on the whole the northern stars are nearer the Sun than the southern stars, but that the distribution in absolute magnitude appears to be essentially the same for the greater volume and depth of space now sampled.

TABLE IV a

Sp.	*M*	*n*
O 6	−4·95	4
O 6·5	−5·5	1
O 7·5	−5·35	4
O 8	−4·35	2
O 8·5	−5·80	2
O 9	−4·91	8
O 9·5	−4·48	14
B 0	−4·17	11
B 0·5	−4·30	15
B 1	−3·16	20
B 1·5	−2·2	1
B 2	−1·89	25
B 3	−1·62	13
B 5	−1·10	2
B 7	−1·5	1

TABLE IV b

Mean type	Mean *M*	Spectral range	*n*
O 7·2	−5·15	O 6 − O 8·5	13
O 9·3	−4·64	O 9 + O 9·5	22
B 0·3	−4·25	B 0 + B 0·5	26
B 1·0	−3·02	B 1 + B 1·5	21
B 2·0	−1·89	B 2	25
B 3·5	−1·46	B 3 − B 7	16

7. *A uniform system of southern star magnitudes and colour indices.*

7.1. To obtain the distances of the stars with which we are dealing, we need to know both the apparent visual magnitude V and the interstellar absorption. The absorption has to be estimated from the colour excess, so that we need to know the star colours. Examination of the available data revealed a rather heterogeneous material of magnitudes and colours on different "systems". An attempt has been made to reduce all of these to a common system. The majority of the stars have Cape magnitudes, and reduction formulae to adjust Cape measures to the $(B-V)$-system have been given by Stoy, so that what may be called the "Cape $(B-V)$-system" has been used as a standard in the present paper. The colour

excess has been taken to be the difference between the $(B-V)$-value, found in this way, and the unreddened $(B-V)_0$ given by Johnson (1958) for spectral types O8 to B7 and three luminosity groups (Iab, II, and III-V). The interstellar absorption for the V-magnitudes has been assumed to be $3{\cdot}0 \times$ CE, i.e., three times the colour excess, following discussions by Johnson–Morgan (1953), Morgan–Harris–Johnson (1953) and Morgan (1958).

Entering the calibration-formula with the measured W, we obtain the absolute magnitude M'; the addition of the spectral-type correction $\Delta M'$ gave M in Column 14 of Table III, which together with Column 8 and Column 10 led to the distances r (in kiloparsecs) of Column 16:

$$r = 10^{-3}\,[\text{antilog } 0{\cdot}2\,(V - M' - \Delta M' + 5 - 3\text{CE})]. \tag{7}$$

(I) *Colour indices*

7.2. The available sources of colour indices for our stars are: Stebbins (1940); Oosterhoff (1951); Schilt (1952); Sharpless (1952); Morgan, Code and Whitford (1955); Johnson (1955); Hiltner (1956); Stoy (1958a, 1960a); Willstrop (1959).

7.2.1: *Stoy.*—The Cape colour-indices SCI may be converted to $(B-V)$ by a relation given by Stoy (1958a):

$$B - V = 0{\cdot}85\ \text{SCI} + 0{\cdot}26. \tag{8}$$

7.2.2: *Morgan–Code–Whitford.*—A list by Stoy (1958b) has 12 stars in common with Morgan–Code–Whitford (1955); Fig. 5 shows the MCW colour-index C_1 as a function of Stoy's $(B-V)$. The relation is very smooth and can be

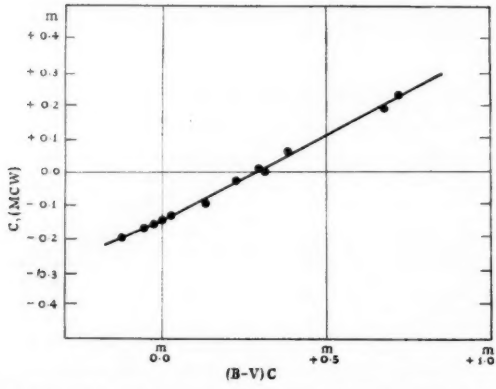

FIG. 5.—*Relation between Morgan–Code–Whitford's C_1 (MCW) and the Cape values (B–V)C.*

used to convert all the relevant MCW-colours to $(B-V)$. Furthermore, this curve agrees closely with a formula given by Morgan–Harris–Johnson (1953, equations (2) and (3)) for the relation between C_1 and $(B-V)$; they found:

$$C_1 = -0{\cdot}144 + 0{\cdot}483\,(B-V).$$

From this we may write

$$B - V = 2{\cdot}07\,C_1 + 0{\cdot}30. \tag{9}$$

The mean of the $(B-V)$-values resulting from Fig. 5 and from the above expression was used to convert C_1 to $(B-V)$. Data were obtained for 29 stars from this source.

7.2.3: *Stebbins.*—The Stebbins-values C_1 have been regarded as the same as the MCW-values C_1.

7.2.4: *Oosterhoff.*—Colour indices measured by Oosterhoff, which he calls C_1 and C_2, may be converted to $(B-V)$ to a first approximation by

$$(B-V)=\frac{1\cdot37}{2}\left[(0\cdot571+0\cdot565\,C_1)+(0\cdot367+0\cdot797\,C_2)\right]+0\cdot16 \qquad (10)$$

This formula results from a combination of the following set of relationships involved

$$C_S'=0\cdot571+0\cdot565\,C_1 \qquad (11)$$
$$C_S''=0\cdot367+0\cdot797\,C_2 \qquad (12)$$
} Oosterhoff, 1951

$$C^*=0\cdot5\,(C_S'+C_S'') \qquad (13)$$
$$ICI=1\cdot50\,C^* \qquad (14)$$ Stebbins, 1940

$$ICI=0\cdot93\,SCI+0\cdot11 \qquad (15)$$
$$B-V=0\cdot85\,SCI+0\cdot26 \qquad (16)$$
} Stoy, 1958a.

Small corrections to the above formula (10) for $(B-V)$ were evaluated by using 87 Oosterhoff-stars for a comparison with $(B-V)$-values deduced from the other sources mentioned. In this way adjusted colour-indices were, in addition, obtained for those 22 of the above Oosterhoff-stars for which there are no other observational values.

Stoy (1960b) has reduced Oosterhoff's indices C_1 and C_2 by the expressions

$$(B-V)_1=1\cdot042\,C_1+1\cdot313, \quad \text{and} \qquad (17)$$
$$(B-V)_2=1\cdot481\,C_2+0\cdot948, \qquad (18)$$

which are based on the comparison of Oosterhoff's colours with the colours for 18 similar reddened B-type stars. The mean of these $(B-V)_1$-and $(B-V)_2$-values makes those of Oosterhoff's stars whose colour-indices exceed $+0^m\cdot05$ by about $0^m\cdot04$ bluer than they are with our above reduction.

(II) *V-magnitudes.*

7.3. After a good deal of intercomparison among themselves and with Cape (based on 80 southern stars) it was decided that the expressions listed below (equations (19), (20), (21), (22)) give the best reduction to a self-consistent system (Cape- $B-V$) that can be obtained from data available at present. This step required certain additional empirical corrections to the various conversion-formulae; the latter can be deduced from the references given below (Sections 7.3.1-4).

7.3.1: *Stoy* (1958*a*):

$$V\,(\text{Cape})=\text{IPv}=\text{SPv}+0\cdot08\,\text{SCI}-0\cdot06. \qquad (19)$$

7.3.2: *Morgan–Code–Whitford* (1955, *p.* 42):

$$V\,(\text{Cape})=[\text{magnitude in MCW, } l.c., \text{ Table II}]-0\cdot12. \qquad (20)$$

7.3.3: *Stebbins* (1940, *p.* 24):

$$V\,(\text{Cape})=m\,(\text{Stebbins})+0\cdot05. \qquad (21)$$

7.3.4: *Oosterhoff* (1951, *p.* 320):

$$V\,(\text{Cape})=0\cdot951\,\text{m (Oosterhoff)}-0\cdot28\,C_2+0\cdot15. \qquad (22)$$

7·3·5: Magnitudes given by the other authors mentioned in Section 7·1 are on the $(B-V)$-system and need no correction. Where a star has been measured by more than one investigator, a straight mean has been taken of the available V-values, if necessary corrected as just described (Table III, Column 8). In the same way, straight means have also been used to combine (in Column 9) the adjusted colour-indices derived from different sources.

8. *Calibration tests with mean proper-motion parallaxes and galactic rotation.* We have seen that, where the measures overlap, the Pretoria and Victoria results agree quite closely. Petrie (1953, 1958b, 1960) has devoted much care to obtaining as reliable a calibration of the (Hγ, M)-relation as is possible with our present knowledge of the stars accessible to northern observers. It does not appear practicable yet to add much calibration evidence from the southern sky, but a number of checks have been made and the results are summarised here.

8.1. *Clusters.*—Stars Nos. 94, 95, 98, 100 and 106 are fairly certain members of the Scorpius-Centaurus cluster. Blaauw's (1946, see also 1958) cluster-parallaxes together with the V- and $(B-V)$-values, lead to a mean absolute magnitude

$$\overline{M}_C = -3^{m}\cdot 0. \quad \text{The mean from H}\gamma \text{ is } \overline{M}_C = -2^{m}\cdot 1.$$

8.2. *Individual parallaxes.*—Table III includes 14 stars for which there exist other parallaxes (trigonometric, dynamic, etc.). The mean of the differences of the corresponding Hγ-parallaxes minus the other values is $\overline{\Delta\pi} = -0''\cdot 001 \pm 0''\cdot 001$. The similar result for 53 northern stars was $+0''\cdot 002 \pm 0''\cdot 004$ (Petrie 1953, p. 265).

8.3. *Proper motions.*—We have followed the procedure that Petrie (1956b) used for the northern stars. Proper motions for the southern stars were taken from the *Cape Annals*, the *Yale Transactions* and the *General Catalogue*. Of 132 stars with known colour excesses, there were 99 stars for which μ_α and μ_δ were also available. Although not used here, new Cape proper-motion data for 11 more became available later (Stoy 1960a) and are included in Table III.

8.3.1: The v-components of the proper motions were obtained using the convenient diagrams devised by Pearce (1927), which assume the solar apex to be at $\alpha = 271^\circ$, $\delta = +28^\circ$ (1900). Then

$$\bar{\pi}_v = \frac{k \sum v \sin\lambda}{V_0 \sum \sin\lambda^2}, \tag{23}$$

where $k = 4\cdot 738$,
$V_0 = 20\cdot 0$ km/sec, (solar velocity), and
λ = distance from star to apex.

The stars are arbitrarily separated into three groups (although this makes each group undesirably small), viz.,

"dwarfs"	with	$M_{sp} > -2^{m}\cdot 0$
"intermediates"	with	$-2^{m}\cdot 0 \geqslant M_{sp} \geqslant -4^{m}\cdot 0$
"giants"	with	$M_{sp} < -4^{m}\cdot 0$

The frequency-distributions of our 19 dwarfs, 32 intermediates, and 48 giants are shown in Fig. 6 (*a*). The comparison with the northern stars in Fig. 6 (*b*) demonstrates the very different distribution of the northern material (Petrie 1956a, 1956b, 1958): the giants in the latter are concentrated at about 1000 parsecs, while for the southern stars the maximum lies at about 2700 parsecs.

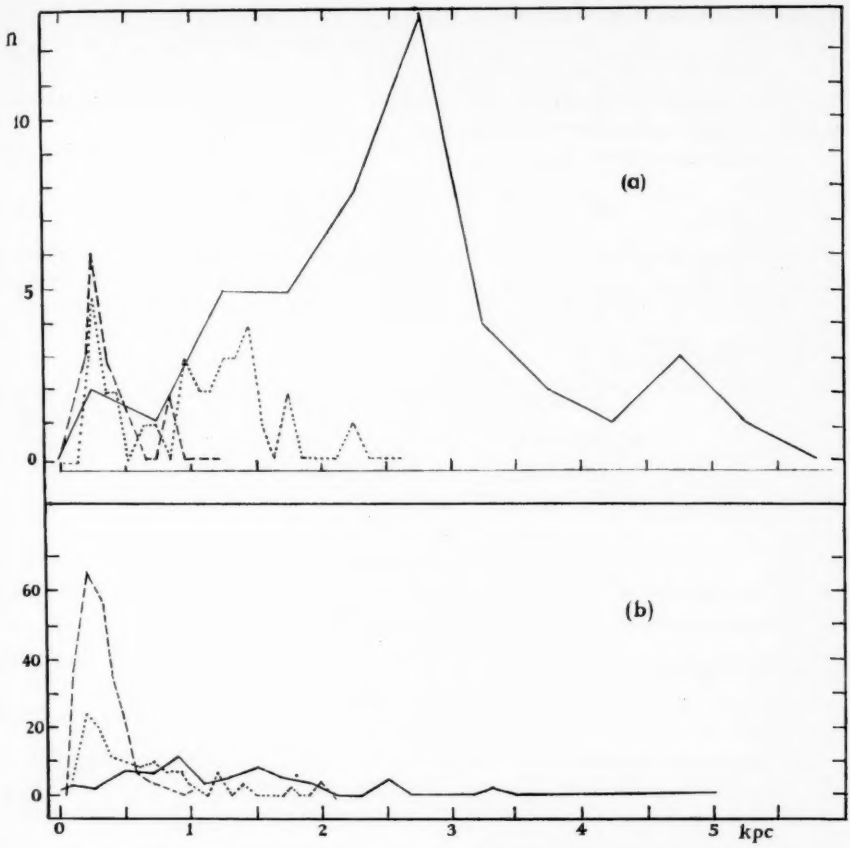

FIG. 6.—*Frequency-distribution of n B-star distances derived from Hγ-intensities: (a) southern, and (b) northern stars.*

– – – – – – – – – – –: *dwarfs*
. . . . . : *intermediates*
————— : *giants.*

8.3.2: We need to estimate the standard errors of both the means of the Hγ parallax $\bar{\pi}_{sp}$, and of the mean proper motion parallax $\bar{\pi}_{v}$.

Since

$$M = m + 5 + 5 \log_{10} \pi,$$

we have

$$\Delta M = 5 \log_{10} e \, (\Delta\pi/\pi) = 2{\cdot}17 \, (\Delta\pi)/\pi. \qquad (24)$$

Petrie (1953, p. 265), on the basis of internal agreement of his measures, gives "as a generous estimate of the probable error of a single spectroscopic absolute magnitude" $\pm 0^{m}{\cdot}33$; or, say, $\pm 0^{m}{\cdot}5$ as the standard error. The corresponding parallax-error would be, therefore,

$$\Delta\pi_{sp} = \pm \frac{0{\cdot}5}{2{\cdot}2} \pi_{sp} = \pm 0{\cdot}2 \, \pi_{sp},$$

or, of the mean parallax of n stars:

$$\Delta\bar{\pi}_{sp} = \pm \frac{0{\cdot}2\,\bar{\pi}_{sp}}{\sqrt{n}}. \tag{25}$$

This takes no account of errors in the correction for interstellar absorption, so that the total $\Delta\bar{\pi}_{sp}$ are probably somewhat greater than estimated here.

For the error of the mean proper-motion parallax we accept the validity of

$$\Delta\bar{\pi}_{v} = \pm \frac{\bar{\pi}_{v}}{\sqrt{n}} \sqrt{\left(\frac{\Delta\mu}{v}\right)^2 + \left(\frac{R}{V_0 \sin\lambda}\right)^2}, \tag{26}$$

where R is the mean linear random motion in one coordinate, taken to be 5 km/sec. The mean $1/\sin\lambda$ is assumed to be 1·75, and for "intermediate" stars the mean $\Delta\mu/v$ is 1·2, as found from the General Catalogue. The mean value of the quantity under the root is then 1·3.

8.3.3: We thus obtain:

$$\Delta\bar{\pi}_{v}\,(\text{intermediates}) = \pm 2{\cdot}0\,\bar{\pi}_{v}/\sqrt{n}, \tag{27}$$

$$\Delta\bar{\pi}_{v}\,(\text{dwarfs}) = \pm 1{\cdot}0\,\bar{\pi}_{v}/\sqrt{n}, \tag{28}$$

$$\Delta\bar{\pi}_{v}\,(\text{giants}) = \pm 3{\cdot}8\,\bar{\pi}_{v}/\sqrt{n}. \tag{29}$$

We then find for 19 "dwarfs":

$$\bar{\pi}_{v} = 0''{\cdot}0033 \pm 0''{\cdot}0009$$
$$\bar{\pi}_{sp} = 0''{\cdot}0039 \pm 0''{\cdot}0002,$$

for 32 "intermediates":

$$\bar{\pi}_{v} = 0''{\cdot}0005 \pm 0''{\cdot}0002$$
$$\bar{\pi}_{sp} = 0''{\cdot}0015 \pm 0''{\cdot}0001,$$

and for 48 "giants":

$$\bar{\pi}_{v} = 0''{\cdot}0008 \pm 0''{\cdot}0004$$
$$\bar{\pi}_{sp} = 0''{\cdot}0005 \pm 0''{\cdot}0000.$$

8.4. *Galactic rotation.*—The spectroscopic distances based on Hγ-intensities may also be compared with distances deduced from the galactic-rotation effect, again following the procedure used by Petrie for northern stars. Petrie calculated a mean distance $\bar{r}_g$ from the formula

$$\bar{r}_g = \frac{1}{A} \frac{\sum \rho \sin 2L \cos^2 b}{\sum \sin^2 2L \cos^4 b},$$

where ρ is the observed radial velocity of each star after correction for the solar motion and the K-term; A is Oort's constant, taken to be 17·5 km/sec/kpc, in accordance with a recent discussion of the B-star material by Feast and Thackeray (1958; see also Petrie 1956b); L is the galactic longitude of the stars measured from the longitude of the centre of the Galaxy; b is the galactic latitude; the distance r is expressed in kiloparsecs.

8.4.1.—The standard error of the spectroscopic distance, by analogy with equation (25), may be taken to be

$$\Delta\bar{r}_{sp} = \pm \frac{0{\cdot}2\,\bar{r}_{sp}}{\sqrt{n}}. \tag{30}$$

The standard error of the mean galactic-rotation distance may then be estimated as

$$\Delta\bar{r}_g \pm = \frac{690}{\sqrt{n}}\,(\text{parsecs}), \tag{31}$$

which follows from the assumption that the random velocity of the average star

plus its observational error add up to a radial velocity $\Delta V = 6$ km/sec; furthermore that ρ has on the average half of that galactic-rotation amplitude which would correspond to the distance r, that is, $\rho = 0{\cdot}00875\, r$ parsecs. We can then calculate the above expression (31) from

$$\Delta \bar{r}_g = \pm \frac{r \,.\, \Delta V}{\rho} \Big/ \sqrt{n}. \qquad (32)$$

8.4.2.—There is, however, a difficulty. The southern stars are on the whole more distant than the northern; thus, the approximate galactic-rotation formula, which assumes that r is small relative to the Sun's distance from the galactic centre, breaks down for roughly half of them. This is unfortunate, for it is precisely with the "giants" which constitute the more distant half of our material that we most need to test the Hγ-results.

Confining ourselves to the approximate formula, we consider only stars not more than 1250 parsecs from us. We divide these into two groups, according to their Hγ-distances:

(A) ... $250 < r_{sp} \leqslant 750$ parsecs (25 stars):
$\bar{r}_g = 459 \pm 144$ pc
$\bar{r}_{sp} = 386 \pm 16$ pc

(B) ... $750 < r_{sp} < 1250$ parsecs (25 stars):
$\bar{r}_g = 1561 \pm 144$
$\bar{r}_{sp} = 1045 \pm 45$.

Both tests, that with proper-motions (Section 8.3.3) and that with galactic-rotation distances, refer to too few stars for the results to have a decisive weight. There is a tendency for the mean Hγ-parallaxes to be larger (or the mean Hγ-distances smaller) than those given by proper motions or galactic rotation. The difference is not significant for the nearer stars, mainly those we have called "dwarfs". It may be just significant for the "intermediates", while about the "giants" we can say nothing.

8.4.3.—If we now attempt to use instead of the velocity-displacement of the usual stellar lines, that of the interstellar K-line, and then deduce "calcium distances" by means of the galactic-rotation formula, we find

	Group A (13 stars)	Group B (22 stars)
calcium	$\bar{r}_g = 525 \pm 190$ pc	1163 ± 148 pc
stars	$\bar{r}_{sp} = 425 \pm 27$ pc	1044 ± 45 pc

We note that the r-values agree reasonably well within each of these groups. This finding, however, is completely in conflict with the expectation that "effectively" the calcium should be only at half the distance of the star in whose spectrum it is observed. As far as the northern stars are concerned, Petrie's (1956b, p. 295) data seemed to confirm this expectation. Although the number of southern stars available for this test is certainly small, this of itself seems an inadequate explanation. The above figures clearly indicate that here, in *our* southern material, the calcium appears to be located at about the *same* distance as the stars. Here we note that the considerable number of stars involved in an Oort-type analysis by Feast and Thackeray (1958, p. 133) did not exhibit such a discrepancy.

There are two remarks which may be made. First, high-resolution measures of the interstellar calcium lines by Adams and others showed that these lines are

almost always multiple, the calcium being concentrated into discrete clouds along the line of sight. Second, while customarily we think of these clouds as being fairly uniformly distributed near the plane of the Milky Way, so that the line of sight intersects a number of clouds of the order of ten per kiloparsec, it seems highly likely that there is some systematic distribution of cloud-frequency related to the spiral arms of the Milky Way. The view is held by some that the Sun is near the inner boundary of a spiral arm. In that case the first kiloparsec or so along the line of sight in the Milky Way north of the equator will be more or less within a spiral arm, while in the southern Milky Way it will mostly run through an inter-arm region. If calcium clouds are a part of the arm population, but are comparatively rarely found between the arms, the results just quoted become a little less puzzling. But in any case, although selection effects cannot be ruled out, we feel inclined to reject the calcium-method as a safe guide to the distances of the southern B-stars.

8.4.4: There is one further point about the B-star distances that must not be forgotten, and that is the uncertainty of the correction for interstellar absorption: there are the ordinary errors in $(B-V)$ and, in addition, the errors in the assumption that the absorption corrections for V-magnitudes is 3·0-times the colour excess in $(B-V)$. In conclusion, we note that the average correction 3CE in Table III is $0^{m}\cdot71$ for "dwarfs", $1^{m}\cdot01$ for "intermediates", and $1^{m}\cdot40$ for "giants".

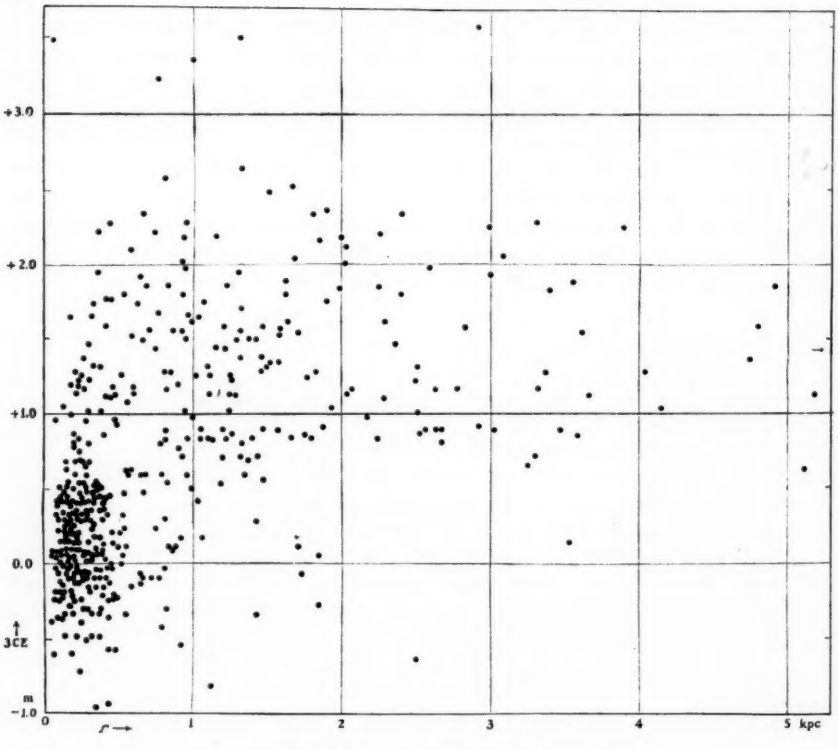

FIG. 7.—*The colour-excess array (both hemispheres).*

9. *Relation of results to the structure of the Milky Way.*

9.1.—It is of considerable interest to try to fit the results of the preceding sections into our present picture of the galactic structure in regions within a few kiloparsecs of the Sun. For this part of the discussion we have also included material from the northern hemisphere, namely 405 O- and B-stars for which Petrie (1953, 1956a, 1956b, 1958) has obtained Hγ-luminosities. To derive distances for these, all published magnitudes and colour indices were re-reduced to the $(B-V)$-system as uniformly as possible, whereby the derivation of the corrections followed a procedure similar to that used for the south. In particular, comparisons of Stebbins- and MCW-data with Hiltner's (1956) list of $(B-V)$-measurements could be based on 48 stars for V-magnitudes, and on 51 stars for $(B-V)$-colours. The details will be omitted here.

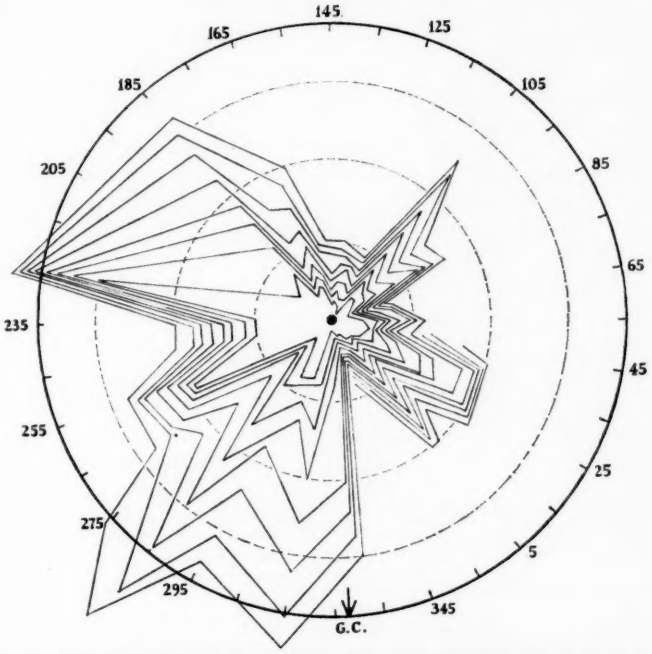

FIG. 8.—*Colour-excess diagram of all B-stars with measured Hγ-luminosities in both hemispheres, out to nearly 4 kiloparsecs. The diagram represents the distance at which the star is affected by a certain absorption, so that where points are far from the centre, the general absorption is small, and vice versa. The three broken circles correspond to distances from the Sun of 1, 2 and 3 kiloparsecs, respectively. The outermost closed " curve " represents the relation between colour-excess and distance for* $CE = 0^{m}.8$. *In addition short extreme " arcs " for* $0^{m}.9$, $1^{m}.0$ *and* $1^{m}.1$ *are indicated in the 60° galactic longitude sector between 345° and 45°. All the iso-absorption lines are drawn at CE-intervals of* $0^{m}.1$.

9.2.—If colour excesses, for both northern and southern stars, are plotted against distance (Fig. 7), a steep increase of reddening appears up to a distance of about 1 kiloparsec, but comparatively little more thereafter. The chief cause of this is probably observational selection. For example, Bo stars beyond 1 kpc will mostly appear fainter than 9^{m} and may have the apparent colour of a G- or K-type star so that many, or possibly most, of those within 3 kpc have not yet

appeared in radial-velocity or photometric programmes. There certainly has been selection in favour of apparently blue stars lying in relatively transparent regions, and against those subject to unusually heavy reddening and general absorption. To some extent even stars within 1 kpc must have been affected by this selection.

9.3.—Taking our results at their face value, we have plotted a series of contours of equal colour-excesses (in steps of $0^{m}\cdot1$) in the plane of the Milky Way (Fig. 8). The interstellar absorption affecting our OB-stars appears to be greater in the region $330° < l^{I} < 165°$, which lies mostly in the northern sky, than in the remainder of the Milky Way, $165° < l^{I} < 330°$, lying mostly south of the equator. Not too much weight should be attached to this until the question of differences in observational selection between north and south has been examined more thoroughly. Here we should also note that, for instance, our data do not even cover all the already known O-B3 stars brighter than $7^{m}\cdot5$ in the southern sky.

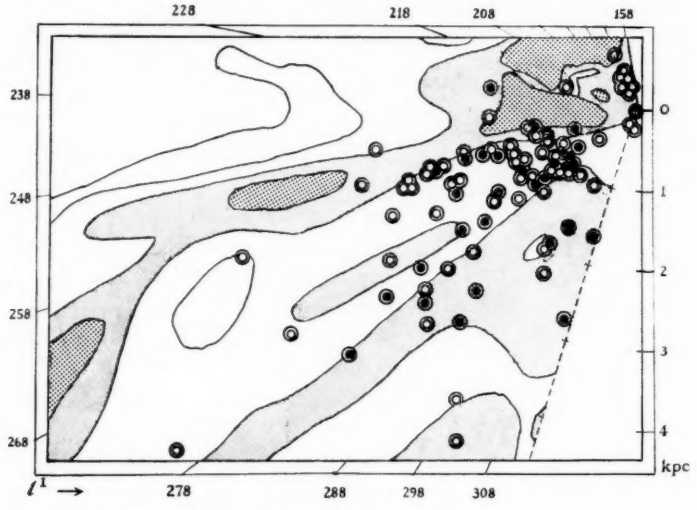

FIG. 9.—*The B-stars in the sector* $l^{I} = 275° \pm$:
◎ = *stars with* $3CE < 1^{m}\cdot5$.
⊙ = *stars with* $3CE \geqslant 1^{m}\cdot5$.
Lightly dotted shading = *HI areas with densities* $d = 0\cdot6$ *atoms/cc.*
Heavily dotted shading = *HI areas with densities* $d = 1$ *atom/cc.*

The large unshaded areas have a density of only 0·2 atoms/cc,—except for an extended region enclosed by the curve on the top left, the smaller elliptical area underneath, and the three very small enclosed regions; for all these five last-mentioned areas the density is only 0·05 atoms/cc.

9.4.—In Figs. 9, 10 and 11 we have plotted, with the Sun as centre, B-star distances as derived from Hγ measurements. Fig. 9 represents the B-stars in the particularly interesting sector around $l^{I} = 275°$ (see Section 9·7); Fig. 10 reaches to $r = 1\cdot5$ kiloparsecs, while Fig. 11 combines all the 465 measured B-stars with known 3CE up to 7 kiloparsecs. A number of characteristic constituents of the Milky Way are added, as described further below in Section 9.5 and in the captions to the figures. It should be noted that of the 333 northern stars with known 3CE only 17 have $r \geqslant 1\cdot5$ kpc. Furthermore, of the 316 northern stars within 1·5 kpc there are 22 stars with $1\cdot5 \leqslant 3CE < 2\cdot0$ and 12 stars with $3CE \geqslant 2\cdot0$. This

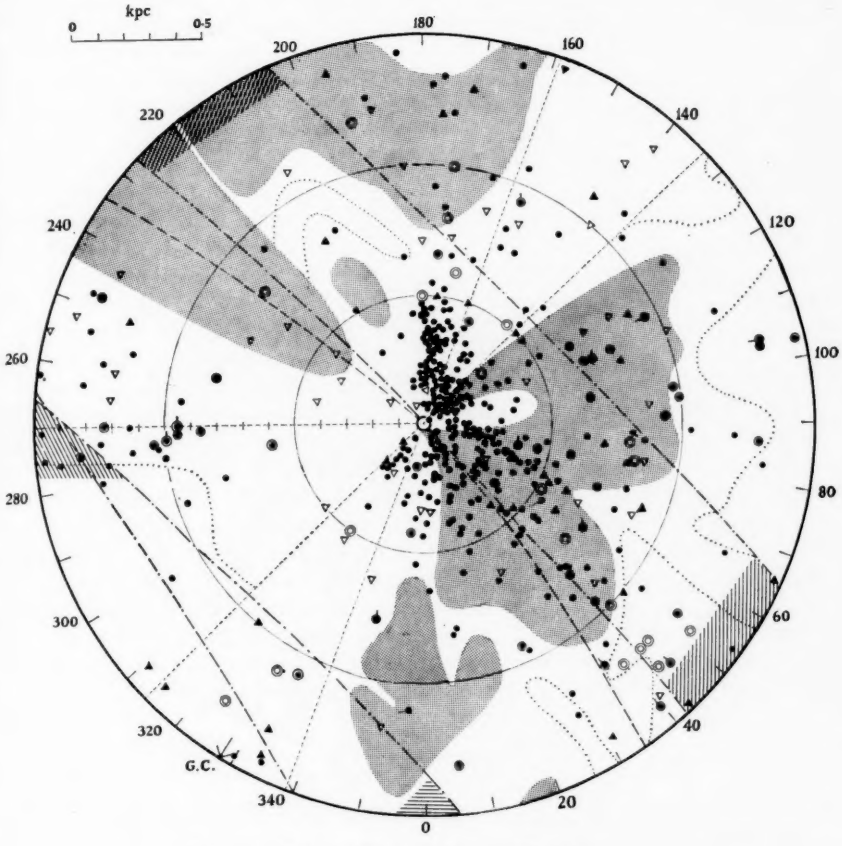

FIG. 10.—*Galactic objects within 1·5 kiloparsecs.*
(B-stars, H I-areas, H II-regions, clusters, associations, spiral-arm patterns.)

● = *B-stars, both hemispheres, with* $3CE < 1{\cdot}5$.
⊙ = *B-stars, both hemispheres, with* $1{\cdot}5 \leqslant 3CE < 2{\cdot}0$.
⊙ = *B-stars, both hemispheres, with* $3CE \geqslant 2{\cdot}0$.
△ = *clusters.*
▲ = *associations.*
Shaded portions = *H I-areas with densities* $d \geqslant 1$ *atom/cc. (The adjacent dotted lines enclose areas of density 0·6 and less.)*
◎ = *H II-regions.*
·–·–·–·–·–·–· = *Becker's spiral-arms.*
Diagonal hatching = *Elsässer-Haug's spiral-arms.*
– – – – – – – – – – – = *Mills' spiral.*

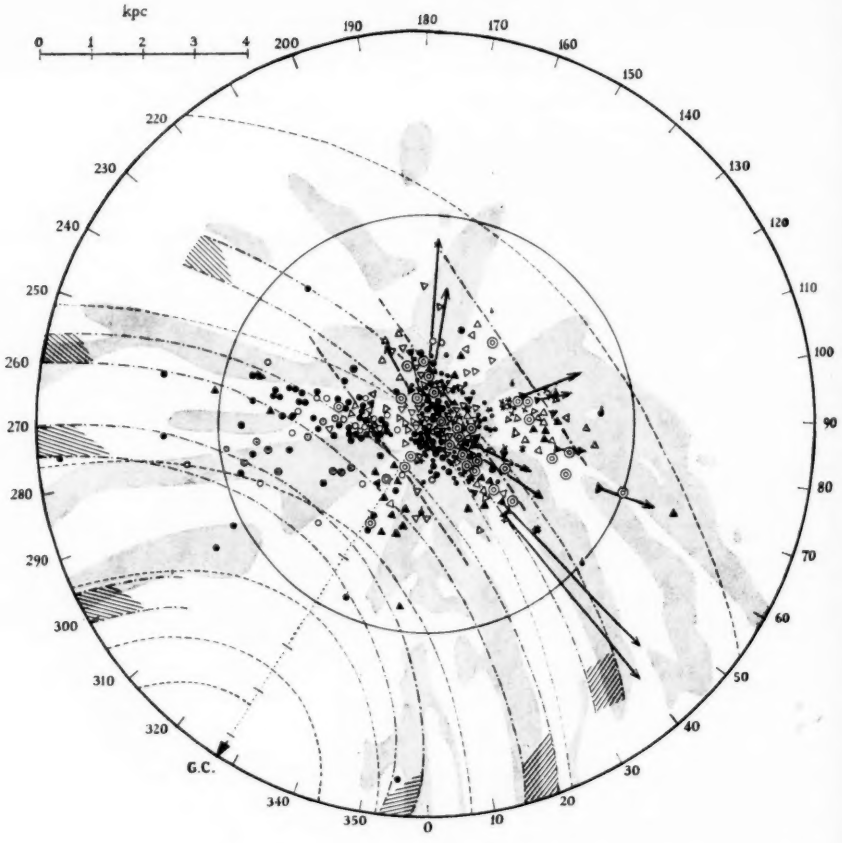

FIG. 11.—*Galactic objects out to 7 kiloparsecs from the Sun;* (465 *B-stars*, 82 *clusters*, 55 *OB-associations*, 36 *H* II*-regions*):

● = *southern B-stars with* $3\,CE < 1{\cdot}5$.
○ = *southern B-stars with* $1{\cdot}5 \leqslant 3CE < 2{\cdot}0$.
⊙ = *southern B-stars with* $3CE \geqslant 2{\cdot}0$.
● = *northern B-stars with* $r < 1{\cdot}5$ *kiloparsecs and with* $3CE < 2{\cdot}0$.
✳ = *northern B-stars with* $r < 1{\cdot}5$ *kiloparsecs and with* $3CE \geqslant 2{\cdot}0$.
🌡 = *northern B-stars with* $r \geqslant 1{\cdot}5$ *kiloparsecs and with* $3CE < 1{\cdot}5$.
× = *northern B-stars with* $r \geqslant 1{\cdot}5$ *kiloparsecs and with* $1{\cdot}5 \leqslant 3CE < 2{\cdot}0$.
✳ = *northern B-stars with* $r \geqslant 1{\cdot}5$ *kiloparsecs and with* $3CE \geqslant 2{\cdot}0$.
Shaded portions = *H* I*-arms* (*density* $d \geqslant 0{\cdot}6$ *atoms/cc*).
△ = *clusters*.
▲ = *associations* (▶ = *Dieter-distances*).
◎ = *H* II*-regions*.
· – – · – – · – – · – – = *Becker-arms*.
Diagonal hatching = *Elsässer-Haug-arms*.
– – – – – – – – – – = *Mills' spiral*.

Note—The star No. 40 ($l = 257$, $r = 5{\cdot}78$) should be added to Fig. 11 above.

distance-range (i.e., Fig. 10) contains, in addition, 44 clusters, 33 OB-associations, and 21 H II regions from our lists (Section 9.5).

When we come to trying to locate our B-stars in supposed spiral arms, we find ourselves faced by a complicated problem and insufficiently supplied with reliable information about the spiral arms, both with respect to the radio- as well as to the optical evidence.

In the first place we have the well-known maps of the neutral hydrogen distribution in the galactic plane, based on 21 cm measures. There is a certain amount of ambiguity in the final interpretation of the observations, and in that part of the sky in which we are chiefly interested here, south of the equator, Australian workers are just revising and improving their results, introducing a different galactic model which involves a specified expansion-motion of the hydrogen gas (Kerr 1961). I am very grateful to Dr F. J. Kerr for this information and for his permission to use some details of his new contour-map in the present discussion of our new B-stars positions, the result of which he considers as "a first clue" in view of the fact that there has been little success in previous attempts to relate optical- and radio-spiral-features.

On the one hand, it is certainly questionable whether spatial structure marked by a concentration of neutral hydrogen is to be identified with spiral arms consisting of a concentration of O- and B-stars, gaseous nebulae, H II regions, etc.

On the other hand, a considerable body of experimental, i.e. observational, evidence has accumulated concerning a possible spatial connection between the H I "arms", the galactic-cluster arms according to W. Becker, the Elsässer-Haug spiral-structure, the Mills-spiral, and the distribution of the southern and northern B-stars, open cluster, OB-associations and H II regions. It is profitable at this stage to attempt a survey of the available evidence.

9.5.—Fig. 11 brings together in one diagram all the above-mentioned objects. Taking this diagram at its face value, it becomes, in particular, at once evident that the stellar objects and the H II regions appear to be situated *between* the H I-arms.

Fig. 11 assembles:

(*a*) Southern B stars (this paper, Table III).

(*b*) Northern B stars, deduced from Hγ-measurements given by Petrie (1953, 1956a, 1956b, 1958).

(*c*) Combined and revised H I-contours from both hemispheres, according to the 21 cm work of the Leiden and Sydney observers; contours restricted to regions denser than, or equal to, 0·6 atoms/cc; after Kerr, 1961; see also Oort-Kerr-Westerhout, 1957, 1958a, b; van de Hulst, 1958; Bok, 1959; Struve, 1959).

(*d*) H II-regions (36); after Morgan-Sharpless-Osterbrock (1952); see Becker (1961); also Bok (1959).

(*e*) galactic clusters (82); after W. Becker (1961; see also 1956); three spiral arms, 1·5 kiloparsecs apart, are suggested by these clusters over an arm-length of 4-5 kpc each (centre arm: Orion; south: Carina, Scutum; north: Perseus); thickness of Orion arm about 1·5 kpc near Sun.

(*f*) spiral arms indicated by Elsässer-Haug's (1960) surface-photometry of the Milky Way; thickness of each arm about 0·6 kpc.

(*g*) spiral arms proposed by Mills (1959) from his observations of the radio-continuum radiation; this structure was suggested as mainly to represent the distribution of ionized hydrogen.

(*h*) OB-associations, after Blaauw, Code, Johnson, Greenchik, Gulledge, Hardie, Hiltner, Morgan, Schulte, Seyfert, Whitford. For references see Becker (1961) and Dieter (1960); these two sources, together with additional data compiled by van de Hulst (1958) and Bok (1959), supplied 55 associations.

(*i*) OB-association-distances discussed by Dieter (1960); positions found photometrically and those derived from galactic-rotation are joined in Fig. 11 by straight lines with arrowheads.

9.6.—Examining the constituents of this diagram in turn, we note that the groups (*a*) and (*b*) clearly fall outside (*c*) and (*g*), but appear well-connected with the groups (*d*), (*e*), (*f*), (*h*), (*i*).

9.7.—A conspicuous branch of B-stars, especially reddened ones, stretches in the galactic direction $l^{\mathrm{I}} = 275^{\circ} \pm$, which lies well *between* two prominent H I arms (Fig. 9). These stars appear to be of particular significance:

If we examine the longitude-colour distribution of all the 132 stars with known colours, and denote with *r* the reddened stars with $1{\cdot}5 \leqslant 3\mathrm{CE} < 2{\cdot}0$, and with *vr* the very reddened stars with $3\mathrm{CE} \geqslant 2{\cdot}0$, we obtain the following distribution, referred to five different ranges in galactic longitude, the last line giving the percentage of the $(r + vr)$-stars in the sector:

0°–60°	130–190	220–270	270–280	280–360
17 stars	15	38	30	32
1*r*	2*r*	6*r* + 3*vr*	9*r* + 6*vr*	4*r* + 5*vr*
6	13	24	50	28 per cent

(None of the stars in our Table III falls into the longitude-ranges 60°–130° and 190°–220°).

The conspicuous concentration of the *r*- and *vr*-stars between 270° and 280° becomes even more emphasized if we widen this range somewhat to cover the sector 265°-287°, centred around 275°. Here we have now 34 stars, of which no less than 10 are *r*-, and 9 *vr*-stars, i.e., together 56 per cent of all the stars in this sector.

We compare this with the material in all the other sectors: there remain 98 stars, comprising only 12 *r* as well as 5 *vr*-stars, i.e., together only 17 per cent of the total. Therefore, we can state that a sector of less than twenty degrees around $l^{\mathrm{I}} = 275^{\circ}$—which lies essentially between the "hydrogen arms"—contains (considered in percentages) no less than $4\frac{1}{2}$ times more "very reddened" stars, and $2\frac{1}{2}$ times more of the ordinary "reddened" stars, than there are in the whole of all the other sections of our southern material.

We may also note other important regions *outside* the H I-areas, situated in northern sectors, particularly those centred about $l^{\mathrm{I}} = 40^{\circ} \pm$ and $l^{\mathrm{I}} = 90^{\circ} \pm$.

The $275^{\circ} \pm$-region is shown in detail in Fig. 9, where the newly-determined B-star positions are compared with neutral hydrogen contours. Most of the stars are seen to appear in a region well outside the Sagittarius arm. Kerr's successful recent Milky Way model, involving, as it does, a combination of two motions,—an outward-flow of the gas from, and its rotation about, the galactic centre—is clearly in general qualitative agreement with the distribution of stars shown in this diagram. Kerr has characterized the conclusions from Fig. 9 by suggesting that if the material of the arms is moving outwards from the central regions of the Milky

Way, the outer part of each arm should contain the oldest gas, and one may therefore conclude that this part of the gas may have been largely condensed by now, i.e., used up to produce stars in the outer part of the arm,—indeed just as indicated by the data shown in Fig. 9. Moreover, it is apparent that any given general H I pattern should, under the influence of these combined motions, have a relatively short life-time, and stars and hydrogen should dissociate from each other at early evolutionary stages.

9.8.—In connection with group (*d*) the extensive recent Mount Stromlo work on the southern H II regions (Rodgers, Campbell and Whiteoak, 1960) is of special importance. Dr Rodgers kindly showed to the author a relevant sheet of the Canberra Hα-atlas now in preparation: it demonstrated that our "reddened sector" around 275° is particularly rich in markedly small H II-regions; more of these appear here per unit area than anywhere else. This points to the radiation of numerous OB-stars and, because of the pronounced reddening-effects observed in this sector, to the presence of strong absorption by dense interstellar dust.

9.9.—As to (*f*), this recent optical work by Elsässer and Haug (1960) is based on a two-colour photoelectric photometry of the Milky Way. From these measurements the authors have deduced outlines of three spiral arms which show little detailed agreement with the H I arms given by the 21 cm work. Plotting histograms of frequencies for our B-star material, however, we find that these stars show some tendency to lie within the Elsässer-Haug arms. We realize, of course, that these spiral arms should at present merely be considered as a schematized picture.

9.10.—Of particular significance for our problem is W. Becker's (1961) extensive analysis of 82 open clusters. Here, it is pointed out that there is no coincidence between the positions of these clusters and the radio-astronomically determined H I regions but, on the contrary, a fundamental difference in their distributions. Becker's method of the photometric determination of cluster-distances is estimated to be correct within 10 per cent of the distance, and there seems no possibility of reconciling the cluster positions and the 21 cm results. As Becker puts it: "the question arises whether a plausible change in the law (of galactic rotation) might lead to a coincidence of the distributions".

9.11.—A similar result can be derived from a recent analysis of the OB-associations: in comparing distances of associations obtained, first by photometry, and secondly from galactic-rotation theory using the observed radial velocities, Dieter (1960) found in most cases appreciable discrepancies. The conclusion was drawn that the "application of such a simple (circular-motion) model to the determination of the distances of neutral hydrogen clouds without independent distance-measurements may lead to serious errors".

It would appear, therefore, that H I-positions in our Fig. 11 may need to be modified. We recognize a suggestion of such a correction indicated in Dieter's Fig. 3 (1960, p. 55), the relevant feature of which is added to our Fig. 11; here, the heads of the arrows denote the galactic-rotation positions, and their tails the corresponding photometric positions. If we assume the photometric distances to be correct, we may apply these vectors (reversed) as tentative corrections to the H I positions: if we do so, the latter ones come to a large extent in coincidence with the plot of stellar objects. Manifestly, much future work is needed.

Finally, it is interesting to note that Dieter found evidence for a coincidence with strong H I-concentrations, situated within the accepted 21 cm arms, for 31 out of the 40 investigated OB-associations.

9.12.—The whole subject of galactic rotation, hydrogen distribution, luminosities and distances appears today more fluid than ever. As a postscript we may mention here another recent paper: Thiessen (1961), investigating the origin of the polarization of star-light, comes to the conclusion that stellar radiation appears to be composed of unpolarized thermal radiation and polarized synchrotron radiation, and that the observed phenomenon is a stellar rather than an interstellar one. As a consequence, Thiessen points to possible implications of the proposed new mechanism, which may require that, e.g., absolute magnitudes, intrinsic colours, colour-magnitude diagrams, etc., may "partially have to be corrected". We also mention important discussions by Johnson and Iriarte (1958).

10. *Possibilities of photoelectric work.*—Recent investigations carried out at the *f*/18 coudé focus of the 36-inch reflector at the Cambridge Observatories, in which the integrated intensities of selected features of stellar spectra are measured directly, have clearly shown great potentialities. Following the construction of a new spectrometer, R. F. Griffin (1960) made a few exploratory measures during one night in June 1960 of Hγ in B-type stars, which showed that it would be possible, with the present instrumental arrangement, to carry out a programme down to $7^{m}.5$.

Subsequently some 1200 observations were made by the writer on 18 nights during 1960 October and November, giving Hγ-intensities for 187 B-stars. The measurements were made with two photomultipliers, one receiving light from the spectrum range $\lambda\lambda$ 4325-4357 A, the other from two comparison regions, $\lambda\lambda$ 4255-4289 A and 4393-4427 A. The general procedure was that followed in earlier work by Griffin and Redman (1960), Deeming (1960), and Griffin (1960). The "Hγ-ratios" obtained may be calibrated directly with the aid of Petrie's original standard stars (1953, p. 259). Details of this work will be reported in a later paper.

In conclusion, I would like to say again how much I appreciate all the kind help I received,—in the way of observational material, valuable advice, and stimulating discussions,—in particular from Professor R. O. Redman and Dr A. D. Thackeray, and from Dr R. M. Petrie, Dr R. H. Stoy and Dr K. O. Wright.

The Observatories,
Madingley Road,
Cambridge:
1961 *May.*

References

Beals, C. S., 1944. *J. Roy. Astron. Soc. Canada*, **38**, 65, 1944.
Becker, W., 1956, "Vistas in Astronomy", ed. A. Beer (Pergamon Press, London), **2**, 1515.
Becker, W., 1961, *Zeits. f. Astrophys.*, **51**, 151.
Blaauw, A., 1946, *Publ. Astron. Lab. Groningen*, No. 52.
Blaauw, A., 1958, *Astron. J.*, **63**, 186.
Blaauw, A., Gum, C. S., Pawsey, J. L., and Westerhout, G., 1960, *M.N.*, **121**, 123.
Bok, B. J., 1959, *Observatory*, **79**, 61.
Butler, H. E., and Seddon, H.; 1958, *Publ. Roy. Obs. Edinburgh*, vol. 2, 113. (See also papers by E. A. Baker, W. M. H. Greaves, R. Wilson in the same series, Vol. 1, pp. 15 and 115, and Vol. 2, pp. 1 and 61; 1949–1958).
Deeming, T. J., 1960, *M.N.*, **121**, 51.
Dieter, N. H., 1960, *Ap. J.*, **132**, 49.

Elsässer, H., and Haug, U., 1960, *Zeits. f. Astrophys.*, **50,** 121.
Feast, M. W., Thackeray, A. D., Wesselink, A. J., 1955, *Mem. R.A.S.*, **67,** Pt. II.
Feast, M. W., Thackeray, A. D., Wesselink, A. J., 1957, *Mem. R.A.S.*, **68,** Pt. I.
Feast, M. W., and Thackeray, A. D., 1958, *M.N.*, **118,** 125.
Griffin, R. F. Thesis, Univ. of Cambridge, 1960.
Griffin, R. F., and Redman, R. O., 1960, *M.N.*, **120,** 287.
Hiltner, W., 1956, *Ap. J. Suppl.*, **2,** 389.
Johnson, H. L., and Morgan, W. W., 1953, *Ap. J.*, **117,** 313.
Johnson, H. L., 1955, *Ann. Astrophys.*, **18,** 292.
Johnson, H. L., 1958, *Lowell Obs. Bull.* Vol. 4, No. 90, p. 45, Table III.
Johnson, H. L., and Iriarte, B., 1958, *Lowell Obs. Bull.*, Vol. 4, No. 91, p. 47.
Kerr, F. J., 1961, *M.N.*, **123** (in the press).
Kopylov, I. M., 1958a, *Crimea Obs. Publ.*, **20,** 127.
Kopylov, I. M., 1958b, *Crimea Obs. Publ.*, **20,** 156 and 195.
Mills, B. Y., 1959, *P.A.S.P.*, **71,** 267.
Morgan, W. W., Sharpless, S., Osterbrock, D., 1952, *Sky and Telescope*, **11,** 138.
Morgan, W. W., Harris, D. L., Johnson, H. L., 1953, *Ap. J.*, **118,** 92.
Morgan, W. W., Code, A. D., and Whitford, A. E., 1955, *Ap. J. Suppl.*, **2,** 71 (Table II on p. 72; see also p. 42).
Morgan, W. W., 1958, I.A.U. Symposium No. 5, p. 60.
Ohlsson, J., 1932, *Lund. Medd.* No. 3.
Oort, J. H., Kerr, F. J., and Westerhout, G., 1958a, *Bull. Astron. Inst. Netherlands*, **113,** No. 475, p. 246.
Oort, J. H., Kerr, F. J., and Westerhout, G., 1958b, *M.N.*, **118,** 382.
Oosterhoff, P. Th., 1951, *Bull. Astron. Inst. Netherlands*, **11,** No. 425, p. 299.
Pearce, J. A., 1927, *Publ. Domin. Astrophys. Obs. Victoria*, Vol. 4, No. 4.
Petrie, R. M., 1953, *Publ. Domin. Astrophys. Obs. Victoria*, Vol. 9, No. 8.
Petrie, R. M., 1956a, " Vistas in Astronomy ", ed. A. Beer, (Pergamon Press, London), **2,** 1346.
Petrie, R. M., and Moyls, B. N., 1956b, *Publ. Domin. Astrophys. Obs. Victoria*, Vol. 10, No. 13.
Petrie, R. M., Cuttle, P. M., Andrews, D. H., 1956c, *Astron. J.*, **61,** 289.
Petrie, R. M., 1958 a, *M.N.*, **118,** 82.
Petrie, R. M., 1958 b, *Astron. J.*, **63,** 181.
Petrie, R. M., 1958 c, *Astron. J.*, **63,** 189.
Petrie, R. M., 1960, *P.A.S.P.*, **72,** 462.
Rodgers, A. W., Campbell, C. T., Whiteoak, J. B., 1960, *M.N.*, **121,** 103.
Schilt, J., 1952, Contrib. Rutherford Obs., Nos. 31–32.
Sharpless, S., 1952, *Ap. J.*, **116,** 251.
Sinnerstad, U., 1961, *Stockholms Obs., Annaler*, **21** No. 6, and **22** No. 2.
Stebbins, J., 1940, *Ap. J.*, **91,** 20.
Stoy, R. H., 1958a, Cape Annals, vols. 17–20; see vol. 20, p. xii.
Stoy, R. H., 1958b, *M.N.A.S.S.A.*, **17,** 142.
Stoy, R. H., 1960a, Cape data; private communication; to be published in Cape Annals.
Stoy, R. H., 1960b, private communication.
Struve, O., 1931, *Ap. J.*, **94,** 233.
Struve, O., 1959, *Sky and Telescope*, **19,** 364.
Thiessen, G., 1961, *Astron. Abhandl. d. Hamburger Sternwarte*, **5,** No. 9.
van de Hulst, H. C., 1958, *Review Modern Physics*, **30,** 913.
Willstrop, R. W., 1959, Thesis, Univ. of Cambridge.

OBSERVATIONS OF THE SOLAR CORONA OUT TO 100 SOLAR RADII

O. B. Slee

(Received 1961 June 19)

Summary

Observations are described of the scattering suffered by 13 discrete sources of radio emission, having ecliptic latitudes between $+15°$ and $-29°$, as they passed closest to the Sun in the 5-month interval June to October, 1960. The equipment used was an E–W interferometer with a base-line of length 2920λ, operating at 85·5 Mc/s.

It is shown that the average shape of the scattering corona over this time interval was elliptical, being more extended in equatorial than polar regions. On the average, scattering could be detected out to angular separations of about 55 $R\odot$ and 40 $R\odot$ in equatorial and polar regions respectively; in addition, in the equatorial regions, sporadic increases in scattering occurred out to angular separations of 120 $R\odot$. Evidence is presented to show that the greater equatorial extension of the scattering corona is probably related to the active belt on the visible Sun.

Detailed measurements of coronal scattering obtained by daily observation of a relatively intense radio source (MSH 12+08) indicated that significant changes in scattering of a random kind occurred in the interval of 24 hours between observations. This can be interpreted as due to the relative movement of the radio source and a quasi-static system of scattering regions, such as coronal rays, if temporal changes in scattering properties can be neglected.

By combining the present results with earlier measurements of the scattering angles at closer angular separations, it is shown that the average scattering varies as $R^{-2\cdot3}$ out to an angular separation of 100 $R\odot$ in the equatorial regions during sunspot maximum. A similar variation in the r.m.s. electron densities of the scattering irregularities is suggested if the scattering regions can be identified with extensions of the coronal rays.

1. *Introduction.*—Up to the present the solar corona has been traced out to angular distances of the order of 30–40 $R\odot$ by means of measurements of the scattering of radio waves from the intense discrete radio source, Taurus A (for example, Hewish (1958), Erickson (1959), Vitkevitch (1960), Hogbom (1960), Gorgolewski and Hewish (1960)). However, these observations have been restricted to defining the scattering produced in a very limited volume of the corona since the apparent path of the radio source with respect to the corona changes little from year to year. By using very long base line interferometers consisting of elements having a large collecting area, which are now coming into use, it is possible not only to detect the smaller scattering produced by coronal electron irregularities at much larger angular separations but also to study its effects on many other weaker radio sources. The latter desirable characteristic is due to the fact that the radio Sun, subtending an angle much greater than the interferometer fringe spacing, does not produce an interference pattern which would obscure or confuse the patterns due to the weaker radio sources. The present communication describes observations of 13 discrete

XUM

radio sources made with an E–W interferometer with a 2920λ base line operating at 85·5 Mc/s during the months June–November 1960. Since these sources possessed ecliptic latitudes ranging from 0°·5 to 15° and −0°·5 to −29°, it was possible by systematic examination of their fringe visibilities as they passed closest to the Sun, to obtain a fairly detailed picture of the spatial extent of the scattering corona.

2. *Observations.*—The radio sources used in the experiment are set out in Table I, in which they are identified according to the catalogues of Mills, Slee and Hill (1958), Edge *et al.* (1959), and given I.A.U. numbers where applicable. In addition to the necessity of possessing a low value of ecliptic latitude, the sources selected needed to exhibit a sufficiently large amplitude 2920λ Fourier component to make their detection certain above the noise fluctuation level when well clear of the solar corona. For the present equipment this requirement was fulfilled for sources having a 2920λ Fourier component greater than 25×10^{-26} w.m^{-2} (c/s)$^{-1}$. The brightness distributions of the sources are not important in determining the scattering introduced by irregularities in the intervening medium; as far as the effect of the scattering on the interferometer is concerned, the radio source may be regarded as a point having an intensity equal to the amplitude of the particular Fourier component. The phase-switched interferometer consisted of the E–W arm of the 85·5 Mc/s cross situated at Fleurs, near Sydney, N.S.W., and a smaller array of dipoles at a location 10 km due West, which was connected to

TABLE I

Particulars of radio sources observed during the scattering experiments

Source designation			Ecliptic co-ordinates (1950)		Observational period (1960)
MSH	3C	I.A.U.	λ	β	
			°	°	
...	144	05N2A	84	−1	May 30–July 3.
06−04	161		97	−29	June 7–June 29.
08−05	...		126	−22	June 27–August 2.
09+08	230		150	−12·5	July 22–August 29.
10+02	238		151	− 4·5	July 27–September 12.
10−021	249		167	− 7	August 6–September 30.
11−18	...		181	−15	August 12–October 5.
12+08	273		185	+ 5	August 26–October 31.
...	274	12N1A	181	+15	September 4–October 4.
12−013	275		190·5	− 0·5	August 31–October 31.
12−020	279		194·5	+ 0·5	August 31–October 31.
13−23	283		204·5	−13·5	September 18–October 31.
13−011	...		204·5	+ 3·5	October 5–November 2.

the base site *via* a radio link (Goddard, Watkinson and Mills 1960). The primary directivity of the system was 0°·8 arc E–W and 3°·7 N–S to half power points, the beam being sufficiently narrow to exclude the intense solar radiation on all except the days of closest approach of a source to the Sun. Pointing of the primary beam to the required declination was affected by phasing the dipoles at the remote site; on any one day it was usual to record up to 6 discrete sources over a period of about 4 hours around midday, the aerial beam being changed to the appropriate declination settings between observations.

Fig. 1 shows reproductions of some of the records obtained from the relatively intense discrete source MSH 12 + 08 while it was in the range of angular separations

$19 R_\odot$ to $109 R_\odot$. It is clear from these records that for a source giving rise to such reasonable signal-to-noise ratios it is possible to measure in some detail the variations in apparent size of the radio source from day to day. It should be noted that, although there was a general decrease in fringe visibility as the angular separations decreased, there were, on many days, large departures from the average degree of scattering. Sporadic large increases in the scattering first became noticeable when the angular separation was as much as $100 R_\odot$ and at separations less than $60 R_\odot$ the effects of scattering could be detected on every record.

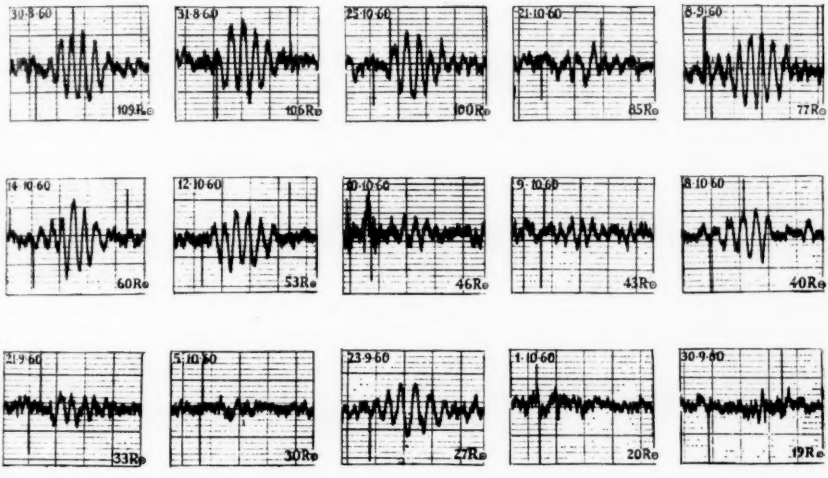

FIG. 1.—*Reproductions of interference fringes obtained from source 12+08. The angular separation for each record is noted near the lower right and generally decreases from left to right and top to bottom. The vertical line at the lower left of each record occurs at* $12^h\ 30^m$ *sidereal time.*

For the majority of sources used in this experiment, the signal-to-noise ratios were between $\frac{1}{4}$ and $\frac{1}{2}$ of those shown for the records of Fig. 1; under these conditions of recording it was possible to say no more than that the source appeared about normal intensity or that it was very weak if present at all. It has been estimated for such cases that the interference pattern would be classed as "not present" when the fringe amplitude dropped to below half its normal value. Although the weaker sources cannot be used to define the details of scattering in the corona, they are still useful as indicators of the average degree of scattering, since the points at which their interferometer patterns first disappear and later reappear may be used to trace around the Sun a line of constant E–W scattering.

3. *Results.*—The visibility of the interference fringes for source 12+08 is plotted as a function of angular separation from the Sun in Fig. 2. On the assumption that the scattered brightness distributions are Gaussian with circular symmetry, a scale has been constructed on the right of the figure to show the corresponding angular sizes to half-brightness points. We use these equivalent angular sizes as a measure of the degree of scattering.

The vertical bars inserted at two locations on the diagram indicate the expected chance deviations from the curve of best fit and were obtained by computing the standard deviations in the amplitudes of fringe patterns due to radio sources far removed from the Sun; the half-lengths of the bars represent these standard deviations. An examination of Fig. 2 reveals two interesting effects. First, departures from the un-occulted mean fringe amplitude became significant on sporadic occasions at angular distances as great as $98\,R\odot$; the fringe visibility was always noticeably reduced at angular separations less than $60\,R\odot$. If the reduction in fringe visibility is interpreted as due to scattering in terms of the model outlined earlier, then it can be stated from these results that the average width of the scattered brightness distributions was about 12″ of arc to half-brightness points at an angular separation of $65\,R\odot$ and increased rapidly to about 58″ of arc at $25\,R\odot$.

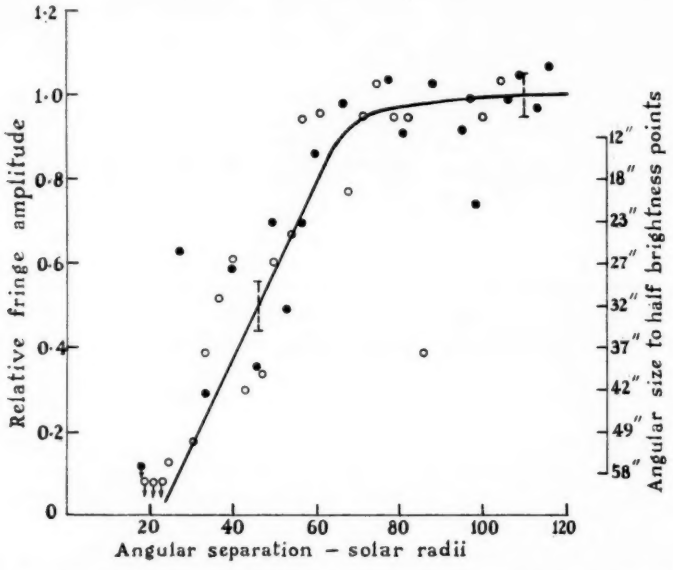

FIG. 2.—*Daily measurements of the fringe visibility for source 12+08 as a function of angular separation from the Sun. The full and open circles refer respectively to observations before and after conjunction. The scale on the right gives the equivalent angular size to half power points. The vertical bars inserted at fringe amplitudes of 0·5 and 1·0 have half lengths corresponding to the expected r.m.s. chance deviations from the average fringe amplitude.*

No measurements were possible at smaller angular separations due to the loss of the interference pattern in the receiver noise fluctuation level. Secondly, we note the large dispersion of the points about the average scattering values defined by the line of best fit. These random variations depart from the mean values by, in many cases, more than 2 or 3 standard deviations and hence must be regarded as indicative of real changes in the properties of the coronal irregularities in the 24 hours from one observation to the next. The question of whether they should be attributed to spatial or temporal coronal variations will be left for later discussion.

The results for all 13 radio sources observed between the end of May and beginning of November 1960 have been plotted in Fig. 3; here, the open circles

refer to observations on days when the interference fringes appeared to be unaffected by scattering, while the filled circles define days for which the fringe amplitude was greatly reduced. The position of the Sun is marked by a cross and the concentric circles are drawn at intervals of 20 $R\odot$. Over this period the tilt of the solar axis with respect to the terrestrial north–south line varied considerably and in Fig. 3 the co-ordinate system is fixed with respect to the solar axis. A curve has been drawn to enclose the majority of the filled circles and is, as far as can be judged, the contour within which the average scattered distribution exceeded 30″ arc to half power points in the E–W direction.

FIG. 3.—*Coronal diagram showing scattering suffered by 13 radio sources listed in Table I. Open circles refer to observations which show no detectable scattering, while the filled circles denote fringe visibilities of about 0·5 or less. The distance scale is defined by circles, concentric with the Sun (marked +), having radii increasing in increments of 20 R⊙. The closed contour, shown dashed, marks the average extent of the scattering corona.*

An examination of the coronal diagram shows that the average shape of the scattering corona over the 5-month interval was elliptical, being more extended in the equatorial regions. In the east equatorial sector, the 30″ contour extended out to 60 $R\odot$, while in the west it appeared to reach about 50 $R\odot$. In the south

polar region, the line of 30″ scattering almost certainly extended to 40 $R_\odot$ and the less numerous data to the north would be consistent with a similar extension. The observed axial ratio for the constant scattering ellipse of about 55/40 is similar to the general form of the visible corona at this intermediate phase of the sunspot cycle.

Fig. 3 also indicates that significant sporadic increases in scattering were recorded on 14 occasions at angular separations in the range 60–120 $R_\odot$ between position angles of 0° and 20° with respect to the solar equator. However, on no occasion was scattering measurable beyond about 50 $R_\odot$ at larger position angles. The significance of the greater extension of the scattering corona in the equatorial regions will be discussed in the next section.

4. *Discussion.*—The coronal scattering diagram (Fig. 3) showed clearly that the contour of constant E–W scattering extended further in equatorial than in polar regions; in addition, 14 cases of significant scattering were observed in equatorial regions in the range of angular separations 60–120 $R_\odot$, although no such events were recorded in the polar regions. These results are consistent with the hypothesis that the electron irregularities which cause the scattering are maintained by the active equatorial belt on the visible solar disk, probably through the ejection of material from disturbed regions.

This suggestion has been tested further by examining the data on the solar activity (CRPL, Part B, Solar–Geophysical Data) for the 14 scattering events mentioned above and also for 7 cases of abnormally low scattering observed during the 5-month interval. Since it was possible that these occurrences were related to the presence or absence of active areas near the appropriate limb of the Sun, various indications of solar activity were examined over the period concerned. There was no significant relationship between the degree of scattering and occurrences of important solar flares, intense solar radio emission or severe geomagnetic disturbances; however, there appeared to be a connection between the presence of calcium plages and abnormal scattering occurrences. In order to investigate this relationship, a daily limb activity index was constructed consisting of the sum of the products of calcium plage area and intensity for plages within 40° of each limb. Table II summarises the relationship between the 21 scattering events and the computed limb activity index and is indicative of a close correlation between them. It should be noticed, however, that this is a one way correlation in that the presence of a high activity index was not necessarily associated with excessive scattering of the radiation from any particular radio source. Such a result is to be expected if each active area on the Sun influences the scattering

TABLE II

Correlation between scattering events and solar limb plage activity

Scattering	Above average	Below average
Limb activity index	No. of occasions	
Above average	11	1
Below average	3	6

properties of only a limited volume of the corona so that it becomes a matter of chance whether, during any particular observation, the radiation is traversing a disturbed region of the outer corona. The latter conclusion is supported by the

detailed observations of fringe visibility for source 12+08 (Fig. 2) in which the scattering angles show a large dispersion about the average for any particular value of the angular separation and exhibit random changes from one day's observation to the next.

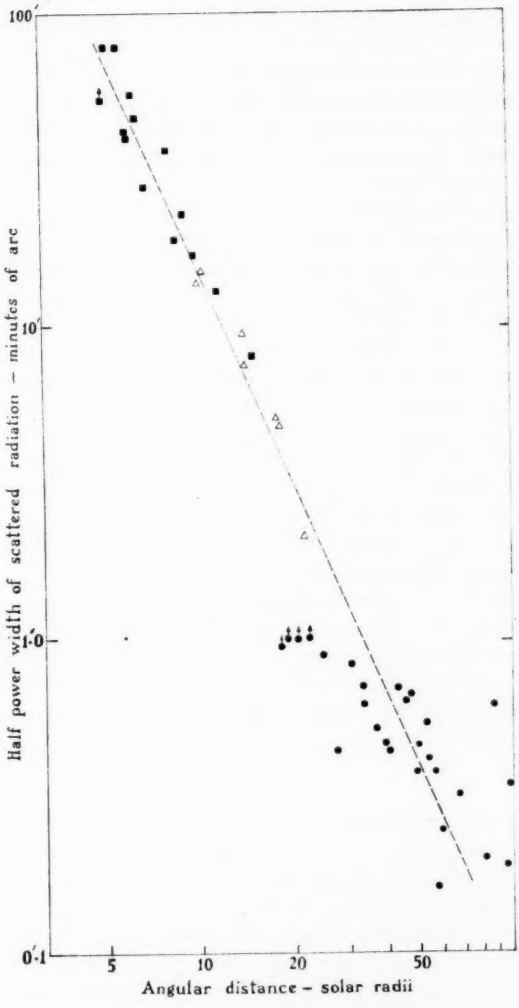

FIG. 4.—*Measured equivalent angular sizes as a function of angular separation from the Sun during the 4 years 1957–1960. Points marked ■: 85·5 Mc/s fan-beam observations of Crab Nebula 1957–1959; △: 26·3 Mc/s results of Erickson in 1959; ●: 85·5 Mc/s interferometer results from source MSH 12+08 during 1960.*

It is not possible to decide from these observations whether the changes in scattering in the 24-hour interval between successive observations of the same radio source are due to the relative movement of the radio source and a quasi-static

system of scattering irregularities or whether dynamic processes related to time variations in solar activity play an important part. If temporal variations in the scattering properties of the corona over the 24-hour interval can be neglected, it is obvious that the physical characteristics of the irregularities in the range 25–120 $R\odot$ vary in an irregular manner over a distance less than 3·5 $R\odot$ which is the average daily change in angular separation. Such a figure would be consistent with the transverse sizes of the visible coronal rays if extended outwards to the distances considered here. However, in order to account for the observed multiple scattering, which depends upon the simultaneous reception of incoherent scattered waves from a number of irregularities lying in the plane perpendicular to the line of sight, the presence is required of a fine structure having dimensions much less than 3·5 $R\odot$ or $2{\cdot}5 \times 10^6$ km.

Finally, it is interesting to inquire whether the present scattering measurements form a logical extension of the scattering angles already observed at smaller angular separations. Measurements of the E–W scattering angles observed between 5 and 100 $R\odot$ have been plotted in Fig. 4. Those measurements between 5 and 15 $R\odot$ were made by the author by means of a 36′ arc E–W fan beam operating on 85·5 Mc/s with the Crab Nebula as source of radiation during the conjunctions of 1957, 1958, 1959; the points plotted between 19 and 100 $R\odot$ are the present measurements on source 12+08. Scattering angles observed by Erickson (1959) at 26·3 Mc/s during the 1959 conjunction of the Crab Nebula have been scaled to 85·5 Mc/s on the assumption that the scattering angle varies as λ^2 and plotted in the diagram to complete the region between 10 and 22 $R\odot$. It can be seen that the present measurements are entirely consistent with an extrapolation of the scattering angles observed at much closer angular separations and suggest that, for the 4 years near the maximum of solar activity, the average scattering varies as $R^{-2\cdot3}$ out to an angular distance of 100 $R\odot$.

Before inquiring into the corresponding electron densities of the scattering irregularities, it would be advisable to examine the factors which influence its calculation. It can be shown from the geometrical optics scattering theory developed by Chandrasekhar (1952) that the r.m.s. scattering angle, ϕ, is related to the r.m.s. electron density variation, ΔN, above (or below) that of the surrounding medium by:

$$\phi \propto \lambda^2 \Delta N n^{1/2}$$

where λ is the wavelength of the scattered radiation and n the number of irregularities along the line of sight. The theory assumes that the irregularities possess, on the average, identical properties throughout the scattering layer and that the scattered brightness distributions display circular symmetry about the direction of propagation (i.e. approximately spherical irregularities). It has been shown, however, by Hewish (1958) and Vitkevitch, Panovkin and Sukhovei (1959) that the irregularities are probably significantly elongated in the radial direction from the Sun so that the scattering would be expected to be greatest in the direction perpendicular to their long axes. In this case, provided the scattering region is small enough so that the directions of the filaments remain approximately constant, the above proportionality would remain valid. If the line of sight traverses several scattering layers, each having different properties, then the equation must be replaced by the appropriate summation.

It is obvious that in order to estimate r.m.s. electron densities from the observed values of the scattering angle it is essential to know the relevant values of n, which,

in turn, necessitates a knowledge of the depth of the scattering region, the sizes of the irregularities and the spacing between them. Since none of these quantities is at present known, it seems futile to attempt calculations of electron density. However, if we are justified in identifying the scattering regions as extensions of the visible coronal rays, it becomes possible to predict the relationship between ϕ and ΔN and how the latter varies, on the average, with angular distance from the Sun.

It seems reasonable to assume that the transverse dimensions of both the ray as a whole and its fine structure would continue to increase approximately in proportion to the radial distance from the Sun. Under these conditions, the value of n in the equations would tend to remain constant with the result that $\Delta N \propto \phi$. Using the present result that $\phi \propto R^{-2\cdot3}$ in the equatorial regions during sunspot maximum, it seems reasonable to suppose that ΔN exhibits a similar variation.

Acknowledgment.—The author wishes to express his gratitude to Mr C. F. Fryar whose assistance made these observations possible.

C.S.I.R.O.,
Radiophysics Laboratory,
Sydney, Australia:
1961 *May* 2.

References

Chandrasekhar, S., 1952, *M.N.*, **112**, 475.
Edge, D. O., J. R. Shakeshaft, W. B. McAdam, J. E. Baldwin, and S. Archer, 1959, *Mem. R.A.S.*, **68**, 37.
Erickson, W. C., 1959, Convair Sci. Res. Lab. Res. Note 31.
Goddard, B. R., A. Watkinson, and B. Y. Mills, 1960, *Aust. J. Phys.*, **13**, 665.
Gorgolewski, S., and A. Hewish, 1960, *Observatory*, **80**, 99.
Hewish, A., 1958, *M.N.*, **118**, 534.
Hogbom, J. A., 1960, *M.N.*, **120**, 530.
Mills, B. Y., O. B. Slee, and E. R. Hill, 1958, *Aust. J. Phys.*, **11**, 360.
Vitkevitch, V. V., 1960, *Ast. Zhurnal*, **37**, 32.
Vitkevitch, V. V., B. N. Panovkin, and A. G. Sukhovei, 1959, *Izvest. Vyss. Ucheb. Zaved. Radiofiz.*, **2**, 1005.

RADIAL VELOCITIES OF FUNDAMENTAL SOUTHERN STARS, II

William Buscombe and Pamela M. Morris

(Received 1961 June 19)

Summary

Newly determined radial velocities are given for 15 standard velocity stars and 115 other bright stars south of the equator. Measurements from two-prism spectrograms (dispersion 90 A/mm at $H\gamma$) taken at the Newtonian focus of the 74-inch reflector are now entirely consistent with velocities determined elsewhere. Most of the present data are from the 30-inch Cassegrain spectrograph (dispersion 36 A/mm at $H\gamma$).

Nearly all the stars in this list are in the FK3 and N30 position catalogues, of the fifth or sixth visual magnitude. At least three spectrograms of each star have been measured. 34 new constant velocities are announced, and variability has been detected for the first time in 23 other stars. Observations have been resumed on 33 stars previously known to have variable velocity. A luminosity class on the revised Yerkes system is assigned where possible.

This paper continues, in the same form, the data presented for stars observed earlier on the programme in Paper I (**1**). The object of the work has been to obtain more reliable radial velocities for certain southern stars whose positions and proper motions are known with high accuracy. Of the 198 stars in the FK3 for which no radial velocity was known in 1940 (**2**), 133 are south of the equator. At least three observations have been completed for each of 34 of these stars at Mt Stromlo, and velocities have been published for 21 more by other observatories. Progress with the stars having uncertain (usually variable) velocities is slower, but orbits have appeared for η Mus, ζ Cen and α Oct.

A major improvement in the quality of observations has been noticed since May 1960, when the faulty temporary camera objective of the three-prism Cassegrain spectrograph was replaced. Craftsmen of the Defence Standards Laboratory in Melbourne prepared the new lens system which Mr T. Feuerriegel designed specifically for this purpose.

Although the Zeiss Newtonian spectrograph (**3**), with its two light flint prisms and the 137·5 mm camera, gives a dispersion of 90 A/mm, the optical resolution compares favourably with the slower Cassegrain system when the optimum spectral purity is maintained behind a slit whose projected image on the photographic emulsion is not wider than 18μ. Difficulties in keeping this instrument at constant temperature, experienced during its initial period of operation, have been overcome. Rubber insulation on the base casting inhibits heat loss by conduction, and a circulating fan and hose prevent thermal stratification of the air within the double enclosure. Dr Heinz Gollnow has taken expert care of all these instrumental problems.

XUM

Since the sensitivity of Eastman Kodak emulsions, especially 103aO, available during the past four years has declined steadily by more than a factor of two, we have been obliged to abandon observation of K stars of sixth magnitude, which would now require prohibitively long exposures, and to fill up gaps in the nightly observing lists with A and B stars. When a sufficient array of MK standard spectra has been observed with the new Cassegrain camera, luminosity classification from the recent plates will be resumed. Plans are in hand to extend this work to the G and K stars.

The practice of observing an internationally accepted star of standard velocity, at least once per night when practicable, has been continued. Results of measures are presented in Table I not only for Cassegrain spectrograms, which are homogeneous with most of the observations of this programme, but also for Newtonian plates photographed with the 74-inch reflector, all reduced with the same wavelength system. From the list of lines used in the earlier Cassegrain spectrograms (**1**) only minor omissions were required to obtain consistent results among Miss Morris's measures of the Newtonian spectrograms. In the past two years, no deviation from standard velocity, in excess of about twice the internal probable error of the mean velocity for a single plate, has been found for either instrument. Combined with recent results from the Cape observers, these data may help the International Astronomical Union to decide on the suitability of a few additional standards considered necessary for the southern hemisphere.

Following the lists of stars with constant velocities (Table II) and with variable velocities (Table III), the individual plate velocities of the double-line binary α Oct (HD 199532) are presented in Table IV. Our preliminary spectrographic orbit for this star has recently appeared (**4**).

TABLE I

Standard velocity stars

HD	Star	$m(HP_v)$	Spec.	$\bar{V}$ km/s	p.e. ±	Obs.	Prev. vel.	References
2151	β Hyi	2·80	G1 IV	+21·6	0·5	17 C	+21·7 a 6 C	*Cape Ann.* **10**
				+23·0	0·4	9 N	+23·0 a 9 L	*Lick Pub.* **16**
							+23·3 a 6 C	*M.N.* **117,** 534
18884	α Cet	2·54	M2 III	−27·1	0·7	7 C	−25·8 a 27	*I.A.U. Tr.* **9**
				−24·4	0·9	2 N		
20794	87 Eri	4·15	G5 V	+86·4	1·0	5 N	+88·3 b 3 W	*Ap. J.* **57,** 149
							+86·8 b 6 L	*Lick Pub.* **16**
							+86·8 a 6 C	*Cape Ann.* **10**
							+88·3 a 7 St	*M.N.* **118,** 609
							+87·5 a 19 C	*M.N.* **119,** 638
29139	α Tau	0·77	K5 III	+53·2	1·1	4 C	+54·1 a 171	*I.A.U. Tr.* **9**
62509	β Gem	1·13	K0 III	+ 4·3	0·6	3 C	+ 3·3 a 167	*I.A.U. Tr.* **9**
80170	120G Vel	5·16	K5	− 0·9	0·4	7 N	0·0 a 6	*I.A.U. Tr.* **8**
							− 0·5 a 27 C	*M.N.* **119,** 638
94510	246G Car	3·78	K0	+ 8·4	0·7	7 C	+ 8·4 a 9 L	*Lick Pub.* **16**
				+ 7·7	0·3	7 N	+ 8·9 b 3 C	*Cape Ann.* **10**
128898	α Cir	3·34	F0 V(Sr)	+ 7·3	0·6	6 C	+ 7·1 b 17 L	*Lick Pub.* **16**
				+ 7·6	2·0	3 N	+ 7·6 a 6 C	*Cape Ann.* **10**
							+ 6·5 a 5 C	*M.N.* **117,** 534
157457	κ Ara	5·09	K0 III	+16·0	0·5	4 C	+17·6 a 6	*I.A.U. Tr.* **8**
							+16·9 a 44 C	*M.N.* **119,** 638

TABLE I—*continued*

Standard velocity stars

HD	Star	$m(HP_v)$	Spec.	$\bar{V}$ km/s	p.e. ±	Obs.	Prev. vel.	References
171759	ζ Pav	3·94	Ko	−16·3	0·8	5 C	−16·9 b 8 L	*Lick Pub.* **16**
				−15·7	0·4	6 N	−16·9 b 3 C	*Cape Ann.* **10**
196171	α Ind	3·05	Ko III	− 1·2	0·2	2 N	−1·8 a 9 L	*Lick Pub.* **16**
							0·0 b 6 C	*Cape Ann.* **10**
							− 0·8 a 5 St	*M.N.* **118,** 609
203608	γ Pav	4·22	F6 V	−29·3	0·4	4 N	−30·1 a 10 L	*Lick Pub.* **16**
							−31·5 b 3 C	*Cape Ann.* **10**
							−28·8 a 5 C	*M.N.* **117,** 534
							−30·3 a 3 St	*M.N.* **118,** 609
203638	33 Cap	5·27	Ko III	+23·2	0·2	3 C	+22·0 a 7	*I.A.U. Tr.* **8**
				+22·1	0·3	2 N	+22·1 a 39 C	*M.N.* **119,** 638
218594	88 Aqr	3·75	Ko III	+22·8	0·5	4 C	+21·1 a 6 L	*Lick Pub.* **16**
							+21·4 a 5 C	*Cape Ann.* **10**
223647	γ^1 Oct	4·99	G5 III	+13·5	0·2	3 N	+14·5 b 3 L	*Lick Pub.* **16**
							+12·0 a 4 St	*M.N.* **118,** 609
							+13·3 a 9 C	*M.N.* **119,** 638

TABLE II

Stars with constant velocities

HD	Star	$m(HP_v)$	Spec.	$\bar{V}$ km/s	p.e. ±	Obs.	Prev. vel.	References
2363	69G Scl	5·77	G5	− 3	0·3	3		
8810	9G Hyi	5·62	K5	+23	1·5	3		
*9362	δ Phe	3·84	Ko	− 8	1·6	9	−6·5 a 8 L	*Lick Pub.* **16**
							−7·1 b 7 C	*Cape Ann.* **10**
10476	107 Psc	5·18	K1 V	−34	1·4	2	−34 b 4 W	*Ap. J.* **42,** 175
							−33 a 3 L	*Lick Pub.* **16**
11937	χ Eri	3·61	G5 IV	− 6	1·0	3	−6 c 8 L	*Lick Pub.* **16**
							−6 a 15 C	*Cape Ann.* **10**
12363	σ Hyi	6·15	F2	+ 6	0·4	3		
12477	26G Hyi	5·97	K2	+ 5	0·4	4		
12573	201G Cet	5·59	A5	+13	0·2	3	+9 d 1 D	
14728	239G Cet	5·77	Ko	− 3	0·7	3		
15248	κ Hyi	5·84	Ko	+22	0·8	3		
15471	29G For	5·95	G5	− 2	0·5	3		
16538	ι^2 For	5·67	F5	+28	0·7	3		
16975	40G For	5·77	G5	+17	1·6	3		
20640	40G Hor	5·68	Ko	− 9	0·4	3		
23719	51G Hor	5·44	Ko	− 4	0·8	2	−2 d 1 L	*Lick Bull.* **15**
24188	61G Hyi	6·46	Ao	+ 2	0·6	3		
25371	163G Eri	5·78	Ao V	+21	1·3	4		
27256	α Ret	3·26	G6 II	+35	0·4	3	+36 b 7 L	*Lick Pub.* **16**
							+36 b 9 C	*Cape Ann.* **10**
27563	210G Eri	5·77	B5 III	+ 8	1·3	5		
29116	ν Men	5·72	Fo	+14	1·9	4		
30127	264G Eri	5·46	A1 V	+ 5	1·4	4		
30432	15G Cae	5·82	Ko	− 6	1·3	3		
32515	26G Cae	5·78	Ko	+29	1·0	3		
33256	68 Eri	5·10	F5 V	+ 7	1·0	2	+10 a 3 L	*Lick Pub.* **16**
							+ 8 b 3 C	*Cape Ann.* **10**
							+10 a 2 W	*Ap. J.* **111,** 223
*36673	α Lep	2·63	Fo Ib	+22	0·5	9	+24·7 a 19	*I.A.U. Tr.* **9**
39780	31G Men	6·17	A1 V	− 4	0·8	3		

TABLE II—*continued*

HD	Star	m(HP$_v$)	Spec.	$\overline{V}$ km/s	p.e. ±	Obs.	Prev. vel.	References
40972	82G Lep	5·90	A1 V	+12	0·6	4		
*45348	α Car	−0·79	Fo Iab	+18	0·4	7	+20·5 a 114	*I.A.U. Tr.* **9**
48915	α CMaA	−1·68	A1 V	− 6†	0·6	3	− 8 a 101 L	*Lick Bull.* **9**, 184 (orbit)
*50877	o^1 CMa	3·79	K3 Iab	+37	0·3	3	+37 b 5 L	*Lick Pub.* **16**
							+36 b 4 C	*Cape Ann.* **10**
54605	δ CMa	1·90	F8 Ia	+34	1·2	4	+35 a 46 L	*Lick Pub.* **16**
							+33 a 20 C	*Cape Ann.* **10**
56855	π Pup	2·44	Ko III	+16	0·6	2	+15·5 a 10 L	*Lick Pub.* **16**
							+16·1 a 7 C	*Cape Ann.* **10**
*57623	δ Vol	3·94	F8 II	+22	1·8	6	+22·6 a 6 L	*Lick Pub.* **16**
							+21·7 b 3 C	*Cape Ann.* **10**
59612	97G Pup	4·74	A3	+40	2·0	5	+37 c 8 L	*Lick Pub.* **16**
							+36 c 3 Y	*Yerkes Pub.* **7**
68434	80G Car	5·75	A2	+25	0·7	3		
69267	β Cnc	3·42	K2	+23	1·5	5	+22 b 5 L	*Lick Pub.* **16**
							+23 b 3 C	*Cape Ann.* **10**
							+19 a 2 V	*D.A.O. Pub.* **6**
							+18 4 W	
*74006	β Pyx	3·87	G5	−12	0·6	13	−14·8 a 9 L	*Lick Pub.* **16**
							−15·4 b 3 C	*Cape Ann.* **10**
89388	187G Car	3·23	K5 Ib	+ 6	0·6	2	+ 8 a 9 L	*Lick Pub.* **16**
							+10 b 3 C	*Cape Ann.* **8**
90853	196G Car	4·00	Fo II	+10	0·6	5	+10 b 11 L	*Lick Pub.* **16**
							+ 6 a 3 C	*Cape Ann.* **10**
119938	268G Cen	6·01	A3	+16	0·8	4		
123123	π Hya	3·22	K2 III	+27	0·7	2	+27 a 19 L	*Lick Pub.* **16**
							+28 b 6 C	*Cape Ann.* **10**
139233		6·56	B9	+ 5	1·2	5		
141891	β TrA	2·97	F2 V	0	1·3	7	0 a 15 L	*Lick Bull.* **15**
							+ 3 b 6 C	*M.N.* **117**, 534
154783	124G Sco	5·83	A3	−30	0·5	4		
159877	9G Ser	5·83	A5	− 8	1·0	4		
163917	ν Oph	3·22	G9 III	+14	0·4	2	+13 a 7 L	*Lick Pub.* **16**
							+13 a 6 C	*Cape Ann.* **10**
165259	67G Aps	5·84	F5	+11	0·2	3		
182509	59G Tel	5·39	K2	− 5	0·4	3		
188584	μ^1 Pav	5·57	Ko	+28	0·7	4		
197725	48G Cap	5·86	Ao	+18	0·4	3		
199684	37G Mic	6·05	Fo	+15	0·4	3		
200702	η Mic	5·34	Ko	+11	0·4	3		
201647	55G Mic	5·76	F5	+12	1·2	2	+11 d 1 W	
203532	57G Oct	6·37	B3 IV	0	0·7	4		
209529	κ^2 Ind	5·40	K5	−11	1·2	4		
210853	ψ Oct	5·58	A6 IV	+17	1·1	3		
214632	10G Tuc	5·75	Ko	−32	0·6	3		
221323	5G Phe	5·70	Ko	+ 8	0·5	4		
224930	85 Peg	5·72	G2 V	−32	0·9	2	−33 c 5 W	*Ap. J.* **57**
							−35 a 3 V	*D.A.O. Pub.* **6**
							−37 8 Y	

* Possibly slightly variable in velocity
† Epoch 1954.1.

TABLE III

Stars with variable velocity

HD Star	$m(HP_v)$ Sp.	JD 243....	V km/s	p.e. ±	Prev. vel.	References
2834	4·82	5385·094	−24	1·9	− 5 c 9 L	*Lick Pub.* 16
λ^1 Phe	A0 V	7122·257	+ 8	1·8		
		7148·223	− 7	1·6		
		7153·210	+39	2·8		
4150	4·45	5711·182	− 5	2·3	+10 c 3 L	*Lick Pub.* 16
η Phe	A0 IV	5740·108	−12	3·0		
		5742·081	−24	1·7		
		5777·988	−22	2·0		
6767	5·10	4967·248	+18	3·4	+ 9 c 9 L	*Lick Pub.* 16
υ Phe	A3 V	5385·132	+ 7	2·0		
		7115·332	+37	2·5		
		7122·277	+41	2·2		
9132	5·11	6094·213	+40	2·2	− 8 b 4 L	*Lick Pub.* 16
157G Cet	A1 V	6799·244	+ 9	2·0		
		6852·103	− 9	2·7		
		6910·965	+ 2	2·1		
10144	0·60	4971·242	+ 3	1·8	+19 c 7 L	*Lick Pub.* 16
α Eri	B5 IV	5812·927	+ 2	1·6		
		7140·310	+21	5·5		
10148	5·63	5720·213	+11	1·6	+18 c 5 W	*Ap. J.* 111, 223
172G Cet	Fo	5754·122	+ 2	1·7		
		7173·233	+17	1·8		
		7211·129	+10	2·2		
10538	5·60	5385·144	+ 8	2·4	+20 c 4 L	*Lick Bull.* 15
129G Scl	A2 V	7122·307	+12	1·1		
		7131·325	+39	1·6		
13709	5·18	5443·995	+ 6	2·4	+17 c 6 L	*Lick Pub.* 16
μ For	A2 V	7122·332	+11	1·7		
		7171·257	+11	2·2		
		7206·153	− 2	3·1		
15427	5·10	5705·265	+38	1·9	+16 c 8 L	*Lick Pub.* 16
ϕ For	A2 IV	5740·160	+32	2·2		
		5760·140	−15	2·4		
		7122·348	+42	1·8		
		7150·327	+29	2·0		
16754	4·48	5720·240	+14	2·2	+20 c 6 L	*Lick Pub.* 16
18G Eri	A2 V	5734·232	+13	1·7		
		5742·201	+26	2·0		
		5800·028	+ 1	1·9		
18149	5·78	5720·257	+31	1·6		
ψ For	F2	5798·044	− 8	4·7		
		5825·981	+16	2·6		
		6536·025	+17	2·0		

TABLE III—*continued*

HD Star	$m(HP_v)$ Sp.	JD 243....	V km/s	p.e. ±	Prev. vel.	References
20313	5·63	5001·236	− 8	1·0	+ 3 c 5 L	*Lick Bull.* **15**
55G Hyi	Fo II	7217·191	+37	1·2		
		7234·115	+40	1·0		
20320	4·80	5444·031	−10	2·6	0 c 6 L	*Lick Pub.* **16**
ζ Eri	A7 m	7171·275	+23	1·1	−15 c 3 Y	*Yerkes Pub.* **7**
		7206·176	+ 7	2·8	−14 d 2 V	*D.A.O. Pub.* **7**
					− 4·5 b	*Ap. J. Supp.* **52***
26591	5·81	7288·963	+ 32	0·9		
187G Eri	Ao		− 96	9·0		
		7298·991	− 77	1·3		
			+122	4·8		
		7299·915	+ 31	0·8		
			− 91	5·7		
27710	5·81	7217·231	+22	0·9	+24 d 1 W	
214G Eri	Fo	7245·129	+16	1·2		
		7299·019	+20	1·2		
		7304·941	+16	1·3		
		7307·935	+12	1·5		
30478	5·30	5743·235	− 4	1·9	+ 2 d 5 L	*Lick Pub.* **16**
κ Dor	A3	7329·921	0	1·4		
		7335·910	− 4	1·4		
31203	5·46	5385·264	− 5	1·3	+ 5 d 7 L	*Lick Bull.* **15**
i^1 Pic	Fo IV	6178·048	+10	0·7		
		7217·268	−14	1·0		
33875	6·17	5826·083	+16	1·7		
20G Men	Ao	7234·224	−11	1·4		
		7303·050	+17	2·2		
		7329·948	−13	1·7		
		7335·942	+29	1·6		
37507	4·79	6863·241	+22	5·3	+ 1 d 5 Y	*Yerkes Pub.* **7**
49 Ori	A3	6921·115	+ 5	3·0	− 1 d 5 L	*Lick Pub.* **16**
		7299·045	−17	1·9		
39937	5·87	6536·137	+31	1·8		
38G Pic	F5	6553·109	− 7	1·0		
		6555·106	− 1	0·5		
40535	6·24	6921·122	+ 6	1·3		
1G Mon	F2 II	7299·074	+18	1·0		
		7303·984	+ 4	1·6		
41534	5·62	6151·189	+72	5·7	+81 c 6 L	*Lick Bull.* **15**
72G Col	B2 IV	7329·976	+64	2·9	+94 c 5 L	*Lick Pub.* **16**
		7335·976	+74	3·1	+99 3 W	
					+105 c 5 C	*M.N.* **117**, 534

TABLE III—*continued*

HD Star	$m(HP_v)$ Sp.	JD 243....	V km/s	p.e. ±	Prev. vel.	References
45320	5·69	5028·289	+33	1·9		
36G Mon	A7 IIIp	6916·103	+20	2·7		
		7291·996	− 8	1·6		
		7304·978	0	2·7		
		7308·009	+ 4	1·8		
46933	4·56	5775·274	+31	1·8	+35 b 5 L	*Lick Pub.* **16**
ξ^2 CMa	A0	7299·096	0	2·3	+26 b 3 Y	*Yerkes Pub.* **7**
		7355·945	+ 6	2·1		
49147	5·57	5809·188	+12	1·9	+21 d 3 Y	*Yerkes Pub.* **7**
75G Mon	A0 IV	6918·142	+22	2·9		
		6954·003	+ 2	3·1		
49333	5·98	7289·012	+30	2·5		
76G CMa	B8	7307·973	+15	3·6		
		7337·985	+15	4·1		
49643	5·61	5058·174	+36	1·1		
80G Mon	B8 V	6916·131	− 1	2·6		
		6979·974	+ 2	2·6		
		7292·083	+ 3	2·5		
50506	5·58	5084·165	−13	3·6	+ 9 e 1 L	*Lick Bull.* **15**
ζ Men	A4 IV	6536·167	+26	3·5		
		6600·031	+ 3	2·4		
		6914·156	+ 2	2·4		
		6978·975	+18	1·7		
52312	5·80	5062·222	− 6	4·7		
101G Mon	B9 III	5086·177	+23	6·0		
		7308·046	+22	5·5		
		7356·005	+ 2	6·0		
53244	4·02	4822·918	+58	4·6	+28 c 4 L	*Lick Pub.* **16**
γ CMa	B8 II	5084·194	+24	3·4	+34 c 5 Y	*Ap. J.* **64**, 11
		6979·997	+30	2·8		
55344	5·74	5822·147	+26	2·6		
130G CMa	A0	7308·125	+11	1·8		
		7338·010	+18	3·3		
75416	5·53	6536·225	−17	3·0	+18 e 1 L	*Lick Bull.* **15**
η Cha	B9 IV	7308·203	+20	6·0		
		7330·114	+37	5·2		
97495	5·61	6979·099	+ 1	2·1	−28 c 6 L	*Lick Bull.* **15**
9G Cen	A2	7002·056	+21	1·9		
		7088·881	+ 6	2·0		
		7299·209	+44	2·2		
104671	4·42	4848·044	− 1	1·4	−2·8 a 63 L	*Lick Bull.* **15***
θ^1 Cru	Ap	5203·042	− 6	1·3	−2·0 a 48 C	*Cape Ann.* **10***

TABLE III—*continued*

HD Star	m(HP$_v$) Sp.	JD 243	V km/s	p.e. ±	Prev. vel.	References
104841	4·79	5531·124	+49	3·8	+16·3 a 26 L	*P.A.S.P.* **38**,
θ^2 Cru	B3 IV	5555·099	+49	5·6		393*
122532	6·36	6714·987	+20	2·9		
307G Cen	Aop	7114·896	+12	2·1		
		7120·883	− 8	1·7		
		7123·890	+ 1	2·3		
125473	4·13	6719·996	+ 3	2·4	− 4 c 3 L	*Lick Pub.* **16**
ψ Cen	Ao IV	7098·960	−16	1·7		
		7114·931	−11	1·9		
		7125·871	− 1	2·8		
133880	5·94	6646·207	+22	5·7		
56G Lup	Aop	6715·023	+20	4·2		
		7120·926	+13	3·0		
		7123·928	+ 9	2·4		
		7154·901	− 4	3·0		
134481	4·04	6392·910	− 9	5·4	+ 3 c 3 L	*Lick Pub.* **16**
κ^1 Lup	B9 V	7114·945	−29	2·3		
		7163·892	− 6	2·5		
		7170·873	− 8	3·0		
144844	5·84	7120·977	− 3	2·9		
27G Sco	B9	7123·977	−29	4·0		
		7147·931	−24	3·9		
		7152·900	− 6	4·3		
166114	5·86	6739·107	−31	4·6	−32 e 1 L	*Lick Bull.* **15**
2G CrA	A5		+52	3·5		
		6793·953	−23	2·3		
		7065·208	+36	1·5		
		7077·159	+18	1·0		
169033	5·65	7124·043	+17	3·4		
2G Sct	B8	7170·922	+ 1	2·7		
		7182·910	−17	4·4		
		7417·222	+34	4·2		
171819	5·99	6793·988	−16	1·9		
22G Tel	A5	6798·987	−13	1·7		
		7099·133	− 2	1·3		
		7115·080	− 8	1·6		
		7122·097	− 8	1·5		
186543	5·48	5291·162	+17	2·8	−16 c 3 L	*Lick Bull.* **15**
ν Tel	A5p	6828·986	−13	3·2		
		7150·079	−21	2·3		
		7172·008	− 1	2·5		
		7174·994	− 7	1·9		
191829	5·48	5264·278	+21	1·9		
81G Tel	K5	6739·189	+16	1·7		
		7124·149	+11	0·6		
		7148·083	+10	0·9		

TABLE III—*continued*

HD Star	$m(HP_v)$ Sp.	JD 243 ...	V km/s	p.e. ±	Prev. vel.	References
202627	4·73	5293·203	− 1	2·2	− 1 c 8 L	*Lick Pub.* **16**
ϵ Mic	A2p	6380·188	+19	3·2		
		7065·309	+22	2·0		
		7115·173	+ 6	0·9		
		7122·204	+37	2·7		
		7150·099	+14	2·1		
205767	4·71	5290·233	+30	1·5	−20 c 15 L	*Lick Pub.* **16**
ξ Aqr	A7 V	5379·960	−26	2·5	− 6 c 4 Y	*Yerkes Pub.* **7**
		6803·087	− 1	3·8		
		7177·013	− 4	4·2		
208321	5·50	5645·290	+41	2·8	+28 c 4 L	*Lick Bull.* **15**
20G Gru	A3 V	5646·239	+38	2·6		
		6034·195	+11	4·9		
		6354·313	+45	3·3		
		6380·205	+ 2	3·1		
209014	5·37	4998·041	−22	4·4	− 5 c 5 L	*Lick Pub.* **16**
η PsA	B8 V	7121·205	+26	5·3		
		7150·116	+34	3·9		
		7171·076	+ 6	4·7		
209522	5·84	5289·242	+ 5	4·3		
25G PsA	B5 Vn	5362·008	+ 8	3·5		
		5646·276	+33	9·7		
		6380·226	+44	3·5		
		6768·172	0	2·5		
		6778·164	+27	2·8		
209819	4·24	5290·250	+27	6·3	− 4 d 4 L	*Lick Pub.* **16**
ι Aqr	B8 V	5379·984	−27	5·7	−14 d 5 Y	*Ap. J.* **64**, 11
		5386·006	−26	6·2		
213320	4·79	5256·328	+15	2·1	+14 c 20 L	*Lick Pub.* **16**
σ Aqr	A1 IV	7065·334	+17	1·5	+ 5 b 6 W	*Ap. J.* **111**, 223
		7122·220	+17	2·3	+ 7 c 3 V	*D.A.O. Pub.* **7**
		7124·205	+19	0·7		
214484	5·55	5293·253	+ 9	1·8	+ 4 d 5 L	*Lick Bull.* **15**
49G PsA	A2 Vp	5646·297	+19	2·0		
		7121·230	+37	1·9		
		7124·231	−31	1·5		
		7150·150	+30	1·9		
		7184·165	+12	1·4		
219263	5·55	7183·066	+ 8	1·1	+26 d 1 L	*Lick Bull.* **15**
92G Gru	Ko	7240·965	− 6	1·1		
220729	5·48	5315·231	+30	1·6	+18 d 6 L	*Lick Bull.* **15**
107G Gru	F3 IV	5325·195	+20	2·0		
		7121·281	− 2	0·8		
		7131·236	+42	0·7		
		7148·182	+39	1·0		

TABLE III—*continued*

HD Star	$m(HP_v)$ Sp.	JD 243...	V km/s	p.e. ±	Prev. vel.	References
224990	4·91	4998·106	+ 3	4·9	o c 6 L	*Lick Pub.* **16**
ζ Scl	B5 III	7173·170	+ 9	3·6		
		7211·048	+21	3·9		
		7218·128	+13	5·2		
		7245·967	+ 8	4·8		
225253	5·54	5361·123	+12	2·7	− 3 d 4 L	*Lick Bull.* **15**
45G Tuc	B8 III	5380·081	− 5	2·8		
		6036·251	+ 3	3·5		

* Orbit.

TABLE IV

Radial velocities of HD 199532

JD 243....	V_1	V_2	JD 243....	V_1	V_2
5314·129		+15	6353·222	+ 3	
5356·995		+25	6353·336	+ 5	
5745·997	+10		6379·181	+22	
6036·134	+ 7		6393·178		+ 5
6038·118	+86		6406·151	+ 8	+74
6067·068	+66		6410·122	+96	+ 6
6084·013	+92	− 2	6711·307	+78	+17
6084·088	+88	− 4	6711·317	+68	
6085·969		+34	6718·283		+14
6086·087	+60		6720·267	+66	
6092·025	+64	+20	6737·231	+94	o
6120·923	+82		6778·137	+25	+57
6154·920	+32		6803·045	+72	
6182·937	+66				

TABLE V

Observers and measurers

	Observed	Measured
L. Aller*	5	o
W. Buscombe	366	244
H. Gollnow	67	o
J. Graham	o	25
W. Heintz†	8	o
P. Morris	27	337
A. Przybylski	84	11
D. Sher	19	o
J. Whiteoak	5	o
Totals	581	617

* Michigan University: visiting professor, 1960–61.
† Munich Observatory: guest observer, 1954–55.

Acknowledgments.—Special thanks are due to our colleagues named in Table V who have graciously shared in securing the observations, and to Mr V. Hunt and Mr J. Green, who have taken great care with the photographic processing.

Mount Stromlo Observatory,
Canberra,
Australia:
1961 *May.*

References

(1) W. Buscombe and P. M. Morris, *M.N.*, **118**, 609, 1958.
(2) G. Hagemann, *Astr. Nach.*, **271**, 1, 1940.
(3) K. Röschke, *Jena Review*, **2**, 90, 1957.
(4) W. Buscombe and P. M. Morris, *Observatory*, **80**, 28, 1960.

A STUDY OF THE GALACTIC CLUSTER IC 2602

I. A Photoelectric and Spectroscopic Investigation

John B. Whiteoak

(Communicated by A. W. Rodgers)

(Received 1961 June 20)

Summary

The results are presented of a photoelectric and spectrographic study of the galactic cluster IC 2602. In the investigation, observations of 29 probable and 40 possible members yield a distance of 155 parsecs and cluster age of 10^7 years. It is a poorly-populated cluster and its luminosity function shows a deficiency in the number of stars of spectral type F compared with that predicted by the Initial Luminosity Function. It is suggested that the star-group is a local condensation of the Scorpio-Centaurus association.

Introduction

The galactic cluster IC 2602 (Melotte 102) is an open group of stars distributed about the Bo star Theta Carina. The brightest members are in a group $1\frac{1}{2}°$ in diameter centred at $\alpha = 10^h 42^m$, $\delta = -64°$ (1950) ($l^{II} = 289°{\cdot}7$, $b^{III} = -4°{\cdot}9$). The cluster is shown in Plate 7: a 3-min exposure in visual light, taken with the 20/26-inch Schmidt telescope of the Uppsala Southern Station. The stars with assigned numbers are those measured in the search for cluster members. The small dense group of stars on the outskirts of IC 2602 at $\alpha = 10^h 41^m$, $\delta = -64°{\cdot}9$ is the more distant cluster Melotte 101.

In a recent photoelectric study of the cluster, Braes (**1**) derived a distance of 150 parsecs, a value less than those of former investigators (**2**). From the absolute magnitude of the brightest main sequence star Theta Carina, and the position on the main sequence that gravitational contraction occurs, he derived an age of 15×10^6 years.

Observations

1. *Photoelectric.*—Three telescopes were used to obtain the photoelectric observations of the suspected cluster members. The investigation was begun with the Mt Stromlo 20-inch $f/18$ reflector, but most of the observing was carried out on the Mt Bingar 26-inch $f/12$ reflector and the Mt Stromlo 50-inch $f/18$ reflector. The photoelectric equipment consisted of an EMI photomultiplier, replaced by a refrigerated RCA 1P21 for the more recent observations, a GR amplifier or one built at Mt Stromlo, and a Brown Recorder. The filters used were those recommended by Johnson (**3**) for the linear transformations from instrumental magnitudes to those of the *UBV* system. The combinations of filters and photomultipliers are shown in the following table.

XUM

Telescope	*Cell*	*Filters*
20-inch	1P21	OY4; BG12+GG13; UG2
26-inch	EMI; 1P21	C3384; C5030+GG13; C9863
50-inch	1P21	C3384; BG12+GG13; UG2
		C3384; C5030+GG13; C9863

As mentioned above, the initial observations were carried out on the 20-inch telescope, but rarely were the nights of sufficient quality to compare accurately the cluster stars with the equatorial *UBV* standards of Johnson and Harris (4). Magnitudes and colours measured with this telescope were given lower weight than those obtained elsewhere.

The 26-inch telescope was used primarily for the transformation of the *UBV* system from the equatorial standards of Johnson and Harris to several stars in the vicinity of the cluster. A total of 23 *UBV* standards was measured for the transformations, the average number observed per night being 12. From five nights of good quality, the transformation equations determined were:

$$\begin{aligned} V-V_{26} &= -0{\cdot}102(B-V)+0{\cdot}142 \\ B-V &= 1{\cdot}156(B-V)_{26}+1{\cdot}964 \\ U-B &= 1{\cdot}051(U-B)_{26}-1{\cdot}051 \end{aligned}$$

with a mean error per measurement of 0·012 in V, 0·015 in $B-V$, and 0·018 in $U-B$.

The sensitivity of the photomultiplier was checked during each night with a radium source fitted in the filter wheel. To obtain extinction coefficients each night as well as to check on the constancy of transparency throughout it, two stars, one of early, the other of late spectral type, were observed several times. For nights of doubtful quality, the following mean extinction coefficients were used:

$$\begin{aligned} K_V &= 0{\cdot}18 \\ K_{B-V} &= 0{\cdot}15\text{-}0{\cdot}04\,(B-V) \\ K_{U-B} &= 0{\cdot}28 \end{aligned}$$

In general, stars were observed through focal apertures of 16″ and 29″.

The observational procedure with the 50-inch was the same as with the 26-inch, except that stars were observed with respect to the secondary standards. The following mean extinction coefficients were used on night of doubtful quality:

$$\begin{aligned} K_V &= 0{\cdot}18 \\ K_{B-V} &= 0{\cdot}12\text{-}0{\cdot}04\,(B-V) \\ K_{U-B} &= 0{\cdot}31 \end{aligned}$$

The reduction of observations was effected in the manner recommended by Johnson and Morgan (3). After the installation of an IBM 610 computer at Mt Stromlo early in 1960, subsequent reductions were carried out on it.

2. *Spectrographic.*—To obtain a luminosity and spectral classification of some of the cluster stars, spectrograms taken by Drs H. Gollnow and A. Przybylski for the measurement of radial velocities were kindly made available. They were obtained with a Zeiss two-prism spectrograph mounted at the $f/5$ Newtonian focus of the 74-inch reflector. The dispersion of the spectra is 90 A/mm at H-gamma. With IIaO and 103aO emulsions, and a projected slit-width of 20

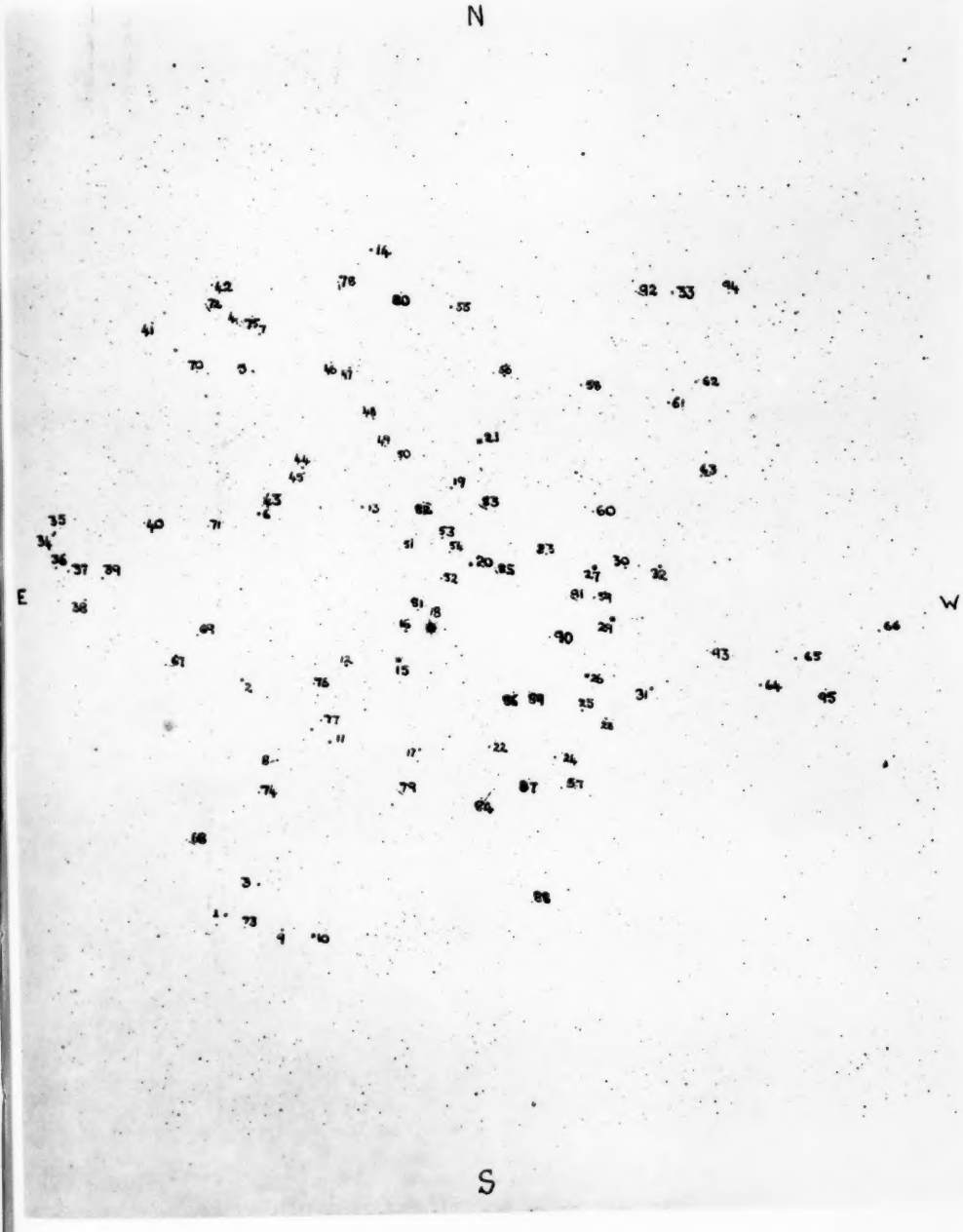

IC 2602

microns, exposure times varied from a few seconds for the star Theta Carina to 100 minutes for a ninth magnitude F2 star.

The spectral and luminosity classification of the stars was effected by comparison of their spectra with those of some of the MK standards listed by Buscombe (**5**) that had been obtained with the same spectrograph. It was based on the ratios of spectral-line intensities shown in the MKK Atlas (**6**) to be sensitive to spectral type or luminosity.

3. *Photographic.*—In a search for fainter possible members of the cluster, plates centred on $\alpha = 10^h 41^m$, $\delta = -64°{\cdot}2$ (1950) were taken in blue and visual light with the $f/3{\cdot}5$, 20/26-inch Uppsala Schmidt by Dr B. Westerlund and Mr D. Sher and kindly made available to the author. Plates in each colour were given exposures of 20 seconds, 30 seconds, and 3 minutes. The limiting stellar magnitude on plates with the last exposure exceeds 17. The photographic emulsion-filter combinations were:

Visual plates	103aD + 2 mm GG14 filter
Blue plates	IIaO + 2 mm GG13 filter

Images of selected stars on the plates were measured with a Haffner iris diaphragm photometer. Only one setting per star per plate was necessary as the setting errors are less than those due to the plate emulsion. The photometer readings were converted to *UBV* magnitudes on the basis of those stars already measured photoelectrically. To correct for the large field errors occurring on the plates, a basic calibration curve was constructed with the stars of Mel. 101 observed with the 50-inch, and the field errors determined from previously-measured stars that are on different parts of the plate. The mean error of a single reduction, $0^m{\cdot}05$, although large, is sufficient to determine whether the star is a possible cluster member.

Approximate spectral types of the stars in and near the cluster were shown on a plate of the field taken with the Schmidt telescope fitted with a 4° objective prism. With an exposure time of 10 minutes, spectra with a dispersion of 480 A/mm at H-gamma of stars as faint as 12th magnitude could be classified. An approximate spectral classification could be achieved by the comparison with the spectra of stars classified in the Henry Draper Extension (**7**).

Results

The stars measured photoelectrically are listed in Table I. The columns are: (1) the star's number in the present study; (2) its HD or HDE designation; (3) right ascension for the epoch 1950; (4) declination for the same epoch; (5) V; (6) $B-V$; (7) $U-B$; and (8) the number of times that the star was observed.

The stars having a great number of observations were those used as secondary standards.

The stars 1–33 were compiled previously at Mt Stromlo in a list of probable members for a radial velocity study of the cluster. The remaining stars are some of comparable brightness situated in the same general direction as the first group. B and V measurements of 27 of the listed stars have been made by Braes. The mean differences are (Braes–Whiteoak):

in V	$-0^m{\cdot}017\,(\pm 0{\cdot}018)$
in $B-V$	$+0^m{\cdot}013\,(\pm 0{\cdot}014)$.

XUM

TABLE I

Stars observed photoelectrically

No.	HD/HDE	1950 R.A.	Dec.	V	$B-V$	$U-B$	n
1	92385	10h36·2	−64°47	6·75	−0·08	−0·30	7
2	92467	10 37·1	−64 14	6·99	0·03	−0·16	8
3	92478	10 37·3	−64 42	7·56	0·05	0·00	9
4	92492	10 37·4	−63 25	9·27	0·12	0·04	11
5	92535	10 37·6	−63 32	8·25	0·21	0·10	9
6	92536	10 37·6	−63 51	6·34	−0·08	−0·31	8
7	92568	10 37·9	−63 26	8·58	0·42	0·14	9
8	92569	10 37·9	−64 26	9·46	0·22	0·15	6
9	92570	10 37·9	−64 50	8·86	0·47	0·02	1
10	92664	10 38·5	−64 50	5·52	−0·17	−0·59	7
11	92715	10 38·9	−64 24	6·82	−0·02	−0·14	9
12	92783	10 39·3	−64 13	6·74	−0·05	−0·22	13
13	92837	10 39·8	−64 00	7·18	0·00	−0·08	13
14	92896	10 40·1	−63 15	7·32	0·22	0·06	7
15	92938	10 40·5	−64 12	4·81	−0·15	−0·58	20
16	92966	10 40·6	−64 08	7·28	−0·01	−0·10	14
17	92989	10 40·8	−64 26	7·58	0·04	−0·01	8
18	93030	10 41·2	−64 08	2·78	−0·23	−1·03	8
19	93098	10 41·7	−63 48	7·61	0·04	0·00	9
20	93163	10 42·1	−63 59	5·79	−0·02	−0·55	11
21	93194	10 42·3	−63 42	4·84	−0·14	−0·62	9
22	93209	10 42·4	−64 25	9·41	0·32	0·25	10
23	93405	10 43·7	−63 58	9·17	0·44	0·01	11
24	93424	10 43·8	−64 27	8·14	0·15	0·08	14
25	93517	10 44·4	−64 20	7·86	0·09	0·07	12
26	93540	10 44·5	−64 15	5·36	−0·10	−0·48	10
27	93549	10 44·7	−64 00	5·26	−0·09	−0·48	12
28	93600	10 44·9	−64 22	8·44	0·50	0·02	15
29	93607	10 45·0	−64 07	4·87	−0·15	−0·65	9
30	93648	10 45·3	−64 00	7·85	0·11	0·08	10
31	93714	10 45·8	−64 17	6·57	0·00	−0·60	7
32	93738	10 46·1	−64 00	6·48	0·00	−0·16	9
33a	93796	10 46·3	−63 21	10·28	0·63	0·13	3
b				9·94	0·58	0·07	3
34	91906	10 33·1	−63 53	7·46	0·03	0·01	2
35	307860	10 33·2	−63 52	8·24	0·22	0·03	1
36	307861	10 33·2	−63 57	10·01	0·50	0·22	2
37	91944	10 33·4	−63 58	8·68	0·05	−0·38	2
38	91997	10 33·8	−64 02	8·95	0·04	−0·33	4
39	92066	10 34·2	−63 59	8·40	0·00	−0·43	4
40	307859	10 35·1	−63 52	10·35	0·20	0·05	1
41	307842	10 35·5	−63 24	9·33	0·73	0·33	1
42	307844	10 36·8	−63 19	9·30	1·41	1·47	1
43	307856	10 37·7	−63 50	10·58	1·22	1·15	2
44	92663	10 38·6	−63 45	7·81	1·51	1·68	17
45	307926	10 38·6	−63 46	9·70	1·34	1·49	6
46	307919	10 39·3	−63 30	10·06	1·14	0·90	1
47	92821	10 39·7	−63 31	8·87	1·28	1·31	1
48	307921	10 40·1	−63 38	9·04	1·58	1·60	2
49	307922	10 40·4	−63 42	9·99	0·60	0·18	2
50	307924	10 40·7	−63 44	10·70	0·62	0·02	1
51	307931	10 40·9	−63 56	10·11	1·21	1·07	14
52	307937	10 41·4	−64 01	9·76	0·11	−0·26	4

TABLE I—*continued*

No.	HD/HDE	R.A. 1950	Dec.	V	$B-V$	$U-B$	n
53	307933	10 41·5	−63 56	8·90	0·43	0·25	1
54	307934	10 41·7	−63 58	10·08	1·63	1·90	10
55	93115	10 41·8	−63 24	7·85	1·52	1·78	6
56	93269	10 42·8	−63 33	8·15	1·14	1·04	6
57	307963	10 43·9	−64 31	10·06	1·15	0·89	3
58	308006	10 44·6	−63 35	9·78	1·53	1·56	5
59	308015	10 44·7	−64 05	8·95	1·19	0·85	8
60	308012	10 44·7	−63 53	10·06	0·49	0·03	2
61	93777	10 46·4	−63 38	8·51	1·16	1·04	3
62	93874	10 47·0	−63 35	8·20	0·17	0·09	2
63	93892	10 47·1	−63 48	8·99	0·50	0·06	1
64	94066	10 48·1	−64 17	7·90	0·08	−0·38	5
65	94174	10 48·8	−64 13	7·76	0·11	0·06	3
66	94422	10 50·6	−64 09	8·24	0·10	−0·39	2

Fig. 1 shows the relation between the colours $B-V$ and $U-B$ of the stars observed. The stars 1–33 are represented by open circles, the remainder by dots. To the former has been fitted the unreddened colour relation given by Arp (**8**), displaced in $B-V$ by $0^m{\cdot}04$, the mean colour excess of the cluster, (E_{B-V}), and in $U-B$ by $0^m{\cdot}03$. From the positions of several of the circles relative to the curve, it appears that the stars whose numbers are 7, 20, 22 and 31 may not be members,

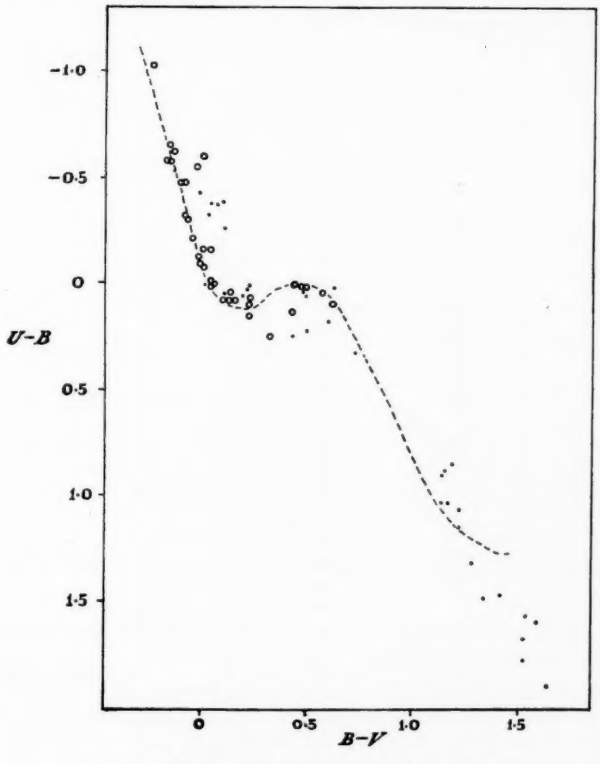

FIG. 1.—*Observed relation between colours of stars.*

assuming they represent normal main sequence stars. Of these, Braes has shown that 20 and 31 have radial velocities differing considerably from the mean value for the cluster. Most of the dots represent either more-reddened main sequence stars or background giants of late spectral type. Stars that may be associated with the cluster are Nos. 34, 35, 36, 41, 43, 49, 50, 60, 62, 63, 65. From the relation $A_V = 3{\cdot}0\,E_{B-V}$, the mean visual absorption for the cluster (A_V) is $0^m{\cdot}12$.

Table II contains the results of the spectral and luminosity classification of the stars. For the stars observed spectrographically with types earlier then Ao, values of $(B-V_0)$ were derived by the "Q" method (Johnson (**9**)). For stars of later spectral types, Arp's calibration (**8**) was used.

The columns of the table are: (1) Star number; (2) spectral type and luminosity class; (3) The number of spectra examined; (4) Spectral type from the "Q" method; (5) E_{B-V}; (6) $(B-V)_0$; (7) V_0; and (8) Notes on the spectra examined.

TABLE II

Determination of cluster reddening

No.	Sp.	n	Sp. ("Q")	E_{B-V}	$(B-V)_0$	V_0	Notes on spectra
1	B9 V	4	B8	·00	−0·08	6·75	
2	B9 IV	5	B9	·09	−0·06	6·72	
3	Ao IV	4	Ao	·06	−0·01	7·38	
4	Ao IV	4	Ao	·12	0·00	8·91	non-member.
5	A3 V	4		·12	0·09	7·89	
6	B8 IV	5	B8	·01	−0·09	6·31	
7	A7 p	5			0·38	8·46	enhanced lines of Sr and Fe.
8	B9·5 IV	7	Ao	·23	−0·01	8·77	non-member.
9	F7 V	4			0·43	8·74	Close visual binary.
	F5 IV	5					
10	B9 p	5	B5		−0·21	5·40	Si star.
11	B9·5 V	3	B9·5	·02	−0·04	6·76	
12	B8 V	5	B9	·01	−0·06	6·71	
13	B9 V	4	B9·5	·03	−0·03	7·09	
14	A5 IV	5		·07	0·15	7·11	
15	B3 V	5	B5	·01	−0·16	4·78	
16	B9·5 V	2	B9·5	·02	−0·03	7·22	
17	A1 IV	6	Ao	·05	−0·01	7·43	
18	Bo V	4	Bo	·05	−0·28	2·63	O9·5 (V).
19	Ao V	5	Ao	·05	−0·01	7·46	
20	B3 V	4	B4	·15	−0·17	5·34	B3: V (V); non-member.
21	B5 V	4	B4	·03	−0·17	4·75	B5 Vn (V).
22	A4 IV	5		·20	0·12	8·81	non-member.
23	F2 V	4		·06	0·38	8·99	
24	A4 IV	5		·03	0·12	8·05	
25	A2 V	4		·03	0·06	7·77	
26	B6 V	5	B6	·04	−0·14	5·24	B7: V (V).
27	B7 IV	4	B6	·05	−0·14	5·11	
28	F7 V	4		·00	0·50	8·44	
29	B4 V	6	B4	·03	−0·18	4·78	B4 IV (V); B3 IV (M).
30	A2 V	4		·05	0·06	7·70	
31	B2 IV	8	B3	·24	−0·24	5·85	non-member.
32	Ao V	5	B9	·05	−0·05	6·33	
33a	G2 IV	2		·00	0·63	10·28	
b	F8 V	2		·05	0·53	9·79	

In Col. (8), previous classifications are shown. Those followed by (V) were observed by Mme de Vaucouleurs (**10**), those by (M) by Miss Morris (**11**). From Col. (5), one can see that the stars Nos. 8, 20, 22 and 31 are more reddened than the remainder and are presumably background stars, as they appear to have normal spectra. Stars with peculiar spectra, Nos. 7 and 10, have been corrected for absorption by the reduction of their values of V and $B-V$ by the means of individually-determined colour excesses and visual absorptions, $0^m{\cdot}04$ and $0^m{\cdot}12$ respectively. In addition to the four excessively-reddened stars, No. 4 is too faint for its spectral type for it to be a member. The stars observed spectrographically are represented in the colour-magnitude array, corrected for absorption, of Fig. 2. The doubtful members are shown as open circles. To the

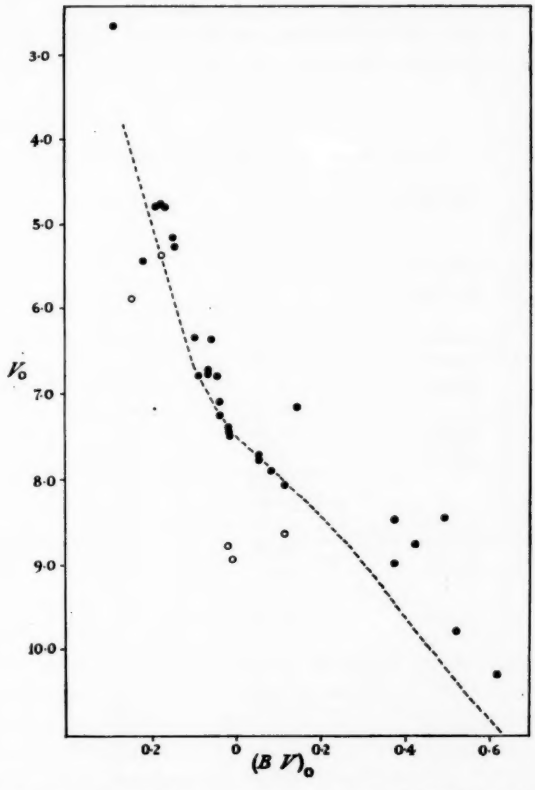

FIG. 2.—*Colour-magnitude array of the cluster, corrected for absorption.*

filled circles has been fitted the 'zero-age' main sequence of Johnson and Iriarte (**12**), displaced $5^m{\cdot}94$ vertically, the distance modulus of the cluster. It is equivalent to a distance of 155 parsecs, similar to the value (150) determined by Braes. A feature of the main sequence is that it does not seem to extend to magnitudes fainter than $V_0 = 8{\cdot}7$. This could be due to the effects of gravitational contraction

for the fainter stars, a lack of stars of spectral type F in the cluster, or the fact that the survey for cluster members is incomplete at the fainter magnitudes.

A spectroscopic parallax for the cluster was not derived, for the MK – M_V calibration would not account for the fact that the brighter stars have already evolved to a position above the main sequence and are therefore more luminous than their main sequence calibration would predict. The same argument applies to the apparently contracting stars, although until some other membership criterion like radial velocities can be considered, it is not certain whether they are contracting cluster stars or foreground objects.

On the visual, blue and objective-prism Schmidt plates, an area of sky $1\frac{3}{4}^\circ$ in diameter was examined in a search for fainter possible members. V and $B-V$ measures were obtained for such stars. The additional possible members are listed in Table III. The columns are: (1) the number of the star in the present survey; (2) the HD or HDE number of the star; (3) V; (4) $B-V$; and (5) its spectral type—either that assigned to it in the Henry Draper Extension or that derived from the spectrum on the objective prism plate.

TABLE III

Possible members observed photographically

No.	HD/HDE	V	$B-V$	Sp.
67		10·75	1·19	K
68		11·01	1·44	K-M
69	308023	9·80	0·96	Ko
70	307849	10·43	0·33	F
71		10·54	0·40	G5
72	307845	10·90	0·50	Go
73	307885	10·83	1·17	Ko
74	308011	9·82	1·16	Ko
75		10·42	0·53	Go
76	307942	10·03	0·42	F5
77	307944	9·40	1·07	Ko
78		10·93	0·69	Go
79		11·46	0·83	G
80	307918	10·72	0·88	G
81	307938	10·48	0·57	Go
82	307929	10·65	1·03	K2
83		10·96	1·10	G7
84	307960	11·33	0·91	G5
85	307936	10·87	0·70	F7
86	307955	10·84	0·95	Ko
87	307969	10·98	1·32	K7
88	307979	10·96	0·68	Go
89	307956	10·96	0·64	G
90	308016	10·59	0·98	K2
91		10·64	0·56	Go
92		11·08	0·51	Go
93		10·87	1·55	K5
94		10·12	1·26	K2
95		10·70	1·08	G5-Ko

The total population of the cluster is shown in the colour-magnitude array of Fig. 3. The probable members are shown as filled circles, additional photo-electrically-measured stars as open circles, and those measured photographically

as dots. To the first group has been fitted the 'zero-age' main sequence. The additional curve leaving the main sequence at $V=8{\cdot}4$ would define the bright magnitude limits at the faint end of a colour-magnitude array of a cluster with a luminosity function similar to that of NGC 2264 (Walker (**13**)) but with an age similar to that of IC 2602. Despite the fact that in addition to fainter members, several field stars probably are included in the figure, the cluster still shows the lack of F stars mentioned previously.

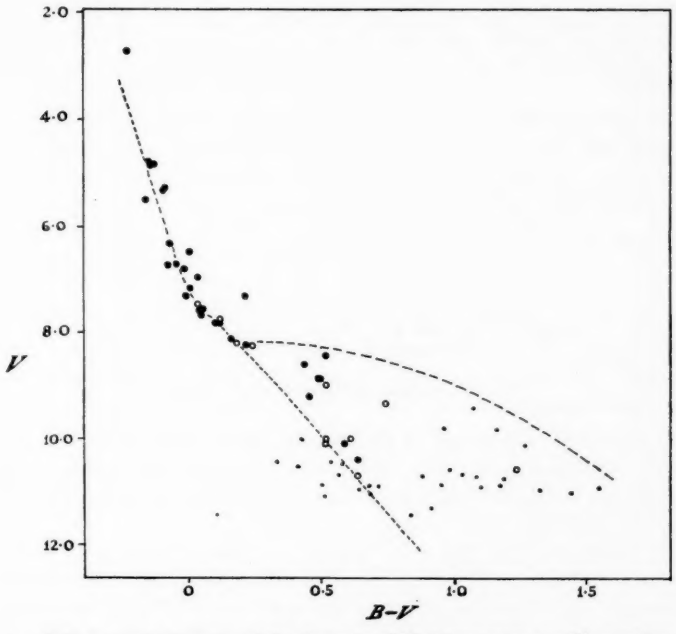

FIG. 3.—*Colour-magnitude array of the cluster in which fainter stars, possibly members, have been included.*

Discussion

Luminosity function.—The luminosity function of the cluster is shown in Fig. 4, the distribution of the number of stars per unit magnitude ($N[M_V]$) with absolute magnitude (M_V). The broken line for M_V greater than 3 represents that part of the luminosity function which is not so well-defined. The curve in the figure is the Initial Luminosity Function adopted by Limber (**14**). It was normalized to the cluster so that the number of members it predicts between the limits of absolute magnitude -1 and $+2$, a range within which the observed membership of the cluster is complete but has not been affected yet by evolution, is equal to the observed number. Compared with the Initial Luminosity Function, that of the cluster appears to be lacking in stars of absolute magnitude $+3$ and $+4$. This is consistent with the conclusions of van den Bergh and Sher (**15**) that galactic clusters do not have a unique luminosity function. Attempts were

made previously to estimate the number of faint cluster members by star counts and the distribution of stars of late spectral types, i.e. stars with objective prism spectra showing pronounced H and K lines. Both were unsuccessful due to the irregular background absorption.

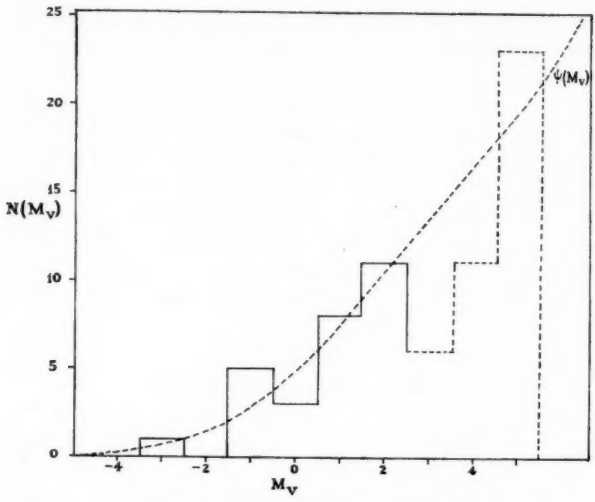

FIG. 4.—*Luminosity function of IC 2602.*

Age of the cluster.—The age of the cluster can be derived by two methods: (1) from the absolute magnitude of the brightest star on or near the main sequence; and (2) the position on the main sequence below which the stars are still in the process of gravitationally contracting on to it.

The brightest star near the main sequence, Theta Carina, at present has an absolute magnitude of $-3{\cdot}3$. It is already evolving from the main sequence and if it is assumed that it has moved almost vertically from it, its absolute magnitude on the main sequence would have been $-2{\cdot}8$. According to the results of recent calculations of star models (Limber (**15**)), such a star would attain an absolute magnitude of $-3{\cdot}9$ in a time of $1{\cdot}2 \times 10^7$ years since its formation before the hydrogen in its core is exhausted and it evolves from the neighbourhood of the main sequence. As the time that it takes to brighten to this magnitude from its value on the main sequence is small compared with the age of the star, then assuming that all the cluster stars are coeval, the cluster would have an age of $1{\cdot}2 \times 10^7$ years. This value is greater than that determined with the older Schönberg–Chandrasekhar theory.

The cluster main sequence appears to terminate at $V_0 = 8{\cdot}7$ i.e. $M_V = +2{\cdot}8$, equivalent to a star of mass $1\frac{1}{2}$ solar masses. Henyey, Le Levier and Levee (**16**) have calculated that a star of such a mass contracts gravitationally on to the main sequence in a time of 8×10^6 years. If it is assumed that the termination is due only to the effects of gravitational contraction, which as mentioned previously is doubtful, then the age of the cluster would be 8×10^6 years. For IC 2602, the age calculated from this method would be expected to be less accurate than the first.

From both considerations, it appears that the age of the cluster is about 10^7 years.

Proper motions.—Proper motions of eighteen of the cluster stars are listed by Boss (**17**). The mean values are:

$$-0^s.0024 \pm 0.0008; \qquad -0''.005 \pm 0.010.$$

at a distance of 150 parsecs in the direction of the cluster, the apparent proper motions due to solar motion are:

$$-0^s.0015; \qquad +0''.007.$$

It appears that most of the apparent motion of the cluster is due to the effects of solar motion. For this reason it is difficult to detect members using the criterion of common proper motions—the General Catalogue lists many stars, obviously non-members of the cluster but in its general direction, that have comparable proper motions.

From an analysis of the proper motions of the members, Markarian (**18**) suggested that the cluster is expanding. A similar conclusion in the case of the association I Lac was criticized by Woolley and Eggen (**19**), and it is quite likely that for IC 2602, any apparent expansion effect is due also to systematic errors in the proper motions, particularly as the determined expansion age (3×10^5 years) is considerably smaller than the age derived in the present study.

The relation of IC 2602 to the Scorpio-Centaurus Association

As the Scorpio-Centaurus association is a close group of young stars, it is of interest to investigate the possibility that IC 2602 is related to it. According to Blaauw's list of certain members (**20**), the association extends from $09^h\,00^m$ to 19^h00^m in right ascension and in the direction of the cluster it has a similar declination. The mean of the radial velocities of the cluster stars listed by Wilson (**21**) is +24 km/sec, a value comparing favourably with that of the association in the direction of the cluster (Buscombe and Morris (**22**)).

From a study of the proper motions of the association stars, Bertiau (**23**) derived a distance of 170 parsecs. Moss Morris (**11**), on the other hand, determined a distance of 220 parsecs from a spectral and luminosity classification of the certain members. She used the relation between MK classification and absolute magnitude of Johnson and Iriarte (**12**), where the luminosity class V is derived from the stars in the vinicity of the Sun. For stars of early spectral type, it includes those stars that are already beginning to evolve from the main sequence, so that the mean absolute magnitude for a star of a certain spectral type is more negative than the value it had on the main sequence. The use of such a calibration would result in an overestimation of the distance. A colour-magnitude array of the association, constructed from the magnitudes and colours of Bertiau for Blaauw's probable members, reveals that the average reddening (excluding the more heavily reddened star Sigma Sco) is $0^m.04$ and the average distance of the group is 150 parsecs. The latter value is only approximate because of the lack of stars of later spectral types. Both of these figures agree with those of the cluster.

The age of the association, determined from the main sequence stars of earliest spectral type (Bo), is about 10^7 years, similar to that of the cluster.

The above evidence suggests that IC 2602 may be a local condensation of the Scorpio–Centaurus Association.

Acknowledgments.—I am grateful to Professor B. J. Bok for his encouragement, and to those astronomers at Mt Stromlo mentioned in the paper. This work was carried out partly with the aid of an Australian National University Research Scholarship and partly with the aid of a General Motors Post graduate Scholarship.

Mt Stromlo Observatory,
Canberra, A.C.T.,
Australia:
1961 *June.*

References

(1) Braes, L. L. E., *M.N.A.S.S.A.*, **20,** 7, 1961.
(2) Alter, G., Ruprecht, J., and Vanysek, V., " Catalogue of Star Clusters and Associations " (Czech. Acad. Sci., 1958.)
(3) Johnson, H. L., and Morgan, W. W., *Ap. J.*, **117,** 313, 1953.
(4) Johnson, H. L., and Harris, D. L., *Ap. J.*, **120,** 196, 1954.
(5) Buscombe, W., Mt Stromlo Mimeogram No. 3, 1959.
(6) Morgan, W. W., Keenan, P. C., and Kellman, E., " An Atlas of Stellar Spectra ", Univ. Chicago Press, 1943.
(7) Cannon, A. J., and Mayall, M. W., *H. A.*, **112,** 1949.
(8) Arp, H. C., *Handbuch der Physik*, **51,** 75, 1958.
(9) Johnson, H. L., Lowell Obs. Bull. No. 90, 1958.
(10) de Vaucouleurs, A., *M.N.*, **117,** 449, 1957.
(11) Morris, P. M., *M.N.*, **122,** 325, 1961.
(12) Johnson, H. L., and Iriarte, B., Lowell Obs. Bull. No. 91, 1958.
(13) Walker, M. F., *Ap. J. Supp.*, Ser. II, 365, 1956.
(14) Limber, D. N., *Ap. J.*, **131,** 168, 1960.
(15) van den Bergh, S., and Sher, D., *Pub. David Dunlap Obs.*, **2,** 203, 1960.
(16) Henyey, L. G., Le Levier, R., and Levee, R. D., *P.A.S.P.*, **67,** 154, 1955.
(17) Boss, B., *General Catalogue*, **3,** 1936.
(18) Markarian, B. E., *Buir. Soob.*, **11,** 19, 1953.
(19) Woolley, R.v.d.R., and Eggen, O. J., *Obs.*, **78,** 149, 1958.
(20) Blaauw, A., Pub. Kapteyn Ast. Lab. Groningen No. 52, 1946.
(21) Wilson, R. E., Pub. Carnegie Inst. Washington No. 601, 1953.
(22) Buscombe, W., and Morris, P. M., *M.N.*, **121,** 263, 1960.
(23) Bertiau, F. C., *Ap. J.*, **128,** 533, 1958.

CAN GRAVITATIONAL FORCES ALONE ACCOUNT FOR GALAXY FORMATION IN A STEADY STATE UNIVERSE?

II. Bondi–Gold Universes

Martin Harwit

(Received 1961 July 10)

Summary

The accretion problem in a Bondi–Gold steady state universe is examined. We show that if galaxies are to be formed in a homogeneous universe by predominantly gravitational means, the cosmic density must be at least

$$\rho_{\min} = 15/4\pi\gamma T^2$$

where γ is the gravitational constant and T^{-1} is Hubble's constant. This is ten times the value initially specified by Hoyle for a steady state universe whose expansion rate is governed by the general relativistic field equations. For a Hubble's constant $2{\cdot}5 \times 10^{-18}$ sec^{-1}, the minimum density $\rho_{\min} = 9 \times 10^{-29}$ g cm^{-3}. This is higher than the usually estimated maximum density of the Universe, but present estimates are not yet well enough established to rule out definitely gravitational galaxy formation in an arbitrary steady state universe.

1. *Introduction.*—In 1948 two different types of steady state cosmologies were proposed in quick succession. Bondi and Gold (**1**) described a steady state (BGSS) universe which was not necessarily governed by the laws of general relativity. The authors felt that there was no reason to believe that general relativity was valid on the scale of the entire universe; observations had only verified the theory on the scale of the solar system.

An alternate version of the theory proposed by Hoyle (HSS) (**2, 3**) incorporates the general relativistic field equations and is, therefore, able to relate the expected mean density ρ_0 of the universe to $1/T$, Hubble's constant. The relationship is

$$\rho_0 = 3/8\pi\gamma T^2.$$

A recent (**4**) examination of gravitational galaxy formation in steady state universes showed that in an HSS universe gravitational forces alone cannot bring about galaxy formation. Even in the presence of an existing condensation (galaxy, cluster of galaxies), gravitational forces are not sufficiently powerful to gather large amounts of matter from regions surrounding the condensation. In particular, the HSS theory would require that the mass M of condensations grows at a rate $dM/dt = 3M/T$, whereas it was possible to show that only a small fraction of the mass of the condensation can be replenished by infall of matter during any period $T/3$.

This criticism cannot be directly levelled against the BGSS theory, since its density is not necessarily computed from the general relativistic equations and could be much higher than the HSS density.

Simple calculations performed in (**4**) showed that gravitational forces could play a dominant role in BGSS galaxy formation only if the density of the universe was greater than a certain minimum $\rho_{\min}$. The purpose of the present paper is to tighten the previously used argument and thus increase the value $\rho_{\min}$ more nearly

to its actual value. At the same time, we will investigate just how a steady state galaxy may be defined.

2. *Motion of gas in the neighbourhood of a galaxy.*—Consider an element of gas a distance r from the central condensation. At any given time, momentum conservation requires that

$$(\rho+\delta\rho)(\dot{r}+\ddot{r}\delta t)-\rho\dot{r}=\rho\ddot{r}\delta t+\dot{r}\delta\rho=-\frac{M\rho}{r^2}\,\delta t+\frac{r\rho}{T^2}\delta t+\frac{r}{T}\delta\rho \qquad (1)$$

where the mass of the galaxy, M, now contains the gravitational constant γ and $\delta\rho$ is the mass newly created within unit volume during time interval δt. The first term on the right is the gravitational attraction of the galaxy, the second term is the cosmic expansion force, and the last one represents momentum transfer from newly created matter. Setting the instantaneous density $\rho=\epsilon\rho_0$ and using the creation rate $\delta\rho=(3\rho_0/T)\delta t$, one can rewrite (1) as

$$\ddot{r}=-\frac{M}{r^2}+\frac{r}{T^2}+\frac{3}{\epsilon T^2}\,r-\frac{\dot{r}}{\epsilon}\frac{3}{T}. \qquad (2)$$

Here both M and ϵ are functions of r and t. The mass of the galaxy as seen by an element at distance r is expressed as

$$M(t)=M(0)+\frac{4\pi}{3}\left[\int_0^t r^3\left(\frac{3\rho_0}{T}\right)dt-(r^3-r_i^3)\rho_0\right] \qquad (3)$$

where $M(0)$ is the mass at time $t=0$ when the particle was at a position r_i. The term under the integral sign represents mass gain through continued creation of matter within a sphere described by the radial position of the particle; the last term gives the mass that would be found in the volume swept out by elements moving from r_i to r, if the volume were filled with gas at the general steady state density ρ_0. This last term is necessary since we are only concerned with 'gravitationally active' mass, i.e. mass in excess of the normal steady state mass $\rho_0 V$ enclosed in a volume V.

To determine ϵ we make use of equation (3) and take the mass enclosed by two spherical shells at slightly different radii r_1 and r_2

$$M_1-M_2=M_1(0)-M_2(0)+\frac{4\pi}{3}\left\{\int_0^t (r_1^3-r_2^3)\frac{3\rho_0}{T}\,dt-\rho_0[(r_1^3-r_2^3)-(r_{1i}^3-r_{2i}^3)]\right\}. \qquad (4)$$

We now choose the same initial boundary conditions used in (**4**), namely we assume that at $t=0$ gas at a distance r_i is receding from the galaxy with a speed r_i/T, and the density outside the central condensation is ρ_0 everywhere. Then $M_1(0)=M_2(0)$. Letting $r_1-r_2\equiv\Delta r$ and $r_1+r_2\equiv 2r$, with $\Delta r\ll r$, equation (4) reduces to

$$\epsilon\rho_0=\frac{M_1-M_2}{4\pi r^2\Delta r}+\rho_0=\frac{3\rho_0}{Tr^2\Delta r}\int_0^t(\Delta r)r^2dt+\frac{\rho_0 r_i^2\Delta r_i}{r^2(\Delta r)}. \qquad (4\,a)$$

To simplify the notation we define a distance r_0 by

$$M(0)=27\,r_0^3/8T^2. \qquad (5)$$

(This equation corresponds to equation (5) of (**4**).) We also define a constant K as

$$K\equiv 4\pi T^2\rho_0/3. \qquad (6)$$

We shall express the initial position r_i of a given element of matter by $r_i=nr_0$. Its position at any subsequent time t will be called αnr_0 or αr_i. In this notation

$$\beta\equiv\Delta r/\Delta r_i=r_i[\Delta\alpha/\Delta r_i]+\alpha \qquad (7)$$

and equation (4a) can be rewritten as

$$\epsilon = \frac{3}{\alpha^2 \beta T} \int_0^t \alpha^2 \beta \, dt + \frac{1}{\alpha^2 \beta}. \tag{8}$$

To integrate the equation of motion (2), we multiply both sides by r. Substituting the expression (3) for M in equation (2) and integrating each term on the right side of (2) separately, we obtain, in the new notation of (5) and (6):

$$\dot{\alpha}^2 = \left[\frac{27}{4n^3 T^2} + \frac{2K}{T^2}\right]\left(\frac{1}{\alpha} - 1\right) + \frac{K}{T^2}(\alpha^2 - 1) - \frac{6K}{T^3}\int_0^t \frac{\dot{\alpha}}{\alpha^2}\left[\int_0^t \alpha^3 dt\right] dt$$
$$+ \frac{\alpha^2}{T^2} + \frac{6}{T^2}\int_0^t \frac{\alpha\dot{\alpha}}{\epsilon} - \frac{6}{T}\int_0^t \frac{\dot{\alpha}^2}{\epsilon}\, dt. \tag{9}$$

3. *Mass growth.*—Consider the mass enclosed by a spherical shell at distance α. The mass growth is $\Delta M = M(t) - M(0)$. From equations (3), (5) and (6), this becomes

$$\frac{\Delta M}{M_0} = \frac{8Kn^3}{27}\left[\frac{3}{T}\int_0^t \alpha^3 \, dt - (\alpha^3 - 1)\right]. \tag{10}$$

Suppose one requires that equation (10) satisfies the condition

$$\frac{\Delta M}{M_0} = A^N - 1 \tag{11}$$

at time $t = NT/3$, where $A > 1$ is a constant and $t \gg T$. This equation has the asymptotic solution

$$\alpha = aA^{t/T} \tag{12}$$

where 'a' is constant. Substituting expression (12) into equation (10) one finds that (for large N, which means $\alpha \gg 1$)

$$\frac{\Delta M}{M_0} \to \frac{8n^3 a^3 K}{27}\left[\frac{1}{\log A} - 1\right] A^N. \tag{13}$$

Through proper choice of parameters n and a, this expression can be made equal to any constant multiple of A^N.

One still has to satisfy oneself that the solution (12) also obeys the equation of motion (9), at least asymptotically. This, in fact, is the case. With

$$\alpha \to aA^{t/T}, \quad \dot{\alpha} \to (\log A/T)\alpha, \tag{14}$$
$$\epsilon \to (\log A)^{-1}$$

one can rewrite (9) as

$$\left(\frac{\log A}{T}\right)^2 \alpha^2 \to \frac{K}{T^2}\alpha^2 - \frac{(6 \log A)}{T^3} K \int_0^t \frac{1}{\alpha}\left[\int_0^t \alpha^3 \, dt\right] dt + \frac{\alpha^2}{T^2}$$
$$+ \frac{6(\log A)^2}{T^3}\int_0^t \alpha^2 \, dt - \frac{6(\log A)^3}{T^3}\int_0^t \alpha^2 \, dt \tag{15}$$

where only terms proportional to α^2 are kept. This leads to

$$\left(1 - \frac{1}{\log A}\right) K \to 4(\log A)^2 - 3 \log A - 1 \tag{16}$$

or

$$K \to 4(\log A)^2 + \log A. \tag{17}$$

In the steady state universe one is interested in the case where A equals the natural number e, so that $K \to 5$*.

* In the HSS universe, with $K = \frac{1}{2}$, one has $\log A = \frac{1}{4}$ and the asymptotic mass growth rate $\propto e^{3t/4t}$.

Now consider a situation in which A is chosen slightly lower than e, say $A=e(1-x)$ in the limit $x\to 0$. Then

$$\log A=\log e+\log(1-x)\to 1-x-x^2/2. \tag{18}$$

One notes that in equation (13), the terms depending on A reduce to

$$e^N x(1-x)^N. \tag{19}$$

This means that even for small x, the mass growth will eventually fall behind the required value, no matter how large the coefficient in equation (13) is made through appropriate choice of large n and a values.

One now defines the boundary of a galaxy in the following way. Consider particles that move with speeds corresponding to an A value $A=(1-x)e$. At some large distance from the central condensation there will be particles which move faster than this, and in particular at extreme distances A becomes identical with e. (This implies, of course, that a condensation must be surrounded by a region of density below ρ_0 at some distance.) One can now define the boundary of the galaxy as the location of the furthest element that moves according to the prescription $A=e(1-x)$. Particles moving faster lie beyond this point and do not belong to the Galaxy.

Unfortunately this definition breaks down in the interesting case of primary concern, namely when $A=e$, for then the entire Universe would fall into the domain of the Galaxy.

One might note that for $K>5$ there is no solution of (16) for which $A\leqslant e$. At first sight one might be surprised that there even exist asymptotic solutions of (9) for which $A>e$. However, the reason for this possibility is that an expansion faster than $\exp(t/T)$ leads to a density less than ρ_0 in the volume enclosed by a shell of 'radius' α. This enclosed volume therefore has negative 'gravitationally active' mass which actually repels matter at α.

4. *Stability of the solution.*—To test the stability of the solution (12) one examines a slightly perturbed function

$$\alpha=aA^{t/T}+\eta\equiv\alpha_0+\eta \tag{20}$$

where $\eta\ll\alpha_0$, and one writes the time derivatives as $\dot\alpha=\dot\alpha_0+\dot\eta$. Substituting expression (20) in the equation of motion (9) subject to $\alpha\gg 1$, one obtains an integral equation relating η to $\dot\eta$. We are primarily interested in the sign of $\dot\eta$ relative to η. If η and $\dot\eta$ have opposite signs the solution (12) is stable; otherwise not.

To perform the indicated integrations, one can assume that η and $\dot\eta$ are slowly varying functions and can be replaced by suitable average values $\langle\eta\rangle$ and $\langle\dot\eta\rangle$, for simplicity in integration. This can always be accomplished by choosing a short enough integration interval $t-t_p$, where t_p marks the onset of the perturbation and t is the instant at which $\dot\eta$ is evaluated. Neglecting all terms higher than first order in η and $\dot\eta$, one finds after lengthy but straightforward reduction that terms independent of η again lead to equation (16), while terms linear in η and $\dot\eta$ give

$$\begin{aligned}[14z-6+2Kz^{-2}]\langle\dot\eta\rangle=\langle\eta\rangle T^{-1}\{&[6z+2(K+1)-5Kz^{-1}]\\&+\tfrac{9}{2}[z^2-z]\}+\tfrac{3}{2}[z^2-z]\theta\end{aligned} \tag{21}$$

where, for brevity, we have set $z=\log A$, $\theta=\beta-\alpha$ in equation (7).

We are interested in values of A near the natural number e. When $A=e$, the second and third terms on the right of equation (21) vanish, and the equation reduces to

$$\langle\dot{\eta}\rangle = -\tfrac{7}{18}\langle\eta\rangle T^{-1}.$$

The solution is stable for $A=e$. We rewrite (21) as

$$[14z+2+2z^{-1}]\langle\dot{\eta}\rangle = T^{-1}\langle\eta\rangle[\tfrac{25}{2}z^2-\tfrac{33}{2}z-3]+\tfrac{3}{2}[z^2-z]\theta$$

with the aid of (17). For $A<e$, i.e. when $0<z<1$, the coefficient of $\langle\dot{\eta}\rangle$ is always positive, and that of $\langle\eta\rangle$ is always negative, its absolute value being at least 25/3 times larger than the coefficient of θ. Since $|\theta|$ will usually not exceed $|\eta|$ except possibly in some small regions, the overall effect of the θ term will be small compared with the $T^{-1}\langle\eta\rangle$ term, so that over large regions the solution (12) will be stable for $A<e$. When η is independent of r_i, $\theta=0$ and the perturbation always leads to instability for $A>e$.

5. *Discussion.*—The motion of gas particles can be computed using equation (9). Fig. 1 illustrates the particle trajectories for $K=5$, and n values 0·85, 1·0 and 1·18. Curve c is particularly instructive. One notes an initial decrease in speed at time $t=0$, when the gravitational field of the galaxy M is 'turned on'. As the gas flows outward at this new, reduced speed, the momentum of locally created matter accelerates it away from the central condensation. However, the rate of mass growth determined by equation (3) eventually overpowers the repulsive forces due to newly created matter, and the gas is rather rapidly decelerated, the direction of its motion being reversed shortly after time T.

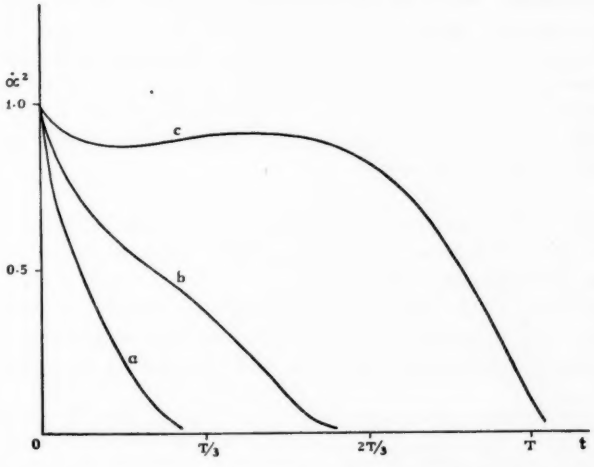

FIG. 1.—*Particle trajectories given in terms of the dimensionless parameter* α. α^2 *is plotted as a function of time for n values (a)* 0·85, *(b)* 1·00, *and (c)* 1·18. *The density of the universe is taken as* $K=5$.

All the trajectories of Fig. 1 were computed by means of an iteration method, working entirely with equation (9) with $\alpha=1$ and $\dot{\alpha}=1$ at $t=0$. In order to keep the labour involved within reason, it was assumed that $\beta=\alpha$ in equation (7). This yields a fair approximation to the actual trajectories since, at short times after $t=0$,

α is only weakly dependent on r_i; even as late as $t = T/3$, $\alpha = 1{\cdot}261$ for $n = 1{\cdot}0$ while $\alpha = 1{\cdot}314$ for $n = 1{\cdot}18$. At later times, when β does appreciably differ from α, the first term on the right of equation (8) dominates the value of ϵ and in this term the influence of β is somewhat limited. Furthermore ϵ appears in only two terms which are roughly equal, opposite in sign, and have integrands directly proportional to ϵ^{-1}. This leads to a weak ϵ-dependence. Still, the actual values shown by the curves should be taken with caution. They are intended primarily to indicate trends in the particle motion.

The mass values for the three curves at times when $\dot{\alpha} = 0$, i.e. when the gas just starts falling back into the galaxy, are

n	Time	M	Expected M
0·85	1/3 T	1·7 M_0	2·7 M_0
1·00	2/3 T	4 M_0	7·4 M_0
1·18	1·02 T	16 M_0	21·5 M_0

One notes that the last value, i.e. 16 M_0, is an appreciable fraction of the ideally expected 21·5 M_0, based on a simple exponential growth expectation. It appears that at time T the transient effects are becoming smaller, and one approaches the mass growth rates expected for $K = 5$. At the same time, one notes that if one wishes the Galaxy to grow sufficiently within just a few periods $T/3$, K should be chosen higher than 5.

This numerical work substantiates the previously derived conclusions based on the asymptotic behaviour of α: the value $K = 5$ represents a minimum density that would be needed if galaxies in a Bondi–Gold universe are to be formed by gravitational means. $K = 5$ denotes a density ten times that initially postulated in Hoyle's relativistic steady state model. For $T = 4 \times 10^{17}$ sec, the minimum density is found to be 9×10^{-29} g cm^{-3}. This is considerably higher than the normally estimated maximum density of the universe, but the next few years should definitely settle on observational grounds whether or not the actual density of the universe is too small to sustain gravitational galaxy formation in a Bondi–Gold steady state universe.

Acknowledgments.—I am greatly indebted to Professor H. Bondi who not only pointed out the need for examining this problem but in a number of discussions offered many guiding criticisms.

This work was made possible through a NATO postdoctoral fellowship and the hospitality of Cambridge University. Partial support was also received from a NSF postdoctoral fellowship currently held at Cornell University.

Cambridge University:
1961 *July*.

Now at: *Cornell University*,
Ithaca,
New York,
U.S.A.

References

(1) H. Bondi, T. Gold, *M.N.*, **108**, 252, 1948.
(2) F. Hoyle, *M.N.*, **108**, 372, 1948.
(3) F. Hoyle, *M.N.*, **109**, 365, 1049.
(4) M. Harwit, *M.N.*, **122**, 47, 1961.

ERRATUM

M.N., **122,** No. 1, 1961 :

M. Harwit, *Can gravitational forces alone account for galaxy formation in a steady-state universe?*

p. 48, equation (5),

for $r_{0\max} = (8M\gamma/3H^2)^{1/3}$ *read* $r_{0\max} = (8M\gamma/27H^2)^{1/3}$

THE DETERMINATION OF THE INCIDENT FLUX OF RADIO-METEORS

II. Sporadic Meteors

T. R. Kaiser

(Received 1961 July 26)

Summary

The theory relating the radio-echo rate to the incident meteor flux is extended to the case of sporadic meteors. It is shown that the relation between total influx and the echo rate observed at the equator with a suitably oriented aerial should be substantially independent of the distribution of sporadic radiants over the celestial sphere. The meteoric influx as a function of limiting magnitude (to $+11^{m}$) has been determined from experimental data. Results for sporadic meteors and for several showers are presented.

---

1. *Introduction.*—In Part I* of this work (**1**) formulae and graphical procedures were developed which enable the radio echo rate obtained with an equipment of given sensitivity and aerial configuration to be related to the absolute incident flux of shower meteors with a well defined radiant point. In extending the analysis to the case of sporadic meteors we must take account of the fact that the observed echo-rate is dependent upon the distribution of sporadic meteor radiants over the celestial sphere as well as upon other factors listed in the summary of Part I.

The incident flux of sporadic meteors whose radiants lie within an element of the celestial sphere of solid angle $d\Omega$ can be represented by (**2**),

$\Phi(\alpha_z)\,d\alpha_z\,d\Omega$ = flux producing zenithal electron line densities between α_z and $\alpha_z + d\alpha_z$,

$\Theta(\alpha_z)\,d\Omega$ = flux producing zenithal line densities greater than α_z.

These are the fluxes across a plane normal to the meteor paths. The mean, over the whole earth, of the sporadic meteor flux through a horizontal plane is therefore

$$\Theta_1(\alpha_z) = \tfrac{1}{4}\int_{4\pi} \Theta(\alpha_z)\,d\Omega \qquad (1)$$

where the integral is taken over the whole celestial sphere. The zenithal electron line density, α_z, is defined as the maximum number of free electrons per unit height produced along the meteor trajectory; it is related to the radio-magnitude, M, by (**3**)

$$M = -2{\cdot}5 \log_{10} \alpha_z + 35 \qquad (2)$$

and to the maximum electron line density, α_m, along the trail by

$$\alpha_z = \alpha_m (\cos \chi)^{-1} \qquad (3)$$

where χ is the radiant zenith distance.

* See corrections to Part I at the end of this paper.

XUM

Since the radio reflection points on the meteor trails are restricted to a narrow height range about a mean height $\bar{h}$ we can, for many purposes, consider the echoes as originating on the *echo surface* defined as the spherical surface at height $\bar{h}$. From a knowledge of the equipment parameters, the minimum detectable electron line density, α, can be calculated for each point on this surface and a set of sensitivity contours plotted for a range of values of the sensitivity factor ρ, as in Fig. 2, Part I*.

Some further concepts from Part I which will be valuable in the following are: (*a*) *The echo plane*; this is defined, for a given radiant point, as the plane normal to the radiant direction and passing through the location of the observer. (*b*) *The echo line*, which is the intersection between the echo plane and the echo surface.

2. *Sporadic meteors observed in a conical element, $d\omega$, of the aerial beam.*— For a given meteor distribution function, Θ, we can derive the rate of radio echoes within a conical element of the aerial beam by arguments similar to those used in a previous work concerned with the meteor height distribution obtained from radio-echo observations (**4**). The geometry is represented in Fig. 1. The conical element has half angle ψ and the radiants of the observed meteors consequently lie in the shaded strip of the celestial sphere of width 2ψ. The elevation of the

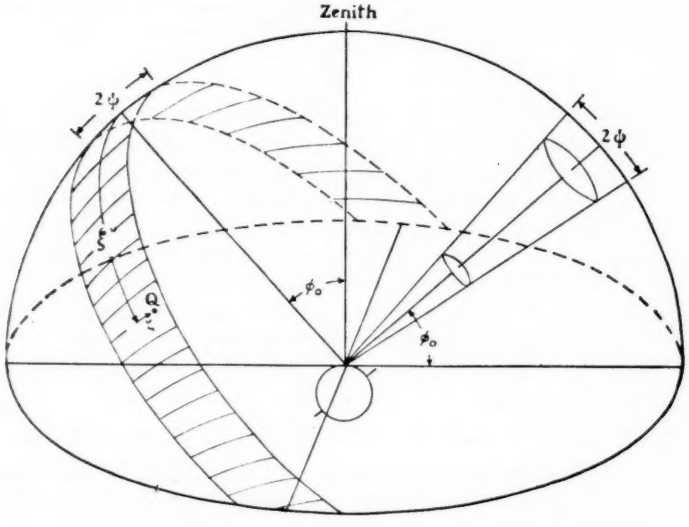

FIG. 1.—*Meteors observed in the conical element of the aerial beam (with semi-angle ψ) have radiant points* Q *(co-ordinates (ξ, ζ)) within the shaded strip of the celestial sphere.*

element above the horizontal is ϕ_0 measured at the location of the observer, and ϕ where it intersects the echo surface.

Let us consider meteors radiating from the point Q with co-ordinates (ξ, ζ) (see Fig. 1). The echo plane corresponding to Q will intersect the conical beam element, the angular intercept being $2(\psi^2-\zeta^2)^{1/2}$ and hence, referring to the echo plane geometry depicted in Fig. 1 of Part I, the linear intercept between the conical element and the echo line is $2R(\psi^2-\zeta^2)^{1/2}(\cos\theta)^{-1}$ where R is the range to the echo surface and θ is the angle between the beam element and the normal to the echo

*ρ is inversely proportional to the minimum detectable line density and may be normalized to a maximum value of unity.

line (in the echo plane). We can now use equation (14) of Part I, which relates the rate of echoes observed over unit length of the echo line to the incident flux of meteors, and obtain the echo rate observed within the beam element due to meteors radiating from an element of solid angle $\mathrm{d}\xi\,\mathrm{d}\zeta$ on the celestial sphere:

$$\text{Rate from } \mathrm{d}\xi\,\mathrm{d}\zeta = \frac{2RHI(\psi^2-\zeta^2)^{1/2}}{\sin\chi\cos\theta}\,\Theta\left(\frac{\alpha}{\cos\chi}\right)\mathrm{d}\xi\,\mathrm{d}\zeta \tag{4}$$

where H = atmospheric scale height,

I is defined by equation (15) of Part I,

χ = zenith distance of Q, measured on the echo line,

α = minimum detectable line density.

Integrating (4) with respect to ζ between the limits $-\psi$ to $+\psi$ and putting $\sin\chi\cos\theta = \sin\phi$ we obtain:

$$\text{Rate from strip } \xi-(\xi+\mathrm{d}\xi) = \frac{\pi RHI\psi^2}{\sin\phi}\,\Theta\left(\frac{\alpha}{\cos\chi}\right)\mathrm{d}\xi. \tag{5}$$

Putting $\pi\psi^2 = \mathrm{d}\omega$ and integrating with respect to ξ, we get:

$$\text{Rate within beam element } \mathrm{d}\omega = \frac{RHI}{\sin\phi}\left[\int_{-\pi/2}^{\pi/2}\Theta\left(\frac{\alpha}{\cos\chi}\right)\mathrm{d}\xi\right]\mathrm{d}\omega. \tag{6}$$

3. *Total rate per unit range interval.*—Consider a beam element of rectangular cross section at elevation ϕ_0 and azimuth ϑ and hence of solid angle $\mathrm{d}\omega = \cos\phi_0\,\mathrm{d}\phi_0\,\mathrm{d}\vartheta$. The range interval on the echo surface intercepted between elevations ϕ_0 and $(\phi_0+\mathrm{d}\phi_0)$ is $\mathrm{d}R = R(\tan\phi)^{-1}\,\mathrm{d}\phi_0$, hence

$$\frac{R\mathrm{d}\omega}{\sin\phi} = \frac{\cos\phi_0}{\cos\phi}\,\mathrm{d}R\,\mathrm{d}\vartheta.$$

Now from equation (32) of Part I

$$\frac{\cos\phi_0}{\cos\phi} = 1 + \frac{\bar{h}}{R_E}$$

where R_E is the earth's radius. To a sufficient approximation $\bar{h}/R_E$ can be neglected, compared with unity, and hence from (6) we get:

Total rate between ranges R and $(R+dR)$ and azimuths ϑ and $(\vartheta+\mathrm{d}\vartheta)$

$$= HI\,\mathrm{d}R\,\mathrm{d}\vartheta\int_{-\pi/2}^{\pi/2}\Theta\left(\frac{\alpha}{\cos\chi}\right)\mathrm{d}\xi. \tag{7}$$

The distribution function Θ may be represented by

$$\Theta(\alpha_Z) \propto \alpha_Z^{(1-s)}.$$

Now $\cos\chi = \cos\phi\cos\xi \simeq \cos\phi_0\cos\xi$ and $\rho = \alpha_0/\alpha$; α_0 is the minimum detectable line density at range R in the direction of the beam axis and ϕ_0 is the elevation to range R on the echo surface. Using (7) we thus obtain the total echo rate $N\mathrm{d}R$, observed between ranges R and $R+\mathrm{d}R$:

$$N\mathrm{d}R = HI\;\mathrm{d}R\iint\Theta\left(\frac{\alpha_0}{\cos\phi_0}\right)(\rho\cos\xi)^{s-1}\,\mathrm{d}\xi\,\mathrm{d}\vartheta \tag{8}$$

where the integral with respect to ϑ is taken across the beam at constant range R. If the aerial beam is sufficiently narrow in azimuth, so that Θ is reasonably constant over a distance on the celestial sphere of the order of the beam width, (8) becomes

$$N\mathrm{d}R \simeq HI\,\mathrm{d}R \int \rho^{s-1}\,\mathrm{d}\vartheta \int_{-\pi/2}^{\pi/2} \Theta\left(\frac{\alpha}{\cos\phi_0}\right)\cos^{s-1}\xi\,\mathrm{d}\xi. \qquad (9)$$

The integral with respect to ϑ can be evaluated graphically, using the sensitivity contours projected onto the echo surface (Fig. 2 of Part I). The difficulty lies in the second integral and the absolute incident flux cannot in general be deduced directly from the echo rate obtained at a single station, unless the form of the radiant distribution and the exponent s are known. The latter can be determined in several ways (Browne *et al.* (**5**), Kaiser (**2, 4, 6**)). Values previously obtained are near to 2·0, while recent determinations at Sheffield (**7, 8**) suggest a small diurnal variation in s, with a mean value of 2·17 for meteors between 8th and 11th magnitude.

4. *The radio-echo rate at the equator.*—The case of an aerial beam, narrow in azimuth, and directed eastwards or westwards at the equator, is important in that the radiants of the observed meteors lie along a great circle from the north to the south pole and in the course of a day this great circle sweeps the whole celestial sphere. Let T radians be the hour angle of this great circle and let $\bar{N}\,\mathrm{d}R$ be the mean diurnal echo rate observed between ranges R and $R+\mathrm{d}R$. Then, from (9) we obtain,

$$2\pi\bar{N}\,\mathrm{d}R = HI\,\mathrm{d}R \int \rho^{s-1}\,\mathrm{d}\vartheta \int_{-\pi/2}^{\pi/2}\int_{0}^{2\pi} \Theta\left(\frac{\alpha_0}{\cos\phi_0}\right)\cos^{s-1}\xi\,\mathrm{d}\xi\,\mathrm{d}T. \qquad (10)$$

Now $\mathrm{d}\Omega = \cos\xi\,\mathrm{d}\xi\,\mathrm{d}T$ is an element of solid angle on the celestial sphere, hence

$$2\pi\bar{N}\,\mathrm{d}R = HI\,\mathrm{d}R \int \rho^{s-1}\,\mathrm{d}\vartheta \int \Theta\left(\frac{\alpha_0}{\cos\phi_0}\right)\cos^{s-2}\xi\,\mathrm{d}\Omega. \qquad (11)$$

Since there are relatively few sporadic meteors with radiants near the poles (i.e. with ξ near 90°), negligible error will be involved if we put $\cos^{s-2}\xi = 1$, hence

$$\bar{N}\,\mathrm{d}R = \frac{2}{\pi} HI\,\Theta_1\left(\frac{\alpha_0}{\cos\phi_0}\right)\left[\int \rho^{s-1}\,\mathrm{d}\vartheta\right]\mathrm{d}R \qquad (12)$$

where $I = 9/4$ for $s = 2$.

Equation (12) can be extended to the case where the echo rate is evaluated over a finite range interval by determining $\int \rho^{s-1}\,\mathrm{d}\vartheta$ as a function of R (using the sensitivity contours of Fig. 2 of Part I) and integrating graphically.

The importance of (12) is that it enables the absolute mean influx, Θ_1, of meteors over a sphere at the Earth's distance from the Sun to be deduced from the mean diurnal rate, $\bar{N}$, irrespective of the form of the distribution of sporadic meteor radiants over the celestial sphere. Thus, for instance, the seasonal variation in the influx of meteors brighter than a given zenithal magnitude can be determined. In addition the results are directly comparable with satellite observations which determine the influx of meteoroids over a sphere as a function of their momenta.

5. *Some preliminary results.*—Since equatorial measurements of sporadic radio-meteor rates have not been made, we are obliged to use data obtained at higher latitudes. A recent analysis (**7, 8**) has been made using sporadic meteor rates obtained with a 17 Mc/s radio echo equipment at Sheffield (latitude 55°N).

The aerial was directed 65°W of N, at low elevation (sensitivity contours are given in Fig. 2 of Part I), and it is considered that the total daily rate during the autumnal equinox (when the apex of the Earth's way is at maximum declination) should approach the equatorial value. The observed mean rate between ranges 300 and 600 km, during September 1958, was 500 per hour. The limiting radio magnitude was $10{\cdot}8 \pm 0{\cdot}5$

$$\left(\alpha_z = \frac{\alpha_0}{\cos\phi_0} = 5 \times 10^9\,\mathrm{cm}^{-1}\right)$$

and the mean influx, Θ_1, was evaluated, using (12), as $1{\cdot}9 \times 10^{-10}\mathrm{m}^{-2}\,\mathrm{sec}^{-1}$ which corresponds to $8{\cdot}2 \times 10^9$ over the whole Earth per day.

The theory of Part I has been used to deduce the magnitude distributions and incident fluxes in the Geminid and Arietid showers using observations made at Sheffield. The results are illustrated in Fig. 2 which gives the shower and sporadic fluxes as a function of limiting magnitude. Some previously reported data (**2, 5, 6**) are also included. To facilitate direct comparison between the shower

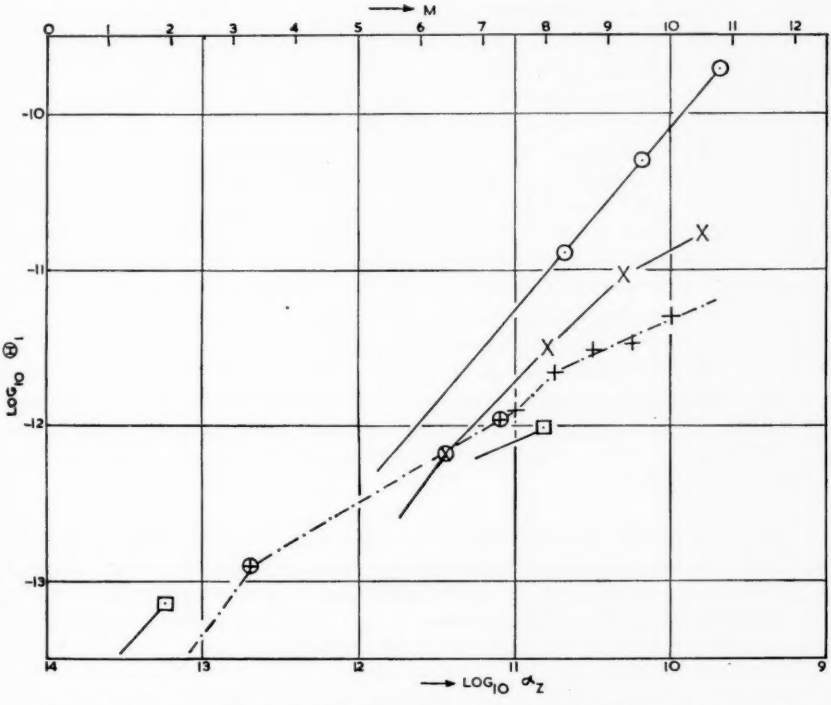

FIG. 2.—Θ_1 m^{-2} sec^{-1} = *mean incident flux over the whole Earth of meteors with zenithal electron line densities greater than* α_z (*brighter than magnitude M*).

- ○ Sporadic meteors (Sheffield, 1958 (**7, 8**))
- × Arietids (Sheffield, 1959)
- ⊗ Arietids (Jodrell Bank data (**2, 6**))
- \+ Geminids (Sheffield, 1958)
- ⊕ Geminids (Jodrell Bank data (**2, 6**))
- □ Perseids (Jodrell Bank data (**2, 6**)).

and sporadic fluxes, the values for the former are given as the mean influx over a sphere (which is one quarter the flux through a plane normal to the radiant direction).

6. *Discussion.*—An important conclusion from the present work is that the relation between the total sporadic meteor influx and the radio echo rate observed with a suitably oriented aerial on or near the Earth's equator is substantially independent of the distribution of sporadic meteor radiants. This makes it possible to determine the variation of activity with solar longitude by making regular equatorial observations over a period of a year. The value of such an observational programme is further enhanced in view of the accumulation of related data concerning the influx of impinging meteoroids on earth satellites.

An interesting feature of Fig. 2 is that the faint shower meteors are swamped by the sporadic background. This is true of the Arietids over the whole range of magnitudes covered by the observations, while the Perseid and Geminid fluxes exceed the sporadic level only for meteors brighter than about magnitude $+5$, (a similar result has been reported by Kresak and Vozarova (**9**) from visual observations). These shower fluxes refer only to the period of maximum shower activity, whereas it is known that in general the magnitude distribution in a particular shower changes during the Earth's passage through the meteor stream (**5**). These effects are particularly important in connection with problems of the evolution of meteor streams and further data are needed. The theory of Part I should prove of value for their quantitative reduction.

Some of the limitations of the theory have been discussed in the previous paper (**1**). One simplifying assumption is that the maximum meteor echo amplitude depends only upon the electron line density in the vicinity of the radio reflection point and on the equipment parameters. It has been shown (**6**) that rapid diffusion may cause a reduction in amplitude, the effect being greater the greater the height and the shorter the radio wavelength; a similar reduction is to be expected due to the finite initial radii of the trails. The consequent reduction to be expected in the echo rate has been discussed by Peregudov (**10**) and Fialko (**11, 12**), while Greenhow and Hall (**13**) have recently presented experimental evidence for a significant initial radius effect. These limitations may be minimized by judicious choice of equipment parameters, particularly the wavelength, but their quantitative effect on the observed echo rate certainly warrants further careful investigation.

Acknowledgments.—I am indebted to my colleagues J. P. Baldwin and D. Brooks for their co-operation in obtaining and reducing the observations presented in Section 5, and to L. M. G. Poole for pointing out some errors in the previous paper (see below). The Sheffield meteor programme is supported by a grant from the Department of Scientific and Industrial Research.

Corrections to Part I (*M.N.*, **121**, 284, 1960).

Equations (1), (2), (3) and (15) in Part I should read

$$\alpha_P = \left(\frac{32\pi^2 R^3 P_R}{P_T G^2 \lambda^3}\right)^{1/2} \left(\frac{mc^2}{e^2}\right) \qquad (1)$$

$$\alpha_P = \left(\frac{54\pi^3 R^3 P_R}{P_T G^2 \lambda^3}\right)^2 \left(\frac{mc^2}{e^2}\right) \tag{2}$$

$$\alpha = \frac{9}{4}\alpha_m(p/p_m)\left(1 - \frac{1}{3}p/p_m\right)^2 \tag{3}$$

$$I = \left(\frac{27}{4}\right)^{s-1} \int_0^1 u^{s-2}(1-u)^{2(s-1)}\,du. \tag{15}$$

The last equation also needs correction where it appears in the title of Fig. 7.

Dept. of Physics,
The University,
Sheffield:
1961 *July.*

References

(1) Kaiser, T. R., *M.N.*, **121,** 284, 1960.
(2) Kaiser, T. R., " Meteors " (Pergamon Press: London), p. 119, 1955.
(3) Kaiser, T. R., " Meteors " (Pergamon Press: London), p. 55, 1955.
(4) Kaiser, T. R., *M.N.*, **114,** 52, 1954.
(5) Brown, I. C., Bullough, K., Evans, S., and Kaiser, T. R., *Proc. Phys. Soc.*, **69B,** 84, 1956.
(6) Kaiser, T. R., *Adv. Phys.* (Phil. Mag. Supp.), **2,** 495, 1953.
(7) Baldwin, J. P., Ph.D. thesis (Sheffield), 1960.
(8) Kaiser, T. R., *Annales de Géophysique*, **17,** 50, 1961.
(9) Kresak, L., and Vozarova, M., *Czech. Astr. Bull.*, **6,** 139, 1953.
(10) Peregudov, F. I., *Soviet Astronomy* (*A.J.*), **2,** 833, 1958.
(11) Fialko, E. I., *Soviet Astronomy* (*A.J.*), **3,** 612, 1959.
(12) Fialko, E. I., *Soviet Astronomy* (*A.J.*), **4,** 711, 1960.
(13) Greenhow, J. S., and Hall, J. E., *M.N.*, **121,** 183, 1960.

SOME NEW SOUTHERN SUBDWARFS

T. J. Deeming

(Communicated by the Director of the Cambridge Observatories)

(Received 1961 August 8)

Summary

Radial velocities and *UBV* colours are presented for 21 newly identified southern subdwarfs. A redetermination of the solar motion relative to the subdwarfs using the new material gives a velocity 131 ± 27 km/sec in the direction of galactic rotation. There is little difference between the kinematic properties of subdwarfs with high, and those with low ultraviolet excesses.

Introduction.—Spectroscopic subdwarfs have mostly been found as a by-product of routine programmes of radial velocity observations of proper motion stars. In view of the scarcity of observatories in the southern hemisphere, and the pressure there of more immediately interesting problems, such work has normally been carried out from northern observatories only. This is apparent in Eggen and Sandage's useful list (**1**) of known spectroscopically identified subdwarfs, the distribution of which with declination is rather strongly non-uniform.

The subdwarfs, however, are mong the most easily identifiable representatives of the "Extreme Population II" component of the Galaxy in the general field, and it is desirable that as many of them as possible should be found. During a recent visit to the Radcliffe Observatory, Pretoria, South Africa, the author conducted a spectroscopic search for southern subdwarfs among likely stars of high proper motion. As a finding list for these, Luyten's useful catalogue of southern proper motion stars (**2**) was used, referred to as LTT in what follows. While this is not the most desirable method of selecting low luminosity stars, since it biasses the selection in favour of stars with high velocities relative to the Sun, it is the only one available, as there are, at present, no suitable lists from work based on objective prism or similar surveys which would not suffer from this selection effect.

Observations.—Spectrograms of selected stars were taken with the "d" camera of the two prism Cassegrain spectrograph attached to the 74-inch Radcliffe reflector (dispersion 86 A/mm at Hγ). Normally, a first exploratory spectrogram was taken at a slit width of 0·20 mm, which gives a projected slit width on the plate of 27 microns, equivalent to about 160 km/sec at $H\gamma$. Further plates of stars with interesting spectra or a high radial velocity were taken at a slit width of 0·14 mm so as to produce purer spectra for radial velocity measurements. Kodak 103aO emulsion was used throughout.

An attempt was made to classify all the spectra from plates of standard stars in the Radcliffe Observatory's plate library. Joy (**3**) has given a definitive description of the spectral peculiarities shown by subdwarfs. The most general feature is a marked weakening of all the metallic absorption lines. Joy's description has to be interpreted in the light of the current belief that most of the stars which were formerly classified as A-type subdwarfs ought properly to be classified F, following analyses of high resolution spectra of some of these (Chamberlain and Aller (**4**), Baschek (**5**), Aller and Greenstein (**6**)). Furthermore, there is

XUM

some doubt as to the existence of spectral differences between K or M dwarfs and subdwarfs; Unsöld (**7**) believes on theoretical grounds that cool subdwarfs should show no spectral peculiarities and disagrees with Joy's reported observations of metal weakening in some M-type stars.

The present results are confined to F- and G-type stars, where the spectroscopic effects are certain, and here weakness of the metallic absorption lines relative to the hydrogen lines is the sole criterion for the selection of subdwarfs. The degree of metal weakening necessary before a star is called a subdwarf is a rather arbitrary quantity. Here the term is restricted to stars showing a quite large deviation from normality, where the use of an MK type, even if modified by a "p", no longer gives even an approximate description of the spectrum. In these stars, all the metallic lines, and the G band of CH are very much weakened relative to the hydrogen lines which, together with the *H* and *K* lines of Ca II are frequently the only lines visible. It is most undesirable to apply an MK classification to a star which is recognisably far from normal, since this can lead to considerable confusion in the interpretation of the results. This difficulty is partly avoided, but not entirely overcome, in the present list by the deliberate use of unsubdivided spectral classes to describe the stars. Thus a type "sdF" implies a general resemblance to an F-type spectrum, although it may be applied to a star which on other evidence seems to have the effective temperature of a normal late-type G star. Beyond refusing to give a spectral class at all (which is possibly the only final answer to the problem), this procedure seems the best that can be followed at present.

Each spectrogram was measured for radial velocity using the Casella projection measuring machine at the Radcliffe Observatory. A set of iron arc wavelengths was used which was substantially the same as one found by Kinman (**8**) to be suitable for use with this camera at this dispersion. All stellar lines in the spectra of subdwarfs are weak, and there are frequently only a few lines suitable for radial velocity measurements: Hγ, Ca I 4226, Hδ, Fe I 4045, 4063, 4071, Ca II K are the most easily measurable. Since the wavelength of an absorption feature is the weighted mean of the wavelengths of its contributors, and since the relative weighting will be different in stars of low metal content, Petrie's wavelengths (**9**) derived for normal stars are not in general applicable to the subdwarfs. The present velocities were reduced using laboratory wavelengths for all the lines. An examination of the residuals from each line showed that no corrections to individual lines were necessary, and none were applied. In any case, the systematic difference in radial velocity between two possible systems occurring through the use of different wavelengths is much smaller in the present case than the average observational error of each determination, since only a comparatively few lines and plates have been available for measurement.

In forming the mean velocity for each star from individual plates, determinations with standard errors (from the internal agreement of velocities from different lines) up to 8·5 km/sec were given unit weight, determinations with standard errors between 8·5 and 15 km/sec were given half weight, and determinations with standard errors greater than this were rejected. These figures were suggested from an examination of the distribution of the individual standard errors from each plate. The average standard error of a final radial velocity is 3·5 km/sec.

During his visits to South Africa in 1960, Dr O. J. Eggen of the Royal Greenwich Observatory, Herstmonceux, measured *U*, *B*, and *V* for most of the

new subdwarfs with the Radcliffe 74-inch reflector and with the 26-inch refractor or the 18-inch reflector at the Cape. I am greatly indebted to Dr Eggen for allowing me to use his results.

Are these stars true subdwarfs? Sandage and Eggen (**10**) and Melbourne (**11**), following a suggestion originally due to Schwarzschild, Searle and Howard (**12**), have shown that the relation between effective temperature and $B-V$ for dwarf stars depends upon the composition of the star, and they suggest that some stars which appear as subdwarfs in, say, the (M_V, $B-V$) diagram, would not lie below the normal main sequence in an (M_{bol}, $\log T_e$) diagram, and in such a diagram would not be called subdwarfs. The usual method of identification of "subdwarfs" from their spectral peculiarities picks out just those stars which deviate most from the normal in their ($B-V$, $\log T_e$) relation. The question therefore arises of whether they should still be called subdwarfs. Since these spectroscopically peculiar stars, more than any other selection of possible "subdwarfs" seem most closely connected with globular clusters and other representatives of Population II, which have similar kinematic, spectroscopic and photometric properties, it would seem that a better name for them would be "Population II dwarfs". This idea is strengthened by the fact that the main sequences of globular clusters in the (M_V, $B-V$) diagram lie one or two magnitudes below the normal main sequence when the RR Lyrae stars in the clusters are fitted to an absolute magnitude of about $0^m{\cdot}5$. However, in order to avoid unnecessary confusion, and since these stars probably *are* subdwarfs in some HR diagrams, the usual term "subdwarf" has been retained here.

Finally, one should emphasise that normal spectroscopic luminosity criteria are not present in these stars, since all the metal lines are so weak. Almost the only information we have from the spectra concerns the degree of metal weakness, i.e. (perhaps) the "population" type. The supposition that the stars are dwarfs is based on their high proper motions alone. In particular there is no direct evidence to indicate that these stars lie below the "normal" main sequence although indirect evidence (e.g. the ultraviolet excesses) suggests that they do. It is just possible that some of the stars could be intrinsically brighter than normal main sequence stars (perhaps like those stars just above the "turn-off" point in globular clusters) although, in view of the high proper motions, this is unlikely.

Results.—Table I gives the results of radial velocity and photometric measurements for the new southern subdwarfs, which are identified by their LTT number. The values of V, $B-V$, and $U-B$ are by Dr O. J. Eggen. Where the value of $U-B$ is given in brackets, it is a measure on the Cape refractor $(U-B)_C$ system. These new stars provide a useful complement to the previously known F and G subdwarfs in Eggen and Sandage's list (**1**), and it has therefore seemed worthwhile to use the new data in a redetermination of the solar motion relative to the subdwarfs. The restriction to F- and G-type spectroscopic subdwarfs ensures homogeneity of the data, and provides probably as pure a sample of extreme Population II dwarfs as is available at present.

Eggen and Sandage's subdwarfs, plus the new southern ones, give a total of 103 stars for analysis. Preliminary least-squares solutions for the solar motion included a K term in the analysis to represent a possible expansion or contraction of the system of subdwarfs. However this was found to be not significantly different from zero, and the solution was repeated omitting the K term. For

TABLE I

Radial velocities, spectral types and photoelectric colours for 21 new subdwarfs

LTT	Spectrum	V	$B-V$	$U-B$	R.V (km/sec)	n
877	sdF–G				+227±8	(5)
2237	sdF	10·63	+0·54	(+1·50)	+320±6	(5)
2679	sdF	9·05	+0·46	(+1·56)	+ 71±2	(3)
2744	sdG				+247±5	(3)
3483	sdF–G	10·10	+0·48	−0·07	−110±5	(4)
3774	sdF	10·01	+0·43	−0·13	+194±2	(5)
4226	sdF	8·96:	+0·47	−0·21	+222±3	(5)
4519	sdF–G	10·39	+0·44		+121±2	(3)
4859	sdF	9·87	+0·47	−0·16	+220±5	(5)
5145	sdF				+144±3	(3)
5468	sdF	8·68	+0·48	−0·18	− 23±6	(5)
7043	sdF				+104±3	(4)
7182	sdF–G	10·22	+0·57	−0·19	+364±2	(6)
7321	sdF	10·92	+0·50	−0·15	+106±3	(5)
7662	sdF	10·72	+0·50	−0·28	...	
7668	sdF	9·62	+0·44	−0·28	+ 17±7	(2)
7862	sdF	10·12	+0·42	−0·26	−146±4	(3)
8578	sdF	10·52	+0·40	(1·45)	+112±1	(5)
9074	sdF	9·64	+0·40	−0·24	+ 47±3	(4)
9201	sdF	10·05	+0·41	−0·25	− 83±7	(5)
9509	sdF	10·15	+0·66	−0·05	+ 72±4	(4)

103 stars, the mean subdwarf motion relative to the Sun, in equatorial components (epoch 1950), was found to be

$$X = -67 \pm 25 \text{ km/sec}$$
$$Y = +84 \pm 27 \text{ km/sec}$$
$$Z = -103 \pm 27 \text{ km/sec}.$$

(For a discussion of the application of the least-squares method to this problem, see Trumpler and Weaver (**13**), p. 181). On transforming to galactic velocity components U, V, W, where U is directly away from the galactic centre, W in the direction of the north galactic pole, and V perpendicular to U and W in the direction of galactic rotation, and using the solar motion determined by Woolley (**14**), we find the mean subdwarf velocity relative to the local standard of rest to be:

$$U = -9 \pm 27 \text{ km/sec}$$
$$V = -131 \pm 27 \text{ km/sec}$$
$$W = +3 \pm 26 \text{ km/sec}.$$

There is thus no significant deviation of the vertex of the subdwarf motion from the direction of galactic rotation. In a similar analysis of the radial velocities of 79 subdwarfs, Fricke (**15**) found a velocity of the Sun relative to the subdwarfs of 148 ± 28 km/sec directed toward galactic longitude $l^{\text{I}} = 75° \pm 8°$ (old system). Applying Woolley's value for the solar motion relative to the local standard of rest, this becomes 135 ± 28 km/sec directed toward $l^{\text{I}} = 77°$. The agreement between the two velocities is good, but Fricke's result shows a deviation of 19° in the vertex of the motion from the direction of galactic rotation. This may be due to his inclusion of some trigonometrical subdwarfs based on rather uncertain parallaxes, as well as some high velocity stars, whose subdwarf nature must be in doubt. The present results indicate a mean velocity dispersion of 135 km/sec; Fricke's value was 110 km/sec.

Further information about the subdwarf motions may be obtained from the proper motions and parallaxes. For most of the known F and G subdwarfs, trigonometrical parallaxes are not available. However the blanketing theory of subdwarfs (**10**) gives a method of estimating the absolute magnitude of a subdwarf from its observed $B-V$ colour, and its ultraviolet excess, $\delta(U-B)$. Hence we can derive a "photometric parallax". The accuracy of these parallaxes depends on the accuracy of the measurements of U, B, and V, and on the correctness of the table of blanketing corrections given by Sandage and Eggen (**10**). Of these two, the latter is almost certainly much the greater source of error. There is not yet sufficient information to give a judgement on the correctness of this, but we may tentatively suppose that an error not greater than $\pm 0^{m}\cdot 5$ in absolute magnitude may be expected, giving a relative error in parallax, $\delta\pi/\pi$, of 0·23, and a similar error in the derived transverse velocity component.

The proper motions (mostly from the extensive publications of the Cape Observatory), the radial velocities, and the photometric parallaxes were combined to compute space velocities in galactic velocity components for each star which has been measured on the *UBV* system, and which has an ultra-violet excess greater than $0^{m}\cdot 10$. The stars were then divided into two groups according to ultraviolet excess: (*a*) those with ultraviolet excess between $0^{m}\cdot 10$ and $0^{m}\cdot 21$, and (*b*) those with ultraviolet excess greater than $0^{m}\cdot 21$, and mean motions and dispersions in each velocity component determined for each group. The results were:

(*a*) *Low excess stars*

$$U = -\ 29 \pm 22\ \text{km/sec} \qquad \sigma_U = 105 \pm 15\ \text{km/sec}$$
$$V = -113 \pm 20\ \text{km/sec} \qquad \sigma_V = \ 93 \pm 14\ \text{km/sec}$$
$$W = +\ 12 \pm 12\ \text{km/sec} \qquad \sigma_W = \ 55 \pm \ 8\ \text{km/sec}$$

(*b*) *High excess stars*

$$U = -\ 11 \pm 22\ \text{km/sec} \qquad \sigma_U = 100 \pm 16\ \text{km/sec}$$
$$V = -141 \pm 17\ \text{km/sec} \qquad \sigma_V = \ 75 \pm 12\ \text{km/sec}$$
$$W = +\ \ 2 \pm 18\ \text{km/sec} \qquad \sigma_W = \ 78 \pm 12\ \text{km/sec.}$$

Note that the velocity dispersions, σ_U, σ_V, σ_W are not corrected for possible errors in the adopted photometric parallaxes, since these are probably systematic rather than random errors. There is apparently a slight deviation of the vertex of subdwarf motion for the stars with low ultraviolet excess which is in the same direction as that found by Fricke in his analysis of subdwarf motions, but it is hardly significant. The high excess subdwarfs show no evidence of a deviation of the vertex of the motion. There is only a slight difference of 28 ± 26 km/sec in mean motion between the low excess stars and the high excess stars. There is a significant difference in the velocity dispersion in the W direction between the low excess and the high excess stars, and this implies a different distribution of stars with height above the galactic plane. The low excess stars with the smaller dispersion of W velocities must extend less far above the galactic plane than the stars with the higher velocity dispersion.

It is interesting to compare these results with similar results derived by Kinman (**16**) for the globular clusters and RR Lyrae stars. He finds a mean solar motion relative to the globular clusters of 167 ± 30 km/sec, similar to that for RR Lyrae stars with periods between $0^{d}\cdot 5$ and $0^{d}\cdot 6$. This is just in agreement, within the

limits of the observational errors, with the value for all the subdwarfs. The mean velocity of all the "Population II" objects—globular clusters, RR Lyrae stars, and subdwarfs—is then 131 ± 18 km/sec, but this value has no particular astrophysical significance unless one has grounds for supposing that all the Population II objects had an almost identical galactic origin, in which case their kinematic properties should be the same. Some of Eggen's moving groups of subdwarfs (1) suggest that this may be the case, but the evidence is by no means conclusive.

Note that if the commonly accepted value for the circular velocity of Population I objects at the Sun, of about 220 km/sec, is true, then the Population II stars have, on average, a quite appreciable galactic "rotation" of about 90 km/sec at the Sun. The circular velocity is only very imperfectly known, and it might be possible to accept a smaller value than 220 km/sec. In this case, however, we should find that several of the subdwarfs have retrograde orbits, and it can be argued that a retrograde orbit is *a priori* improbable, since a very close (and statistically improbable) stellar collision is required to reverse the direction of a star's orbit, and a star is unlikely to have been formed initially with a retrograde galactic orbit, unless there was a very high degree of turbulence in the protogalactic gas cloud, of the order of 100 km/sec, r.m.s. velocity. It will be interesting to await the development of proper motion systems based on the extragalactic nebulae, since this seems to offer the most promising line of approach for a precise determination of the local circular velocity.

Acknowledgments.—The author would like to thank the Radcliffe Trustees and the D.S.I.R. for the opportunity to work in South Africa, and he particularly expresses his thanks to Drs A. D. Thackeray, A. J. Wessenlink, and M. W. Feast for their encouragement and hospitality during his visit to Pretoria. He would also like to thank Dr O. J. Eggen for the use of his photoelectric results and for much helpful discussion.

The Observatories,
Cambridge:
1961 *July.*

References

(1) O. J. Eggen and A. R. Sandage, *M.N.*, **119**, 255, 1959.
(2) W. J. Luyten, "A catalogue of 9867 stars in the southern hemisphere with proper motions exceeding 0″·2 annually", The Lund Press, Minneapolis, Minnesota, 1957.
(3) A. H. Joy, *Ap. J.*, **105**, 396, 1957.
(4) J. W. Chamberlain and L. H. Aller, *Ap. J.*, **114**, 52, 1951.
(5) B. Baschek, *Zs. f. Astrophys.*, **48**, 95, 1959.
(6) L. H. Aller and J. L. Greenstein, *Ap. J. Suppl.*, **5**, No. 46, 1960.
(7) A. Unsöld, *M.N.*, **118**, 3, 1958.
(8) T. D. Kinman, *M.N.*, **119**, 157, 1959.
(9) R. M. Petrie, *Publ. D.A.O.*, **10**, No. 22.
(10) A. R. Sandage and O. J. Eggen, *M.N.*, **119**, 278, 1959.
(11) W. Melbourne, *Ap. J.*, **132**, 101, 1960.
(12) M. Schwarzschild, L. Searle, and R. Howard, *Ap. J.*, **122**, 353, 1955.
(13) R. Trumpler and H. N. Weaver, "Statistical Astronomy", University of California Press, 1953.
(14) R.v.d.R. Woolley, *M.N.*, **118**, 45, 1958.
(15) W. Fricke, *Astr. Nach.*, **278**, 121, 1950.
(16) T. D. Kinman, *M.N.*, **119**, 559, 1959.

THE RADIO EMISSION FROM NORMAL GALAXIES

III. Observations of Irregular and Early-type Galaxies at 158 Mc/s and a General Discussion of the Results

R. Hanbury Brown and C. Hazard

(Received 1961 August 31)*

Summary

A survey of the radio emission at 158 Mc/s has been made from twenty bright spiral, four irregular and four early-type galaxies. This paper reports the measurements of the irregular and early-type galaxies; the results obtained from the spirals were given in the two previous parts. The variation of the radio index R with type of galaxy is discussed; R is defined by the equation $R=m_r-m_{pg}$ where m_r and m_{pg} are the radio and photographic magnitude respectively. It is shown that the value of R for irregular galaxies is significantly greater than that for Sb and Sc spirals, and that this is probably also true of early-type galaxies.

---

1. *Introduction*

The present paper completes an account of a survey of bright *normal* galaxies which was carried out in 1958 with the 250 ft steerable paraboloid at Jodrell Bank working at 158 Mc/s. A *normal* galaxy, following Baade and Minkowski (**1**), is taken to be a normal member of the population of galaxies observed photographically. In Paper I (**2**) we described the apparatus and also the results obtained on M31 and M33; in Paper II (**3**) we reported measurements on twenty spirals of type Sb and Sc. In the present paper (III) we report some observations of a few irregular and early-type galaxies; we also discuss how the radio emission from a *normal* galaxy depends upon type.

2. *Observations*

An attempt was made to observe the radio emission at 158 Mc/s from four irregular galaxies of magellanic type and four early-type galaxies. A radio source was observed close to the position of IC 1613; the regions of sky near the other galaxies were complicated by the proximity of other sources and irregularities in the general background radiation and it was possible only to set an upper limit to their emission. The results are shown in Table I. We have tabulated m_{pg}, the photographic magnitude according to Holmberg (**4**) or de Vaucouleurs (**5**), m_r, the observed integrated radio magnitude at 158 Mc/s, and R the radio index, where $R=m_r-m_{pg}$. We have not corrected the values of R, as discussed in Paper II, for the absorption of light; an estimate of these corrections shows that they are less than 0·5 mag. and for the purposes of the present paper they can be neglected.

* Received in original form 1961 July 10.

TABLE I

Observations at 158 Mc/s of irregular and early-type galaxies

Galaxy NGC	Type	m_{pg}	m_r	$R=m_r-m_{pg}$
4449	Irr	9·9	$\geqslant$ 10·6	$\geqslant$ +0·7
4214	Irr	10·1	$\geqslant$ 11·0	$\geqslant$ +0·9
6822	Irr	9·2	$\geqslant$ 10·7	$\geqslant$ +1·5
IC 1613	I	8·9*	9·1	+0·2
4594	Sa	9·2	$\geqslant$ 10·6	$\geqslant$ +1·4
3368	Sa	10·1	$\geqslant$ 10·4	$\geqslant$ +0·3
4472	E	9·3	$\geqslant$ 10·2	$\geqslant$ +0·9
1023	SO	10·5	$\geqslant$ 9·8	$\geqslant$ −0·7

* The optical data for this galaxy has been taken from de Vaucouleurs (**5**).

3. *The radio index of different types of galaxy*

3.1. *The radio index of Sb and Sc spirals.*—It was shown in Paper II that the average radio index of Sb and Sc spirals is +1·4 and +1·2 respectively, the associated r.m.s. deviations about these mean values being ±0·8 and ±0·7. These conclusions were based on measurements of sixteen galaxies selected from a survey of twenty bright spirals.

3.2. *The radio index of early-type galaxies.*—In view of the scarcity of observational data we shall assume that types E, SO and Sa all have the same average radio index and consider these three types as a single group.

Table II is a list of all the early-type galaxies which have been surveyed individually for radio emission. For the purpose of comparison the measurements at different frequencies have been scaled to 158 Mc/s on the assumption that the spectral index is −0·6 since this was the median value found by Harris and Roberts (**10**) for all sources in their survey. If also, following Harris and Roberts, we assume that the dispersion about this mean spectral index is such that 50 per cent of the sources have values in the range −0·4 to −0·8, then we can calculate the associated uncertainty in scaling the values in Table II; the greatest uncertainty, which arises in scaling the 1400 Mc/s results, is about ±0·5 mag. and is not significant in the present discussion.

The table shows that, out of a total of eighteen galaxies, in only one case (NGC 4526) was a radio source observed; the remainder were below the limit of detection and may therefore have any value of radio index greater than that shown in Table II. The results cannot, therefore, be used to derive a mean radio index, but they can be used to estimate a lower limit if we assume a value for the dispersion about the mean. Thus if we assume that individual early-type galaxies have radio indices which are distributed about the mean with a similar dispersion to that observed for Sb and Sc spirals (±0·7 mag.), then the probability of occurrence of the distribution of limits given in Table II can be calculated for different values of the mean. This calculation shows that there is roughly a 50 per cent probability that the observed distribution would arise by chance if the mean index is as low as +2·5, and only a 10 per cent probability, if the mean value is +2·0. Thus, given the assumed dispersion, it is probable that the mean radio index of early-type galaxies is greater than +2·0 and is therefore greater than that (+1·3) of Sb and Sc spirals.

TABLE II

Observations of single early-type galaxies

Galaxy NGC	Type	m_{pg}	m_r(158 Mc/s)	R (158 Mc/s)
185	E	10·3	> 11·0 (H)	> +0·7
205	E	8·9	> 10·2 (L)	> +1·3
1023	SO	10·5	> 9·8 (BH)	> −0·7
1052	E	11·7	> 11·0 (H)	> −0·7
1291*	SBO	9·4	> 11·1 (M)	> +1·7
3115*	E	10·2	> 11·3 (M)	> +1·1
3368	Sa	10·1	> 10·4 (BH)	> +0·3
3379*	E	10·3	> 10·8 (Le)	> +0·5
3623	Sa	10·2	> 10·8 (Le)	> +0·6
4278	E	11·2	> 11·0 (H)	> −0·2
4382	SO	10·1	> 10·0 (Le)	> −0·1
4472	E	9·3	> 10·2 (BH)	> +0·9
4494*	E	10·8	> 10·1 (Le)	> −0·7
4526*	Sa	10·5	10·0 (Le)	−0·5
4594	Sa	9·2	> 11·2 (M)	> +2·0
4636*	E	10·0	> 10·3 (Le)	> +0·3
4649*	E	9·9	> 10·3 (Le)	> +0·3
5866*	SO	11·1	> 11·0 (H)	> −0·1

H D. S. Heeschen (6) at 1400 Mc/s.
L M. I. Large (7) at 408 Mc/s.
BH Present survey at 158 Mc/s.
M B. Y. Mills (8) at 85 Mc/s.
Le P. R. R. Leslie (9) at 178 Mc/s.
* Optical data according to de Vaucouleurs (5); the data for the other galaxies was taken from Holmberg (4).

3.3. *The radio index of irregular galaxies.*—Table III is a list of the available observations of irregular galaxies. The measurements have been adjusted to 158 Mc/s on the assumption that the spectral index of the sources is −0·6. All the galaxies in the list contain a substantial proportion of Population I; in the classification of Holmberg they appear as type Ir1, and in the system of de Vaucouleurs they are referred to as Magellanic. One galaxy, IC 1613, appears to have a radio emission which is markedly different from the others. We have therefore surveyed this galaxy also at 240 Mc/s and have confirmed the presence

TABLE III

Observations of single magellanic irregular galaxies.

Galaxy	m_{pg}	m_r (158 Mc/s)	R (158 Mc/s)
LMC	0·6	3·3 (M)	+2·7
SMC	2·5	5·4 (M)	+2·9
NGC 55	7·8	10·8 (M)	+3·0
NGC 4449	9·9	⩾ 10·6 (BH)	⩾ +0·7
NGC 4214	10·1	⩾ 11·0 (BH)	⩾ +0·9
NGC 6822	9·2	⩾ 10·7 (BH)	⩾ +1·5
IC 1613	8·9	9·1 (BH)	+0·2

M B. Y. Mills (8) at 85 Mc/s.
BH The present survey at 158 Mc/s.

of a source close to the optical position; however, the value of radio index measured at 240 Mc/s was $+1{\cdot}3$ which differs considerably from the value of $+0{\cdot}2$ obtained at 158 Mc/s. This discrepancy suggests that the observations are affected by confusion with other sources and that the association of this radio source with IC 1613 must be regarded as doubtful, although the possibility cannot be excluded that IC 1613 is an excited or *radio* galaxy.

If we exclude the result on IC 1613, then the data in Table III indicate that the average radio index of magellanic galaxies is certainly greater than that of spirals; the measurements on NGC 55 and the Magellanic Clouds suggest that it has a value of about $+3{\cdot}0$

3.4. *Summary.*—Fig. 1 summarizes the results of the previous sections. It shows that the ratio of total radio emission to the total light, as measured by the radio index is greatest for Sb and Sc spirals and decreases significantly for irregular galaxies. It also seems likely that it decreases for early-type galaxies, although this conclusion cannot be established by the data. These results confirm the conclusions reached by Mills (**11**) from earlier surveys.

There appears to be no simple correlation between the radio index of normal galaxies and their mass, linear size or colour index. However, the results in Fig. 1 suggest one particular conclusion. It appears that the ratio of coronal to disk radiation in an irregular galaxy is much less than that found in an Sb or Sc spiral. The absence of a corona around irregular galaxies is suggested by an examination of the radio isophotes of the Magellanic Cloud (**8**), but their large angular size and proximity to our own Galaxy makes this conclusion somewhat uncertain. However, if we assume that NGC 55 and the other four irregulars in Table I are similar to the Magellanic Clouds, then all the measurements taken together show that irregulars do not have extensive and powerful radio coronae

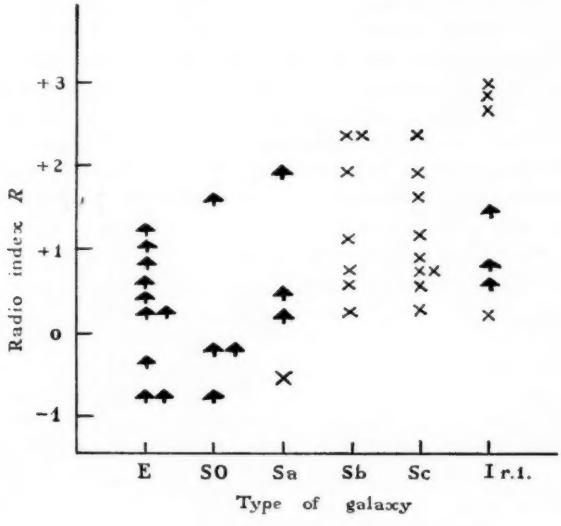

FIG. 1.—*The radio index of different types of galaxy.*

similar to those found in Sb and Sc spirals, otherwise we would expect their radio indices to be much lower than the radio indices of the Clouds. It follows that any corona which may exist in an irregular must emit less than the main body of the nebula.

The above conclusion is supported by a comparison of the emission from the disk of a spiral and from the body of an irregular. Thus the radio index of an average Sb or Sc spiral, if we exclude about 90 per cent of the emission which is due to the corona, probably lies between $+3$ and $+4$ and is therefore comparable with the value of $+3$ shown in Fig. 1 for irregulars. This suggests that the radio emissivity of the disk of a late-type spiral is comparable with that of the body of an irregular galaxy and that the emission processes are similar in the two cases.

The present limits to the radio index of early-type galaxies do not permit any positive conclusions to be drawn about their radio emission; nevertheless it appears likely that they are relatively weak radio emitters in comparison with Sb and Sc spirals.

4. *Acknowledgments.*—We thank the Director of the Nuffield Radio Astronomy Laboratories for making available the facilities for this investigation.

Nuffield Radio Astronomy Laboratories,
Jodrell Bank,
Macclesfield, Cheshire:
1961 *July.*

School of Physics,
University of Sydney,
New South Wales,
Australia.

References

(1) Baade, W., and Minkowski, R., *Ap. J.*, **119**, 215, 1954.
(2) Brown, R. Hanbury and Hazard, C., *M.N.*, **119**, 297, 1959.
(3) Brown, R. Hanbury and Hazard, C., *M.N.*, **122**, 479, 1961.
(4) Holmberg, E., *Medd. Lund. Obs.*, Ser. 2, No. 136, 1957.
(5) de Vaucouleurs, G., *A revision of the Harvard Survey of Bright Galaxies.* Australian National University Mimeograph, 1952/53.
(6) Heeschen, D. S., *P.A.S.P.*, **72**, 368, 1960.
(7) Large, M. I., Matthewson, D. S., and Haslam, C. G. T., *Nature*, **183**, 1250, 1959.
(8) Mills, B. Y., *Handbuch der Physik*, Vol. 53, p. 237, Springer-Verlag, Berlin, 1959.
(9) Leslie, P. R. R., *Observatory*, **80**, 216, 1960.
(10) Harris, D. E., and Roberts, J. A., *P.A.S.P.*, **72**, 237, 1960.
(11) Mills, B. Y., *Aust. J. Phys.*, **8**, 368, 1955.
(12) Mills, B. Y., *Aust. J. Phys.*, **13**, 550, 1960.

XUM

NOTE ON

THE GRAVITATIONAL INSTABILITY OF AN INFINITE HOMOGENEOUS ROTATING VISCOUS MEDIUM IN THE PRESENCE OF A MAGNETIC FIELD

Since the publication of the above paper (*M.N.*, **122,** 455–459, 1961), Professor St. Piotrowski has kindly pointed out that equivalent but more extensive work on this problem has been carried out by his colleagues, A. G. Pacholczyk and J. S. Stodolkiewicz (*Acta Astronomica, Warsaw*, **10,** 1, 1960). I should like to acknowledge the priority of their work, of which the Society and I were unaware at the time of publication.

Similar work has also been carried out more recently by S. S. Kumar (*Pub. Astron. Soc. Japan*, **12,** 552, 1960) and I am grateful to Dr Kumar for pointing out that the term $\frac{1}{3}\nu$ grad div **u** should be included on the right-hand side of the Navier–Stokes equation (1). Nevertheless, this does not affect the conclusion of my paper that the viscosity of the medium does not alter the Jeans criterion for instability.

Department of Mathematics
Imperial College
London, S.W.7:
G. STEPHENSON

1961 *November.*

XUM